

**Characterization of the *Arabidopsis thaliana*
STY8, STY17 and STY46 protein kinase family**

Dissertation der Fakultät für Biologie
der
Ludwig-Maximilians-Universität München

vorgelegt von
Giorgia Lamberti

München

2011

Erstgutachter: Prof.Dr. Jürgen Soll

Zweitgutachter: Prof.Dr. Barbara Conradt

Tag der mündlichen Prüfung: 16. Dezember 2011

SUMMARY

Chloroplasts originated from an endosymbiotic event in which an ancestral photosynthetic cyanobacterium was engulfed by a heterotrophic host cell. During evolution about 95 % of the genetic information was transferred from the chloroplast to the nuclear genome, thus requiring an efficient and well regulated back-transport of nuclear encoded proteins to the chloroplast. Several cytosolic players govern the targeting of preproteins to the chloroplast. Most chloroplast precursor proteins display the feature to bind the heat shock chaperone protein Hsp70. Beside Hsp70, 14-3-3 proteins can bind a subset of chloroplast preproteins. A 14-3-3 dimer interacts with many precursor proteins in their transit peptide, forming together with Hsp70 the so-called "guidance complex" which enhances the import rate of the preproteins. The affinity of 14-3-3 for the substrate increases when the binding site on the substrate is phosphorylated. In *Arabidopsis thaliana* the responsibility for the transit peptide phosphorylation was attributed to three high homologous protein kinases: STY8, STY17 and STY46.

In this work the properties of the three plant specific kinases STY8, STY17 and STY46 have been extensively studied *in vitro* as well as *in vivo*. The intramolecular autophosphorylation of a conserved threonine residue inside the activation segment was demonstrated to be an essential regulatory mechanism of the kinase activity. A conserved small molecule-binding domain called ACT was also shown to play a role in the kinase regulation. STY8 was found to be inhibited by several specific tyrosine kinase inhibitors, although it lacked the ability to phosphorylate tyrosine residues. The substrate phosphorylation occurred on serine and threonine residues after the release of the substrate from the ribosomes.

In vivo analysis of *sty8*, *sty17* and *sty46 Arabidopsis* knockout/knockdown mutants revealed a distinct function of the three kinases in the greening process and in the efficient differentiation of chloroplasts. Mutant plants displayed a delayed accumulation of chlorophyll, a retarded establishment of photosynthetic capacity and a reduction of nuclear encoded chloroplast proteins during the first 6 h of de-etiolation, supporting a role of the cytosolic STY8, STY17 and STY46 kinases in chloroplast differentiation.

SUMMARY (GERMAN)

Der Chloroplast entstand durch Endosymbiose eines den Cyanobakterien ähnlichen, freilebendem Organismus in eine heterotrophe Wirtszelle. Im Laufe der Evolution wurde ca. 95% der genetischen Information aus dem Chloroplasten in das Kerngenom übertragen, weshalb ein effizienter und hochregulierter Transport von nukleär kodierten Proteinen in den Chloroplasten unentbehrlich wurde. Eine Vielzahl cytosolischer Faktoren sind an dem Transport der Präproteine zu den Chloroplasten beteiligt. Die Meisten Präproteine binden HSP70 und ein Teil der Transitpeptide interagiert zusätzlich mit 14-3-3 Proteinen, wodurch der sog. 'Guidance-Komplex' entsteht, welcher die Importeffizienz von Präproteinen steigern kann. Die Affinität von 14-3-3 Proteinen zum Substrat wird durch Phosphorylierung an der Substratbindestelle erhöht. In Arabidopsis wurden drei homologe Proteinkinasen identifiziert, STY8, STY17 und STY46, die plastidäre Präproteine phosphorylieren.

In der vorliegenden Arbeit wurde die Bedeutung und Funktionsweise dieser drei Kinasen sowohl *in vitro* als auch *in vivo* untersucht. Es konnte gezeigt werden, dass die intramolekulare Autophosphorylierung an einem konservierten Threoninrest wichtig für die Regulation der Kinaseaktivität ist. Desweiteren verfügen die Kinasen über eine sog. ACT Domäne, die höchstwahrscheinlich durch die Binding von Metaboliten, ebenfalls die Kinaseaktivität beeinflusst. STY8 kann von tyrosinkinase-spezifischen Inhibitoren gehemmt werden, obwohl Phosphorylierung an Tyrosinresten weder bei der Autophosphorylierung, noch bei der posttranslationalen Substratphosphorylierung stattfindet. Eine *in vivo* Analyse von *sty8*, *sty17* und *sty46 knockout/knockdown* Mutanten wies auf eine Funktion der drei Kinasen bei der Ergrünung und der Chloroplastendifferenzierung hin. Die Mutanten zeigten neben verringertem Wachstum sowohl eine verzögerte Akkumulation von Chlorophyll und eine verminderte Effizienz der photosynthetischen Leistung, als auch eine Reduktion nukleär kodierter plastidärer Proteine während den ersten sechs Stunden der Ergrünung. Ultrastrukturelle Veränderungen der Chloroplasten deuteten ebenfalls auf eine Rolle der STY Kinasen bei der Chloroplastenentwicklung hin.

TABLE OF CONTENT

SUMMARY	I
SUMMARY (GERMAN)	II
TABLE OF CONTENT	III
ABBREVIATIONS	1
1 INTRODUCTION	2
1.1 Preprotein import into chloroplast.....	2
1.2 Targeting to the chloroplast	5
1.3 Plant protein kinases	7
1.4 Plant dual-specificity protein kinases.....	8
1.4.1 The <i>Arabidopsis thaliana</i> STY protein kinases.....	9
1.5 Aim of this work	10
2 MATERIALS	12
2.1 Chemicals	12
2.2 Molecular weight markers and DNA standards	12
2.3 Antibodies	12
2.4 Oligonucleotides	13
2.5 Plasmids	15
2.6 Kits.....	18
2.7 Enzymes	19
2.8 Chromatography media	19
2.9 Bacterial strains	19
2.10 Plant material.....	20
2.11 <i>E.coli</i> media and plates.....	20
2.12 <i>A.tumefaciens</i> media and plates.....	20
2.13 Plants media and plates	20
3 METHODS	21
3.1 DNA cloning	21
3.2 <i>E. coli</i> growth conditions	22
3.3 <i>Agrobacterium tumefaciens</i> growth conditions	22
3.4 Plant growth conditions.....	22
3.5 Expression and purification of recombinant proteins	22
3.6 Size exclusion chromatography.....	23
3.7 SDS polyacrylamide gel electrophoresis and Western Blot.....	23

3.8	Kinase assay	24
3.9	Phosphoamino acids analysis	24
3.10	In vitro transcription and translation.....	25
3.11	Immunoprecipitation	25
3.12	Isoelectric focusing	25
3.13	Isolation of intact chloroplasts from <i>Pisum sativum</i> (pea).....	26
3.14	Protein import experiment.....	26
3.15	<i>Arabidopsis thaliana</i> stable transformation with <i>Agrobacterium tumefaciens</i>	26
3.16	Generation of knockdown mutant plants	27
3.17	Isolation of genomic DNA from <i>Arabidopsis thaliana</i>	27
3.18	Quantitative RT-PCR analysis	28
3.19	Chlorophyll extraction	28
3.20	Spectroscopic analysis	28
3.21	Electron microscopy	28
3.22	Protein extraction from <i>Arabidopsis thaliana</i>	29
3.23	Isolation and transient transformation of <i>Arabidopsis thaliana</i> protoplasts.....	29
3.24	Protein extraction from transformed <i>Arabidopsis thaliana</i> protoplasts	30
3.25	Transient transformation of <i>Nicotiana benthamiana</i>	30
3.26	Isolation of <i>Nicotiana benthamiana</i> protoplasts	30
4	RESULTS	32
4.1	Characterization of STY8, STY17 and STY46 auto- and substrate- phosphorylation <i>in vitro</i>	32
4.1.1	Phylogeny and conserved domains.....	32
4.1.2	Characterization of kinase autophosphorylation activity.....	33
4.1.3	Analysis of the conserved ACT domain.....	37
4.1.4	Identification of kinases specific inhibitors.....	39
4.1.5	Characterization of kinases amino acids specificity	40
4.1.6	Analysis of the substrates phosphorylation	41
4.2	<i>In vivo</i> characterization of STY8, STY17 and STY46.....	42
4.2.1	GFP localization of STY8, STY17 and STY46	42
4.2.2	Association analysis of STY8	43
4.2.3	Generation and characterization of <i>sty8</i> , <i>sty17</i> and <i>sty46 Arabidopsis</i> mutant lines	44
4.2.4	Analysis of the chloroplast ultrastructure in kinase mutant lines	47
4.2.5	Phenotypic analysis of etiolated kinases mutant plants	51
4.2.6	Biochemical characterization of etiolated kinase mutant plants	53

4.2.7	Gene expression analysis of etiolated kinase mutant plants	55
4.2.8	Analysis of preprotein import	57
5	DISCUSSION	64
5.1	<i>In vitro</i> characterization of STY8, STY17 and STY46.....	64
5.1.1	Autophosphorylation of STY8, STY17 and STY46 is important for kinase activity.....	64
5.1.2	The ACT domain might regulate the kinase activity in vivo	65
5.1.3	STY8 differs from other plant STY kinases	66
5.2	<i>In vivo</i> characterization of STY8, STY17 and STY46	67
5.2.1	STY8, STY17 and STY46 are involved in etioplast to chloroplast transition	67
5.2.2	STY8, STY17 and STY46 depletion leads to chloroplast ultrastructure modification	68
5.3	Chloroplast precursor phosphorylation	69
5.3.1	Transit peptide phosphorylation is not essential for import into chloroplasts ...	69
5.3.2	Transit peptide dephosphorylation is essential for import into chloroplasts	70
5.4	Future perspectives	72
6	REFERENCES	74
7	APPENDIX	79
7.1	Phosphorylated residues in STY8, STY17 and STY46	79
7.2	Kinase inhibitory library tested with STY8	80
7.3	Results of microarray analysis for etiolated <i>sty8 sty17 sty46</i>	81
7.3.1	Up-regulated genes in <i>sty8 sty17 sty46</i>	81
7.3.2	Down-regulated genes in <i>sty8 sty17 sty46</i>	84
	ACKNOWLEDGEMENTS	89
	CURRICULUM VITAE	90
	LIST OF PUBLICATIONS	91
	EHRENWÖRTLICHE VERSICHERUNG	92

ABBREVIATIONS

2D	two dimensional
ACT	<u>a</u> spartate kinase, <u>c</u> horismate mutase and <u>t</u> yrA
AMP-PNP	adenosine 5'-(β,γ -imido)triphosphate tetralithium salt hydrate
ATP	adenosine-5'-triphosphate
BLAST	basic local alignment search tool
bp	basepair
CBB	coomassie brilliant blue
cDNA	copy-DNA
CF0	membrane-embedded part of CFOCF1 ATP synthase (complex)
CF1	soluble part of CFOCF1 ATP synthase (complex)
C-terminus	carboxyl-terminus
DMSO	dimethylsulfoxid
DTT	dithiothreitol
<i>E.coli</i>	<i>Escherichia coli</i>
E2YI	pyruvate dehydrogenase
Fv/Fm	variable fluorescence/ maximum fluorescence
g	gravity force
GFP	green fluorescence protein
HCF101	high chlorophyll fluorescence 101
IEF	isoelectric focusing
IEP	isoelectric point
IPG	immobilized pH gradient
kDa	kilo Dalton
LHC	light harvesting complex
MBP	myelin basic protein
MW	molecular weight
N-terminus	amino-terminus
OD	optical density
OE23	oxygen evolving complex protein of 23 kDa
PAC	pale cross
PAGE	polyacrylamide gel electrophoresis
PSI	photosystem 1
PSII	photosystem 2
PVDF	polyvinylidene difluoride membrane
RNAi	RNA interference
Rpm	revolutions per minute
RT-PCR	reverse transcriptase PCR
SSU	ribulose-1,5-bisphosphate carboxylase/oxygenase, small subunit
TEM	transmission electron microscopy
Tic	translocon at the inner envelope of chloroplasts
Toc	translocon at the outer envelope of chloroplasts
w/v	weight per volume
WT	wild type

1 INTRODUCTION

1.1 Preprotein import into chloroplast

Chloroplasts are highly specialized organelles believed to originate from an endosymbiotic event, in which an ancestral photosynthetic cyanobacterium was taken up by a heterotrophic host cell. In order to gain control over the new cellular component, about 95 % of the genetic information was transferred from the chloroplast to the nuclear genome. Therefore proteins encoded by nuclear genes exerting their function in the chloroplast have to be transcribed in the nucleus, translated in the cytosol as preproteins and directed to the chloroplast. The targeting of these proteins to the correct organelle is often sponsored by the presence of a transit sequence at the N-terminus of the newly synthesized protein which is then cleaved after the protein has reached its destination (see Bruce 2000 for review). Once the preprotein approaches the chloroplast surface it interacts with receptors located on the chloroplast membrane and it is transported through the outer and inner envelopes. To be imported across the chloroplast membranes, most of the chloroplast-destined preproteins engage the two multi-protein translocon complexes Toc (translocon at the outer membrane of chloroplast) and Tic (translocon at the inner membrane of chloroplast), also known as “general import pathway” (see Schwenkert et al. 2011 for review). Beside this route, other alternative pathways have been described especially for outer/inner envelope-destined proteins, nevertheless the general import pathway remains the best characterized (Figure 1). The first step of the import is the recognition of the preprotein by the Toc receptors. Toc159 and Toc34 are integral GTPases at the outer membrane both largely exposed at the chloroplast surface and anchored at the outer envelope membrane via their C-termini. These two proteins expose their N-terminal GTP-binding domain to the cytosol and are believed to be responsible for the direct recognition of the preproteins thus acting as receptors. Translocation of the preproteins across the outer envelope of the chloroplast requires energy in the form of GTP, which is hydrolyzed by Toc159 and Toc34 (see Andres et al. 2010 for review). The receptors Toc159 and Toc34 form the Toc core complex together with Toc75,

the translocation channel of the chloroplast outer membrane. Toc75 is a deeply inserted membrane protein and forms a β -barrel-type channel. Toc159, Toc34 and Toc75 have been shown to be sufficient for the translocation *in vitro* of preproteins in lipid vesicles (see Schleiff et al. 2003 for review). Apart from the Toc core complex, further components have been assigned to the Toc complex. Toc64 is a component loosely associated with the Toc core complex and was shown to be not essential for the chloroplast protein import (see Andres et al. 2010 for review). Toc64 is anchored to the outer membrane of the chloroplast exposing its C-terminal domain to the surface. This domain contains three tetratricopeptide motifs (TPR) for protein-protein interaction and it was proposed to be involved in preprotein recognition (Qbadou et al. 2006). A portion of Toc64 also reaches into the intermembrane space interacting with the so-called intermembrane space (IMS) translocation complex. This complex facilitates the translocation of preproteins between the Toc and Tic translocons. Little is known about this complex and so far three components have been identified: Toc12, Tic22 and IMS Hsp70. Toc12 is also described as the fifth components of the Toc complex and it interacts with Toc64 and IMS Hsp70. The role of Toc12 might be to retain IMS Hsp70 close to the Toc complex in order to facilitate the interaction between the chaperone and the preprotein emerging from the Toc75 channel into the intermembrane space. Tic22, the third component of the IMS translocation complex, is loosely bound to the inner envelope membrane and it might function as a linker between the Toc and Tic translocation complexes (see Schwenkert et al. 2011 for review). Once the preprotein has been translocated across the chloroplast outer membrane via the Toc translocon and escorted across the intermembrane space by the IMS complex, it reaches the Tic translocation complex that is responsible for preprotein translocation across the inner envelope membrane. Eight components of the Tic complex have been identified so far (see Kovacs-Bogdan et al. 2010 for review). The only soluble component of the Tic complex is Tic22 which is located in the intermembrane space and as mentioned before is part of the IMS translocation complex. Tic110 is the most abundant component of the Tic translocon and it forms the import pore on the inner envelope membrane. A second component supposed to form a channel is Tic20.

This component might form an alternative import channel for a determined subset of preproteins, nevertheless Tic110 remains the main pore of the Tic translocon. Tic40 is a component anchored to the inner envelope membrane via its N-terminal domain and it exposes its large C-terminal domain to the stromal side. The C-terminal part of this protein comprises domains for protein-protein interaction, allowing the interaction with Tic110 and the stromal chaperone Hsp93. Hsp93 is an ATPase, possesses unfolding capacity dependent of ATP hydrolysis and it is supposed to be the motor chaperone of the Tic translocon. Hsp93 together with Tic40 are believed to form the “motor complex” providing the driving force for the import. The last three components of the Tic translocon are Tic64, Tic55 and Tic32. These three proteins are responsible for the redox regulation of the import process and therefore constitute the so-called redox-regulon of the Tic complex. Tic64 and Tic32 are extrinsic membrane proteins and their association with Tic110 is dependent on the metabolic redox state in the stroma whereas Tic55 is anchored to the inner envelope membrane via its C-terminal domain. The ability of Tic64, Tic32 and Tic55 to regulate the import process according to the redox state of the stroma is provided by the presence of particular domains: NADP(H)-binding site for Tic64 and Tic32 and a Rieske-type iron-sulphur centre for Tic55 (see Balsera et al. 2010 for review). The import of chloroplast precursor proteins across the outer and inner membrane of the chloroplast ends with the release of the preprotein in the stroma where the transit peptide is cleaved off by a metallo-peptidase called stroma processing peptidase (SPP) (see Paetzel et al. 2002 for review) and the mature proteins are finally folded and assembled.

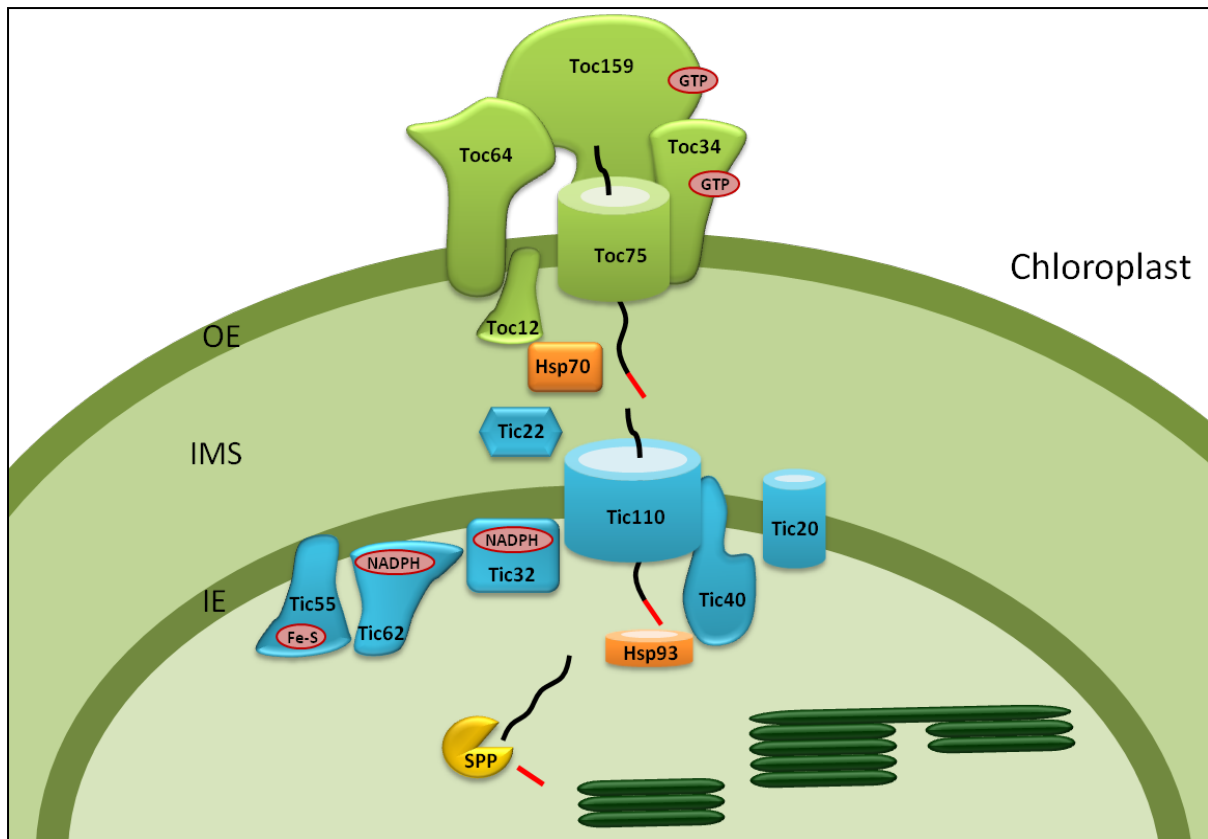


Figure 1. Model of the preprotein import into the chloroplast. Nuclear encoded chloroplast proteins are translocated across the outer (OE) and inner envelope (IE) of the chloroplast via the Toc and Tic translocons. After translocation, the transit peptide is cleaved and the mature protein can fulfill its function in the stroma.

1.2 Targeting to the chloroplast

The import of chloroplast precursor proteins via the general import pathway was extensively studied and it is now a well characterized process. The cytosolic targeting of the preproteins to the chloroplast, which is an important step preceding the import process, is so far not well understood. In the past decade several pivotal cytosolic players involved in protein targeting to the chloroplast have been identified (Figure 2). Most chloroplast precursor proteins display the feature to bind the heat shock chaperone protein Hsp70, a 70 kDa protein that assists a wide range of protein folding processes in an ATP-dependent manner (see Mayer and Bukau 2005 for review). Although binding of Hsp70 has been observed both in the transit peptide (Ivey et al. 2000) and in the mature part (May and Soll 2000) of chloroplast preproteins, the presence of Hsp70 binding site in about 80% of the chloroplast transit peptides denotes a preference for binding in the N-terminal region of precursors (Zhang and Glaser 2002).

Beside Hsp70, two main other cytosolic components have been shown to interact with chloroplast precursor proteins: the chaperone Hsp90 (Qbadou et al. 2006) and a 14-3-3 dimer (May and Soll 2000). Each of these two components seem to bind a subset of chloroplast preproteins (Fellerer et al. 2011), albeit it was not possible to link the preprotein function/properties and the interaction with a particular cytosolic component. The binding of chloroplast precursor proteins with Hsp90, a well-described chaperone in both prokaryotes and eukaryotes, might prevent preproteins aggregation in the cytosol. Most importantly Hsp90 escorts the precursor proteins to Toc64 at the outer membrane of the chloroplast, facilitating the docking of the preproteins to the cytosolic-exposed TPR domain of Toc64 (Qbadou et al. 2006). Alternatively to Hsp90, many precursor proteins interact with 14-3-3. 14-3-3 proteins are eukaryotic, small (~ 30 kDa) acidic proteins, which readily dimerize and interact with a large number of different substrates involved in various cellular processes in plants and animals (Bridges and Moorhead 2005; Dougherty and Morrison 2004). Together with Hsp70, 14-3-3 proteins bind to chloroplast preproteins, most likely very soon after their translation, forming the so-called “guidance complex” which possibly prevents aggregation and enhances the import rate of the preproteins (May and Soll 2000). The affinity of 14-3-3 for its substrates can be dynamically regulated via phosphorylation/dephosphorylation of the 14-3-3 binding motifs present on the substrate. Phosphorylation normally corresponds to an increment in the affinity for the substrates. Beside the diversity in the amino acids compositions and secondary structures, all chloroplast transit peptides present an overall positive charge and the predominance of serine and threonine residues which have been recently shown to often lie within 14-3-3 binding motifs and to be subjected to reversible phosphorylation (May and Soll 2000; Waegemann and Soll 1996). Although lack of phosphorylation does not prevent protein import or lead to mistargeting (Nakrieko et al. 2004), it elevates transport rates mediated by a higher affinity to the receptor protein Toc34 (Schleiff et al. 2002). Additionally, dephosphorylation of chloroplast preproteins has likewise been shown to influence protein import, since it is indispensable for efficient transport of preproteins (Waegemann and Soll 1996). However, it is so far unclear at what stages of

plant development or under which environmental conditions transit peptide phosphorylation is physiologically relevant in chloroplast biogenesis. In *Arabidopsis thaliana* the responsibility for the transit peptides phosphorylation was recently attributed to three highly homologous protein kinases: STY8, STY17 and STY46 (Martin et al. 2006).

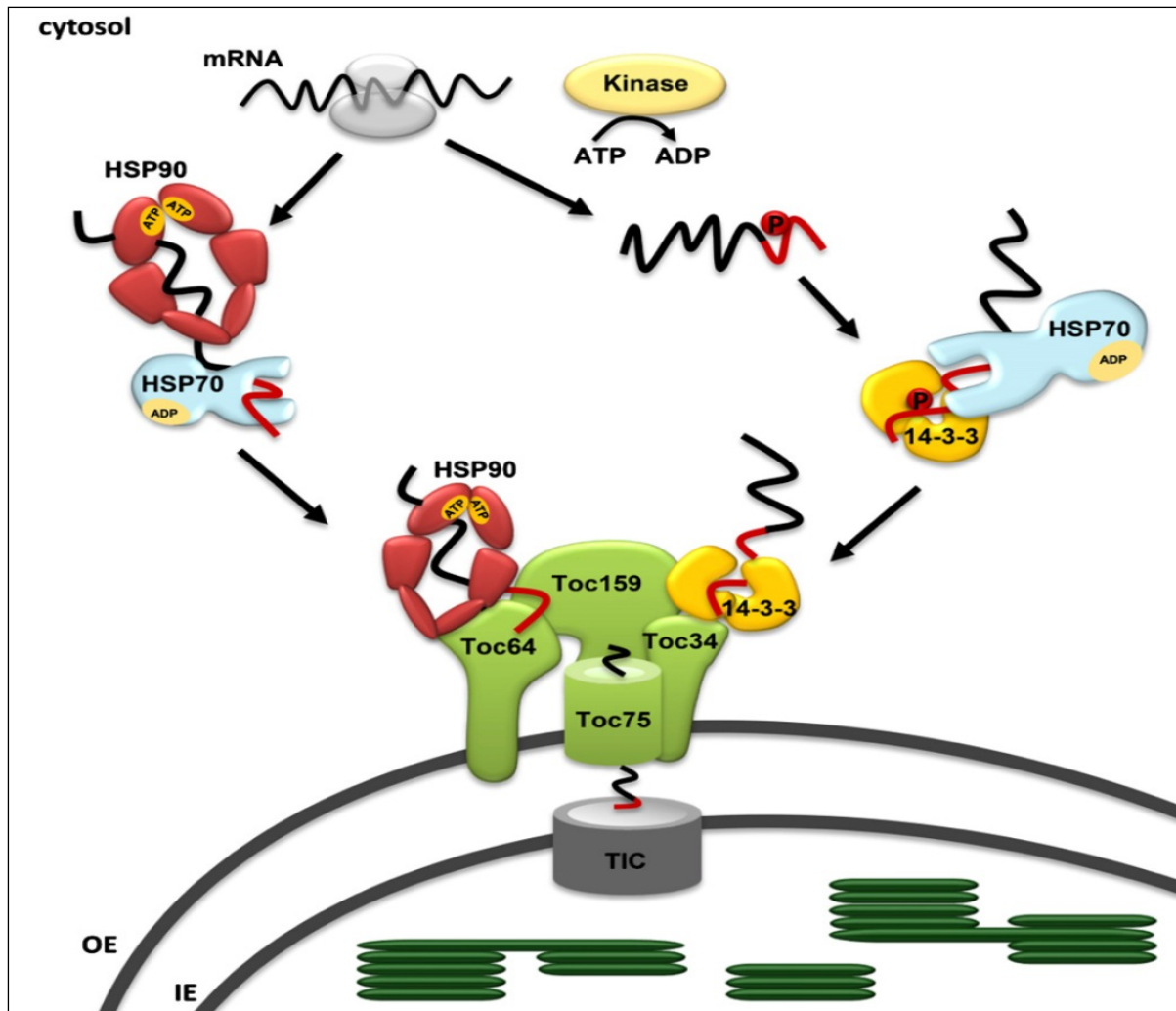


Figure 2. Cytosolic components of the import pathway. Precursors, which are synthesized in the cytosol are recognized by Hsp70, Hsp90 or 14-3-3 proteins, respectively. 14-3-3 binding precursors are initially phosphorylated by a specific kinase and further guided to Toc34. In contrast Hsp90-bound precursors use Toc64 as a first docking station, from where they are passed on to Toc34 and Toc75 (Schwenkert et al. 2011).

1.3 Plant protein kinases

Protein kinases are enzymes designed to phosphorylate proteins or other enzymes. The phosphorylation reaction catalyzed by the kinases consists in general in the transfer of the γ phosphate from an ATP molecule to a serine, threonine or tyrosine hydroxyl group on the

protein substrate. Protein phosphorylation occurs in response to external stimuli, like extracellular messenger molecules and environmental signals, and endogenous stimuli. Substrate phosphorylation in response to a stimulus leads to the on/off switch of the target protein function or to the amplification of the initial signal (see Hunter 1987 for review). Protein phosphorylation is one of the most important regulatory mechanisms in eukaryotic cells and about 2% of the genomes of completely sequenced eukaryotic species consist of protein kinase encoding genes. The percentage of protein kinase encoding genes rises to 3.2 when only the *Arabidopsis thaliana* genome is considered (see Krupa et al. 2006 for review), suggesting that protein phosphorylation is a prominent regulatory process also in plants. Plant protein kinases share characteristics with animal and fungal kinases, however some differences have been observed. These divergences are easily explainable by the fact that plants evolved independently from fungi and animals.

1.4 Plant dual-specificity protein kinases

Traditionally, protein kinases have been divided into two distinct families: the serine/threonine kinases and the tyrosine kinases (Hanks et al. 1988). It has been broadly demonstrated that serine/threonine phosphorylation plays a key role in the regulation of many cellular processes, both in animals and plants. The role of tyrosine phosphorylation has been minutely characterized in animals, however in plants little is known about it. Initially, the occurrence of tyrosine phosphorylation in plants was underestimated because of the impossibility to identify typical tyrosine kinases. This attitude started to change with the identification of protein tyrosine phosphatases in *Arabidopsis thaliana* and other species (see Luan 2002 for review). Additionally, mass spectrometry-based analyses indicated that tyrosine phosphorylation is as extensive in plants as it is in animals (de la Fuente van Bentem and Hirt 2009). Albeit the presence of specific tyrosine kinases still remains unclear, it has been demonstrated that plants present a particular class of dual-specificity kinases able to phosphorylate both serine/threonine and tyrosine residues. Exponents of this class

have been identified in many types of higher plants such as rice, soybean, tomato, wheat, barley, alfalfa, beech and *Arabidopsis thaliana* (see Rudrabhatla et al. 2006 for review).

1.4.1 The *Arabidopsis thaliana* STY protein kinases

In a BLAST search against the consensus protein tyrosine kinase motif CW(X)₆RPXF, 57 catalogued *Arabidopsis thaliana* protein kinases have been identified (Rudrabhatla et al. 2006). The catalytic domains of all these proteins present the 11 conserved sub-domains characteristic of protein kinases. Beside the consensus protein tyrosine kinase motif CW(X)₆RPXF in the sub-domain XI, the catalytic domain of all the 57 kinases also present the KXXN motif in sub-domain VI indicative of serine/threonine specificity. Therefore, it has been assumed that these proteins belong to the dual-specificity kinase family and have been tentatively named as STY (serine/threonine/tyrosine) protein kinases (Rudrabhatla et al. 2006). The 57 genes encoding for the STY kinases are distributed among all five *Arabidopsis* chromosomes and the corresponding proteins have been predicted to localize to the cytosol. *Arabidopsis* STY protein kinases are highly homologous to each other and beside the protein tyrosine catalytic domain also other functional domains are conserved among these proteins. The predicted structures of STY kinases resembles the typical structure of protein kinase catalytic domain, consisting in a small and a large lobes, which are involved in ATP binding and orientation and substrate recognition and catalysis, respectively. The microarray data available suggest that the expression of the different STY kinases is spread through tissues and developmental stages and that these kinases may be involved in different plant cellular processes (Rudrabhatla et al. 2006). The 57 *Arabidopsis* STY kinases can be clustered into four groups including members of many different protein kinase classes. Group I is further divided into four families: the ANT-like kinases, the peanut STY-related kinases, the soybean GmPK6-like kinases and the ATMRK-like kinases. Group II mainly consists of MAP3K/CTR1/EDR1 protein kinases and is further divided in three families: the PB1 domain/GmPK6/EDR1/MAPK3 like kinases, the PAS domain/MAP3K/CTR1/EDR1-like kinases and the MAP3K/CTR1/EDR1-like kinases. Group III consists of protein kinases

containing ankyrin domain repeat motifs and group IV includes light sensory kinases related to *Ceratodon purpureus* phytochrome kinases (Rudrabhatla et al. 2006). Interestingly, the kinases of group I, precisely the ANT-like kinases, the peanut STY-related kinases and the soybean GmPK6-like kinases, have tyrosine consensus sequence RWMAPE in the subdomain VIII in addition to the one in subdomain XI, suggesting that these kinases are evolutionarily more closer to the protein tyrosine kinase family. Furthermore, studies on the activity of the peanut STY-related kinase STY13 indicated that this kinase is actually able to phosphorylate tyrosine beside serine/threonine residues (Reddy and Rajasekharan 2007; Rudrabhatla et al. 2006). Other three members of the peanut STY-related kinase family are particularly interesting: STY8, STY17 and STY46.

The discovery of transit peptide phosphorylation of chloroplast destined precursor proteins (Waegemann and Soll 1996) opened the possibility that the regulation of protein import begins already in the cytosol. To further characterize transit peptide phosphorylation the identification of the responsible kinase became essential. In a first delineation it was proposed that the kinase might localize in the cytosol and that it phosphorylates serine and threonine residues on the consensus motif $(P/G)X_n(R/K)X_n(S/T)X_n(S^*/T^*)$ where $n=0-3$ amino acids spacer and S^*/T^* represents the phosphate acceptor (Waegemann and Soll 1996). Recently, a kinase able to *in vitro* phosphorylate chloroplast transit peptides was isolated from an *Arabidopsis* leaves extract (Martin et al. 2006). This kinase belongs to the *Arabidopsis* dual-specificity kinase family and was previously named STY8 (Rudrabhatla et al. 2006). The two closely related kinases STY17 and STY46 are likewise able to phosphorylate chloroplast transit peptides *in vitro* (Martin et al. 2006).

1.5 Aim of this work

This work aimed at a detailed characterization of the STY8, STY17 and STY46 protein kinases. The first goal of this work is the elucidation of the *in vitro* characteristics of the kinases. The properties of the kinases will be first analysed biochemically *in vitro* with particular attention at the kinases regulation. The autophosphorylation activity of the kinases

will be studied, conserved autophosphorylation site(s) and the autophosphorylation mechanism will be analysed. The kinase specificity for substrates and for the autophosphorylation will also be analysed.

The second aim of this work is the elucidation of the importance of the kinases activity *in vivo*. For this purpose, several *Arabidopsis thaliana* mutant lines will be phenotypically and biochemically characterized. Lastly, the phosphorylation/dephosphorylation state of transit peptides will be analysed in regard of its role in the regulation of the import process.

2 MATERIALS

2.1 Chemicals

All used chemicals were purchased in high purity from Sigma-Aldrich (Steinheim, Germany), Fluka (Buchs, CH), Roth (Karlsruhe, Germany), Roche (Penzberg, Germany), Merck (Darmstadt, Germany), AppliChem (Darmstadt, Germany) or Serva (Heidelberg, Germany). Radiolabeled amino acids ([³⁵S]Met) were obtained from Perkin Elme (Dreieich, Germany).

2.2 Molecular weight markers and DNA standards

*Eco*RI and *Hind*III digested λ-Phage DNA (MBI Fermentas) was used as a molecular size marker for agarose-gel electrophoresis. For SDS-PAGE the “MW-SDS-70L” marker from Sigma-Aldrich (Steinheim, Germany) was used.

2.3 Antibodies

Antibody	Clonality	Species	Immunoblot	Source
anti-Sty8	polyclonal	rabbit	1:500	laboratory of Prof. J. Soll
anti-Sty17	polyclonal	rabbit	1:500	laboratory of Prof. J. Soll
anti-Hcf136	polyclonal	rabbit	1:1000	kindly provided by P. Westhoff
anti-PAC	polyclonal	rabbit	1:1000	kindly provided by J. Meurer
anti-Hcf101	polyclonal	rabbit	1:500	kindly provided by J. Meurer
anti-CF0-II	polyclonal	rabbit	1:1000	kindly provided by S. Greiner
anti-CF1-γ	polyclonal	rabbit	1:1000	kindly provided by S. Greiner
anti-CF1-α/β	polyclonal	rabbit	1:1000	kindly provided by S. Greiner
anti-Lhcb2	polyclonal	rabbit	1:1000	Agrisera
anti-Lhca1	polyclonal	rabbit	1:1000	Agrisera
anti-psaG	polyclonal	rabbit	1:1000	kindly provided by J. Meurer
anti-psaD1	polyclonal	rabbit	1:1000	kindly provided by J. Meurer
anti-pSSU	polyclonal	rabbit	1:1000	laboratory of Prof. J. Soll
anti-E2YI	polyclonal	rabbit	1:1000	laboratory of Prof. J. Soll
anti-pOE23	polyclonal	rabbit	1:1000	kindly provided by S. Greiner
anti-Phospho-Threonine	monoclonal	mouse	1:1000	Cell Signaling Thecnology
anti-Phospho-Tyrosine	monoclonal	mouse	1:2000	Cell Signaling Thecnology
anti-GFP	monoclonal	mouse	1:1000	Roche
anti-rabbit	peroxidase coupled	goat	1:10000	Sigma
anti-mouse	peroxidase coupled	goat	1:10000	Sigma

2.4 Oligonucleotides

Name	Sequence	Purpose
STY8NheI for	cgatgctagcagcatcaagatgagtcgga	cloning in pET21d
STY8NotI rev	cgatgcgccgccactacgacgtttacctc	cloning in pET21d
STY17NheI for	cgatgctagcgcgatcaagaggagacg	cloning in pET21d
STY17NotI rev	cgatgcgccgcacgatggccttttttaggcc	cloning in pET21d
STY46NheI for	cgatgctagcgtgatggaggacaacgagagt tgcgctagtagagtattttcg	cloning in pET21d
STY46NotI rev	cgatgcgccgcgatgatgtgtggtgcttct	cloning in pET21d
STY8 Δ ACT BamHI for	cgatggatccaagcttaaggatcaacctgg	cloning in pET21d (deletion of ACT domain)
STY8 Δ ACT BamHI rev	gcatggatcccggctcgtgtagacaatgttc	cloning in pET21d (deletion of ACT domain)
STY8mut439 rev	catgaccctgattcaatctgcactctggcaac	site directed mutagenesis
STY8T439A for	cagattgaatcaggggtcatggctgctgaaac tg	site directed mutagenesis
STY8T439D for	cagattgaatcaggggtcatggatgctgaaac tg	site directed mutagenesis
STY8T439E for	cagattgaatcaggggtcatggaggctgaaa ct g	site directed mutagenesis
STY8T439S for	cagattgaatcaggggtcatgatggctgaaac tggg	site directed mutagenesis
STY8T439Y for	cagattgaatcaggggtcatgtatgctgaaact ggg	site directed mutagenesis
STY17T445A for	cagactgagtcaggggttatggctgcggaaa cag	site directed mutagenesis
STY17mut445 rev	cataaccctgactcagtctgcactctggcaac	site directed mutagenesis
STY17T445D for	cagactgagtcaggggttatggatgcggaaa cag	site directed mutagenesis
STY46T443A for	gcacaaactggagttatggctgctgaaactg	site directed mutagenesis
STY46mut443 rev	cataactccagttgtgctttcactctagc	site directed mutagenesis
STY46T443D for	gcacaaactggagttatggatgctgaaactg	site directed mutagenesis
STY8mut409 rev	aaggtccctgtgaataatgtgtttgatgc	site directed mutagenesis
STY8K409R for	caacattattcacagggaccttaggactgcga atc	site directed mutagenesis
STY17RNAi for	caccgagagttgcggaagcagagc	cloning in pB7GWIWG2(I)
STY17RNAi rev	gaggtgcaagagacctcgag	cloning in pB7GWIWG2(I)
STY46AttB for	ggggacaagttgtacaaaaagcaggctat ggctagcgtgatggaggac	cloning in pH2GW7
STY46AttB rev	ggggaccactttgtacaagaaagctgggtcct aatgatgtgtggtgcttct	cloning in pH2GW7
STY8 5'UTR for	ctgagatcattcgtctttgtac	screening of T-DNA knockout
STY8Ex4 rev	accaaaaagttggaggagcaagaa	screening of T-DNA knockout

STY46Ex7 for	gcatgttccaataccaatg	screening of T-DNA knockout
STY46Ex10 rev	cccttttgcttgtagatag	screening of T-DNA knockout
LBa1	tggttcacgtagtgggccatcg	screening of T-DNA knockout
STY8QRT-PCR for	aggcattgagcacaac	quantitative RT-PCR
STY8QRT-PCR rev	cttgctagggctctcatc	quantitative RT-PCR
STY17QRT-PCR for	ctacgcgattgtgctg	quantitative RT-PCR
STY17QRT-PCR rev	ctatcaaaccgatcaacca	quantitative RT-PCR
STY46QRT-PCR for	tcagctacgggattgtg	quantitative RT-PCR
STY46QRT-PCR rev	agcaacttacaaaggaaatca	quantitative RT-PCR
CF1-γQRT-PCR for	gagagataaggtagagc	quantitative RT-PCR
CF1-γQRT-PCR rev	gactttgggtaagggaac	quantitative RT-PCR
PAC QRT-PCR for	gatagcctaagggattcg	quantitative RT-PCR
PAC QRT-PCR rev	cggcagctctgatgaagc	quantitative RT-PCR
CF0-II QRT-PCR for	gagcatttctcatctctc	quantitative RT-PCR
CF0-II QRT-PCR rev	ggagagtaatagacctg	quantitative RT-PCR
LHCb.2 QRT-PCR for	catgctgctaccgcaag	quantitative RT-PCR
LHCb.2 QRT-PCR rev	tcaagtaggggttccgag	quantitative RT-PCR
Hcf101 QRT-PCR for	ccgcttctcatccacagt	quantitative RT-PCR
Hcf101 QRT-PCR rev	ctggacatgcgggtgttg	quantitative RT-PCR
Hcf136 QRT-PCR for	cgtctctgcaactctgca	quantitative RT-PCR
Hcf136 QRT-PCR rev	ccaagtgtctccaccatc	quantitative RT-PCR
ACTINE QRT-PCR for	ggtgatggtgtgtct	quantitative RT-PCR
ACTINE QRT-PCR rev	actgagcacaatgttac	quantitative RT-PCR
pSSU 6xHis for	ctaggcgatcgccatgcaccaccaccaccac cacgcttctcagttctttcc	insertion of stalling sequence/cloning in pF3A
pSSU stalling rev	ctaggtttaaacaggaggaatatatttgcaggt cagcaggctgctcagtttttgcactcagcacc agcggttccatgtagccttctggctttag	insertion of stalling sequence/cloning in pF3A
pSSU flexi for	ctaggcgatcgccatggcttctcagttctttcc	cloning in pF3A
pSSU flexi 6xHis rev	ctaggcgatcgccatgcaccaccaccaccac cacgcttctcagttctttcc	cloning in pF3A
pSSU S31/34A for	gcaccttactggccttaaggcagctgccgca ttccctg	site directed mutagenesis
pSSU S31/34A rev	cttaaggcagtgaaagggtgcaaccatgtagc	site directed mutagenesis
pSSU S31/34D rev	cttaaggatgtgaaagggtgcaaccatgtagc	site directed mutagenesis
STY8 TOPO for	cgatcacatggctagcacgaccaaagatga gtcggagag	cloning in pENTR-D-TOPO
STY8 TOPO rev	tcacactacgacgtttacctctttc	cloning in pENTR-D-TOPO
STY17 TOPO for	caccatggctagcgcgatcaaagagg	cloning in pENTR-D-TOPO
STY17 TOPO rev	acgatggccttttttaggcc	cloning in pENTR-D-TOPO
STY46 TOPO for	caccatggctagcgtgatggaggac	cloning in pENTR-D-TOPO
STY46 TOPO rev	atgatgtgtggtgcttctcc	cloning in pENTR-D-TOPO
mSSU-XhoI-rev	cgatgcccgcgtagccttctggctttagg	cloning in pET21d

LHCb2 NheI for	agtcgctagcgcaacatcagctatcc	cloning in pET21d
tpLHCb2-rev	cacacctgcatggatacaccaaccttgccg	generation of chimeric construct
CF0-II NheI for	agtcgctagcgctgctaattcgataatg	cloning in pET21d
tpCF0-II rev	cacacctgcatctccgccatcgacgg	generation of chimeric construct
PAC NheI for	agtcgctagcgcgggcagctgctg	cloning in pET21d
PAC NotI rev	gactgcgccgccactcaagttgagg	cloning in pET21d
Hcf101 NheI for	agtcgctagcccgttcttcatccacag	cloning in pET21d
Hcf101 NotI rev	gactgcgccgccgacttcgactggagacaatg	cloning in pET21d
tpHcf101 rev	cacacctgcattgaagcagcttagctacag	generation of chimeric construct
pSSU TOPO for	caccatggcttctctagttcttcc	cloning in pENTR-D-TOPO
pSSU TOPO rev	gtagccttctggctttaggc	cloning in pENTR-D-TOPO
pSSU Ara T4A 1st for	ggacttaagtctccgctgccgccgagccgcgcca	site directed mutagenesis
pSSU Ara T4A 1st rev	ggcagcggaggacttaagtcggtgaaagg	site directed mutagenesis
pSSU Ara T4A 2nd rev	ggcggcggctgcgccggcagcggaggacttaagtcg	site directed mutagenesis
pSSU Ara T4A 2nd for	cctccgctgccgccgagccgccgccgcccgcg	site directed mutagenesis
pSSU Ara TOPO for	caccatggcttctctatgctc	cloning in pENTR-D-TOPO
pSSU Ara TOPO rev	accggtgaagcttg	cloning in pENTR-D-TOPO
pOE23 TOPO for	caccatggcatctacacaatg	cloning in pENTR-D-TOPO
pOE23 TOPO rev	ggcaacactgaaagaactg	cloning in pENTR-D-TOPO
pOE23 S22A for	ccaactagaaccttagctcaacgccaagtag	site directed mutagenesis
pOE23 S22A rev	taaggttctagttggagttgtaatagc	site directed mutagenesis
LHCb1.3-TOPO rev	cttccgggaacaaagttggtg	cloning in pENTR-D-TOPO
LHC-mSSU fusion rev	ttggtggccacacctgcatcgcggggaaagctg	generation of chimeric construct
mLHC-for	gcatctgaagtccttgaagcggccgtgtgacaatg	generation of chimeric construct

2.5 Plasmids

Gene	Organism	Vector	Description	Source	Purpose
Sty8	<i>Arabidopsis</i>	pET21d	C-terminal His-tag	this work	expression in <i>E.coli</i>
Sty8	<i>Arabidopsis</i>	pET21d	T439A C-terminal His-tag	this work	expression in <i>E.coli</i>
Sty8	<i>Arabidopsis</i>	pET21d	T439D C-terminal His-tag	this work	expression in <i>E.coli</i>

Sty8	<i>Arabidopsis</i>	pET21d	T439E C-terminal His-tag	this work	expression in <i>E.coli</i>
Sty8	<i>Arabidopsis</i>	pET21d	T439S C-terminal His-tag	this work	expression in <i>E.coli</i>
Sty8	<i>Arabidopsis</i>	pET21d	T439Y C-terminal His-tag	this work	expression in <i>E.coli</i>
Sty8	<i>Arabidopsis</i>	pET21d	K409R C-terminal His-tag	this work	expression in <i>E.coli</i>
Sty17	<i>Arabidopsis</i>	pET21d	C-terminal His-tag	this work	expression in <i>E.coli</i>
Sty17	<i>Arabidopsis</i>	pET21d	T445A C-terminal His-tag	this work	expression in <i>E.coli</i>
Sty17	<i>Arabidopsis</i>	pET21d	T445D C-terminal His-tag	this work	expression in <i>E.coli</i>
Sty46	<i>Arabidopsis</i>	pET21d	C-terminal His-tag	this work	expression in <i>E.coli</i>
Sty46	<i>Arabidopsis</i>	pET21d	T443A C-terminal His-tag	this work	expression in <i>E.coli</i>
Sty46	<i>Arabidopsis</i>	pET21d	T443D C-terminal His-tag	this work	expression in <i>E.coli</i>
Sty8- Δ ACT	<i>Arabidopsis</i>	pET21d	deletion of AA 172-239 C-terminal His-tag	this work	expression in <i>E.coli</i>
Sty17	<i>Arabidopsis</i>	pB7GWIWG2(l)	bp 25-424	this work	generation of RNAi lines in plant
Sty46	<i>Arabidopsis</i>	pH2GW7	full lenght	this work	stable expression in plant
Sty8	<i>Arabidopsis</i>	p2GWF7	C-terminal GFP	this work	transient expression in plant
Sty17	<i>Arabidopsis</i>	p2GWF7	C-terminal GFP	this work	transient expression in plant
Sty46	<i>Arabidopsis</i>	p2GWF7	C-terminal GFP	this work	transient expression in plant

pSSU	<i>Tobacco</i>	pET21d	C-terminal His-tag	laboratory of Prof. Jürgen Soll	expression in <i>E.coli</i>
pOE23	<i>Pea</i>	pET21d	C-terminal His-tag	laboratory of Prof. Jürgen Soll	expression in <i>E.coli</i>
pSSU	<i>Tobacco</i>	pF3A	C-terminal His-tag	this work	<i>In vitro</i> translation
pSSU	<i>Tobacco</i>	pF3A	stalling sequence/ C-terminal His-tag	this work	ribosomes stalling/ <i>in vitro</i> translation
mSSU	<i>Tobacco</i>	pET21d	C-terminal His-tag	this work	expression in <i>E.coli</i>
pLHCb2.2-mSSU	<i>Arabidopsis/ Tobacco</i>	pET21d	pLHCb2.2 AA 1-90 C-terminal His-tag	this work	expression in <i>E.coli</i>
pCF0-II-mSSU	<i>Arabidopsis/ Tobacco</i>	pET21d	pCF0-II AA 1-74 C-terminal His-tag	this work	expression in <i>E.coli</i>
pPAC	<i>Arabidopsis</i>	pET21d	C-terminal His-tag	this work	expression in <i>E.coli</i>
pHcf101	<i>Arabidopsis</i>	pET21d	C-terminal His-tag	this work	expression in <i>E.coli</i>
pHcf101-mSSU	<i>Arabidopsis</i>	pET21d	pHcf101 AA 1-64 C-terminal His-tag	this work	expression in <i>E.coli</i>
pSSU	<i>Tobacco</i>	p2GWF7	C-terminal GFP	this work	transient expression in plant
pSSU	<i>Tobacco</i>	p2GWF7	S31/34A C-terminal His-tag	this work	transient expression in plant
pSSU	<i>Tobacco</i>	p2GWF7	S31/34D C-terminal His-tag	this work	transient expression in plant
pSSU	<i>Arabidopsis</i>	p2GWF7	AA 33-41A C-terminal His-tag	this work	transient expression in plant
pOE23	<i>Pea</i>	p2GWF7	C-terminal GFP	this work	transient expression in plant

pOE23	<i>Pea</i>	p2GWF7	S22A C-terminal GFP	this work	transient expression in plant
pSSU	<i>Tobacco</i>	pAMpAT	C-terminal His-tag	this work	transient expression in plant
pSSU	<i>Tobacco</i>	pAMpAT	S31/34A C-terminal YFP	this work	transient expression in plant
pSSU	<i>Arabidopsis</i>	pAMpAT	AA 33-41A C-terminal YFP	this work	transient expression in plant
tpSSU- mLHCb1.3	<i>Tobacco/ Arabidopsis</i>	p2GWF7	C-terminal GFP	this work	transient expression in plant
tpSSU- mLHCb1.3	<i>Tobacco/ Arabidopsis</i>	p2GWF7	C-terminal GFP tpSSU S31/34A	this work	transient expression in plant
tpSSU- mLHCb1.3	<i>Tobacco/ Arabidopsis</i>	pK7FWG2	C-terminal GFP	this work	transient expression in plant
tpSSU- mLHCb1.3	<i>Tobacco/ Arabidopsis</i>	pK7FWG2	C-terminal GFP tpSSU S31/34A	this work	transient expression in plant
pSSU	<i>Tobacco</i>	p2GWF7	AA 1-47	this work	transient expression in plant

2.6 Kits

All the kits were utilized according to the manufacturer instructions.

Kit	Purpose	Source
QIAprep Spin Miniprep Kit	Plasmid DNA isolation	QUIAGEN
QIAGEN Plasmid Midi Kit	Plasmid DNA isolation	QUIAGEN
QIAGEN Plasmid Maxi Kit	Plasmid DNA isolation	QUIAGEN
NucleoSpin Extract II	Purification of DNA	Macherey-Nagel
Rneasy Plant Mini Kit	RNA extraction from plant	QUIAGEN
FastStart DNA Master SYBR-Green Plus kit	Quantitative RT-PCR	Roche
pENTR-D-TOPO Cloning kit	cloning with gateway system	Invitrogen
LR clonase II Enzyme Mix	in vitro recombination	Invitrogen
BP clonase II Enzyme Mix	in vitro recombination	Invitrogen
Wheat germ lysate translation kit	in vitro translation	Promega
Reticulocyte lysate translation kit	in vitro translation	Promega

2.7 Enzymes

The enzymes were utilized according to the manufacturer instructions.

Enzyme	Source
Restriction Endonucleases	Fermentas
T4 DNA ligase	Fermentas
Taq DNA polymerase	5 PRIME
Phusion DNA polymerase	New England Bio Labs
SP6 RNA polymerase	Fermentas
MMLV Reverse Transcriptase	Promega
RNase-free DNase I	Amersham Biosciences
Lambda phopshatase	Sigma
Cellulase Onozuka R10	Serva
Macerozym R10	Yakult Honsha

2.8 Chromatography media

Beads	Purpose	Source
Ni-sepharose fast flow	His-tag purification	GE Healthcare
TALON magnetic beads	Immunoprecipitation	Clontech

2.9 Bacterial strains

Strain	Organism	Genotype
TOP10	<i>E.coli</i>	F ⁻ mcrA Δ(mrr-hsdRMS-mcrBC) φ80lacZΔM15 ΔlacX74 nupG recA1 araD139 Δ(ara-leu)7697 galE15 galK16 rpsL(Str ^R) endA1 λ ⁻
BL21(DE3)pLysS	<i>E.coli</i>	F ⁻ ompT gal dcm lon hsdS _B (r _B ⁻ m _B ⁻) λ(DE3) pLysS(cm ^R)
RIPL (BL21-CodonPlus(DE3)-RIPL strain)	<i>E.coli</i>	<i>E. coli</i> B F ⁻ ompT hsdS(rB ⁻ mB ⁻) dcm ⁺ Tetr gal λ(DE3) endA Hte [argU proL Camr] [argU ileY leuW Strep/Specr]
AGL-1 (Lazo et al. 1991)	<i>Agrobacterium tumefaciens</i>	AGL0 recA::bla pTiBo542ΔT Mop ⁺ Cb ^R
GV3101(pMP90RK)(Koncz and Schell, 1986)	<i>Agrobacterium tumefaciens</i>	C58C1 pMK90RK, Rif ^r , Gmr, Kmr

3 METHODS

Standard methods were performed as described by Sambrook and Russel, 2001.

3.1 DNA cloning

During this work several genes were cloned in the expression vector pET21d+. For the PCR amplification the appropriate pairs of primers were used in order to amplify the desired fragments from a template DNA or from cDNA obtained from *Arabidopsis thaliana* (see 3.18). Different protocols for PCR reactions were utilized according to the size of the amplification product. In order to obtain compatible sticky ends, the amplified DNA and the destination vector were digested with the appropriate restriction endonucleases. After digestion, the DNA was loaded on an agarose gel and purified using the NucleoSpin Extract II (Macherey-Nagel). The ligation reaction between vector and insert was performed using the enzyme T4 DNA ligase (Fermentas) for 1 h at 23°C. The ligation product was transformed in 50 µl of chemical competent *E.coli* TOP10 cells and plated on LB plates with the appropriate antibiotic. Single colonies were inoculated in liquid culture, let grown over night and the plasmid DNA was purified using the QIAprep Spin Miniprep Kit (QUIAGEN). The DNA insert was fully sequenced.

To introduce single point mutations site directed mutagenesis was performed. The whole plasmids were amplified by PCR using the proper pairs of primers carrying the mutation and the protocols for PCR reactions were modified according to the size of the amplification product.

Chimeric constructs were generated by overlap PCR, using appropriate oligonucleotides fusing the desired gene fragments.

Homologous recombination was used for cloning of DNA-fragments / constructs into vectors of the GATEWAY-system (Invitrogen, Karlsruhe, Germany) according to the manufacturer's recommendations. Thereby, *attB*-sequences or CACC- sequence were added by PCR primers.

3.2 *E. coli* growth conditions

E.coli was cultivated in LB medium at 37°C in either liquid culture or on agar-plates supplemented with the appropriate antibiotics according to the resistance (Ampicillin 100 µg/ml, Kanamycin 50 µg/ml and Spectinomycin 50 µg/ml).

3.3 *Agrobacterium tumefaciens* growth conditions

Agrobacterium tumefaciens was cultivated in YEP medium at 28°C in either liquid culture or on agar-plates supplemented with the appropriate antibiotics according to the resistance (Carbenicillin 100 µg/ml, Kanamycin 25 µg/ml, Spectinomycin 100 µg/ml, 40 µg/ml Gentamicin and 100 µg/ml Rifampicin).

3.4 Plant growth conditions

Arabidopsis thaliana WT Columbia ecotype (Col-0) and the respective mutants were grown either on soil or on half-strength MS (Murashige and Skoog) medium supplied with 1% sucrose under controlled conditions in a growth chamber. For phenotyping analysis plants were grown on soil in long day condition (16h/8h light/dark, 22°C, 120 µE m⁻¹ s⁻²). For greening experiments dry seeds were surface-sterilized and vernalized at 4°C for 2 days. Petri dishes were exposed to light (120 µE m⁻¹ s⁻²) for 6 h and were then placed in the dark. After 6 days in the dark, Petri dishes were exposed to light for the indicated period of time. Seedlings for TEM recordings were either grown on half-strength MS (Murashige and Skoog) medium without sucrose (7 days) or on soil (14 days) in long day conditions and were harvested in darkness at the end of night.

3.5 Expression and purification of recombinant proteins

All recombinant proteins used in this work were expressed in *E.coli* BL21(pLysS) or RIPL cells. Cells were grown at 37°C in LB medium to OD₆₀₀=0.6 and 1 mM isopropyl-1-thio-β-D-galactopyranoside was added in order to induce protein expression for 16 h at 18°C. Cells were lysed in lysis buffer (200 mM NaCl, 20 mM Tris/HCl pH 7.5, 20 mM imidazol), centrifuged for 30 min at 18000 rpm and the supernatant was incubated with 350 µl Ni-

sepharose fast flow (GE Healthcare) for 1 h at 4°C. The Sepharose was washed twice with washing buffer (200 mM NaCl, 20 mM Tris/HCl pH 7.5, 40 mM imidazol) and recombinant proteins were eluted by increasing the imidazol concentration up to 200 mM.

For protein purification in inclusion bodies, cells were grown at 37°C in LB medium to $OD_{600}=0.6$ and 1 mM isopropyl-1-thio- β -D-galactopyranoside was added in order to induce protein expression for 16 h at 37°C. Cells were lysed in lysis buffer (100 mM TrisH/Cl pH 8.0, 200 mM NaCl, 5 mM Mercaptoethanol) and centrifuged for 30 min at 18000. The resulting pellet was resuspended in detergent buffer (20 mM Tris/HCl pH 7.5, 1% Desoxycholic acid, 1% Nonidet P40, 200 mM NaCl, 10 mM Mercaptoethanol) and centrifuged for 10 minutes at 10000 rpm. The pellet obtained was washed twice with Triton buffer (20 mM Tris/HCl pH 7.5, 0.5% Triton X-100, 5 mM Mercaptoethanol) and 2 times in Tris buffer (50 mM Tris/HCl pH 8.0, 10 mM DTT). The inclusion bodies were finally resuspended in buffer A (8 M UREA, 50 mM NaPi-buffer pH 8.0, 300 mM NaCl, 2 mM Mercaptoethanol), frozen in liquid nitrogen and stored at -80°C.

3.6 Size exclusion chromatography

Recombinant STY8 (35 μ g) and *Arabidopsis* lysates (1.3 mg) were separated by size exclusion chromatography. Samples were loaded on a Superdex 200 column, the flowrate was 0.3 ml/min and 500 μ l fractions were collected by elution in Tris buffer (50 mM Tris/HCl pH 7.5, 200 mM NaCl). For determination of the molecular weight, a standard curve was generated using marker proteins (aldolase, ferritin, conalbumin, ovalbumin, thyroglobin; GE Healthcare).

3.7 SDS polyacrylamide gel electrophoresis and Western Blot

Polyacrylamide gels (10, 12 or 15 % separating gels, 5 % stacking gels) were prepared as described by Sambrook and Russel, 2001, and the electrophoretic separation was performed at 25 mA/gel for mini gels and 35mA/gel for big gels. The proteins were electrotransferred from the gel to a PVDF membrane by a semi-dry-blotting in a Trans Blot Cell (BioRad) (Anode buffer I: 300 mM Tris, 20 % methanol. Anode buffer II: 25 mM Tris, 20 % methanol.

Cathode buffer: 40 mM aminocaproic acid, 20 % methanol). The transfer was performed for 1 hour at 44 mA/gel for mini gels and 100 mA/gel for big gels. The membrane was blocked in 5 % milk-TBST for 30 minutes at RT and incubated over night with the appropriate primary antibody (see 2.3) diluted in 5 % milk-TBST. The membrane was washed 3 times for 10 minutes in TBST (1 x TBS 0,1 % Tween), incubated for 1 hour at RT with the appropriate secondary antibody diluted in 5 % milk-TBST and washed again 3 times for 10 minutes in TBST. The membrane was developed with ECL as described (Schwenkert et al. 2006).

3.8 Kinase assay

0.1-2 µg of recombinant STY kinases were incubated with 0.2-2 µg of recombinant substrate in the presence of 3 µCi ³²P-ATP and 2,5 µM ATP in a total volume of 50 µl kinase buffer (20 mM Tris/HCl pH 7.5, 5 mM MgCl₂, 0.5 mM MnCl₂). The reaction was carried out for 10 min at 23°C and stopped by adding 12 µl of SDS sample buffer. Kinase reactions with CPK4 were accomplished in kinase buffer containing 7 mM CaCl₂ and 1 mM DTT instead of MnCl₂ and Yes kinase reactions were performed in 20 mM MOPS pH 7.9 and 5 mM MgCl₂. Purified Yes kinase (Summy et al. 2003) was obtained from Proteinkinase.de (Kassel, Germany). The proteins were separated on 12 % SDS-polyacrylamide gel followed by autoradiography.

For the inhibition studies the STY kinase was preincubated for 10 min with the inhibitors (Kinase screening library, Cayman) at different concentrations. The reaction was then carried out as described before. The reaction product was separated on 12 % SDS-polyacrylamide gel, the coomassie stained protein bands were cut out from the gel and the radioactivity was determined by liquid scintillation counting (1215 LKB RACK BETA II liquid scintillation counter, Scintillation fluid :0.5% PPO and 0.05% POPOP in toluene).

3.9 Phosphoamino acids analysis

³²P-labelled phosphorylated proteins were separated on SDS PAGE and extracted from gels by incubation in 10 mM CHAPS, 20 mM Tris/HCl pH 7.5 for 12 h at 20°C. Proteins were precipitated with trichloroacetic acid and resuspended in 50 µl H₂O. For acid hydrolysis proteins were heated at 110°C for 2 h in 6 M HCl. After hydrolysis, amino acids were

lyophilized and dissolved in distilled water. Thin layer chromatography was performed on cellulose plates (TLC Cellulose Plastic sheets 20x20 cm, Merck) for 4 h at 1000 V in a mixture of acetic acid:formic acid:H₂O of 78:25:897 (vol/vol). ³²P-labelled amino acids were detected by autoradiography. Standards of Ser(P), Thr(P) and Tyr(P) were run in parallel and detected by staining with 0.25 % ninhydrin.

3.10 *In vitro* transcription and translation

Linear plasmid DNA was transcribed using SP6 RNA polymerase (Fermentas). Protein synthesis was performed in the presence of 50 % home-made wheat germ lysate for 45 min at 25°C as described (Fellerer et al. 2011).

3.11 Immunoprecipitation

After *in vitro* translation of His-tagged proteins, samples were centrifuged for 10 min at 20,000 g at 4°C and supernatant was added to 15 µl of TALON magnetic beads (Clontech). After incubation for 1 h at 4°C, beads were washed 2 times with washing buffer (50 mM NaPi pH 7.3, 300 mM NaCl, 1x complete protease inhibitor cocktail (Roche), 1x PhosSTOP phosphatase inhibitor cocktail (Roche)) and proteins were eluted from the beads in 15 µl elution buffer (50 mM NaPi pH 7.3, 300 mM NaCl, 250 mM imidazol, 1x complete protease inhibitor cocktail (Roche), 1x PhosSTOP phosphatase inhibitor cocktail (Roche)).

3.12 Isoelectric focusing

Rehydration buffer (7 M urea, 2 M thiourea, 0.2 % biolytes 3-10 (Bio-Rad), 2 % CHAPS, 100 mM DTT, bromophenol blue, 1x complete protease inhibitor cocktail (Roche), 1x PhosSTOP phosphatase inhibitor cocktail (Roche)) was added to protein samples and incubated for 1 h at 20°C. Samples were centrifuged for 10 min at 20000 g, supernatant was added to IPG strips (ReadyStrip IPG strips, pH range 3-10, Bio-Rad) and incubated 1 h at 20°C. Isoelectric focusing was performed using a Protean IEF Cell (Bio-Rad) at 8000 V. After isoelectricfocusing, the IPG strips were incubated for 20 min in equilibration buffer I (6 M urea, 2 % SDS, 50 mM Tris/HCl pH 8, 20 % glycerol, 2 % DTT) and 10 min in equilibration

buffer II (6 M urea, 2 % SDS, 50 mM Tris/HCl pH 8, 20 % glycerol, 2.5 % iodoacetamide). The second dimension was performed on a 12 % SDS-polyacrylamide gel.

3.13 Isolation of intact chloroplasts from *Pisum sativum* (pea)

Chloroplasts from pea were isolated from leaves of 9-11 days old pea seedlings (*Pisum sativum* var. Arvica) and purified through Percoll density gradients as previously described (Waegemann and Soll 1995).

3.14 Protein import experiment

The translation mixture was centrifuged for 10 min at 19000 rpm at 4°C and the postribosomal supernatant was used for import. After chloroplast isolation the chlorophyll concentration was determined according to Arnon, 1949. A standard import assay into chloroplasts equivalent to 20 µg chlorophyll was performed in 100 µl import buffer (2 mM ATP, 10 mM Met, 10 mM cysteine, 20 mM potassium gluconate, 10 mM NaHCO₃, 3 mM MgSO₄, 330 mM sorbitol, 50 mM Hepes/KOH (pH 7.6), 0.2 % BSA) containing 10 % of *in vitro* translated radiolabeled protein. Import was initiated by addition of organelles to the import mixture and was incubated at 25°C in the dark. The reaction was stopped after 1-10 min in the dark. Intact chloroplasts were reisolated through a Percoll cushion (40 % Percoll in 330 mM sorbitol, 50 mM Hepes/KOH (pH 7.6)), washed once in wash buffer (330 mM sorbitol, 50 mM Hepes/KOH (pH 7.6), 3 mM MgCl₂) and resuspended in loading buffer. Samples were analyzed by SDS-PAGE and autoradiography

3.15 *Arabidopsis thaliana* stable transformation with *Agrobacterium tumefaciens*

Agrobacterium tumefaciens (GV3101) carrying the construct of interest was grown in YEP medium supplemented with the appropriate antibiotics until OD₆₀₀=0.8. Cells were centrifuged 15 min at 3500 rpm and pellet was resuspended in a proper volume of Silvet-medium (5 % sucrose, 0.05 % silvet L-77) in order to reach a final OD₆₀₀=0.8. *Arabidopsis thaliana* plants already showing primary and secondary bolts were transformed by floral dip

(Clough and Bent 1998). Seeds obtained from the transformed plants were selected on MS plates supplemented with the appropriate antibiotic (25 µg/ml Hygromycin or 15 µg/ml BASTA).

3.16 Generation of knockdown mutant plants

T-DNA insertion lines SALK 072890 (*sty8*) and SALK 116340 (*sty46*) were obtained from the SALK collection (<http://signal.salk.edu>) and homozygous lines were isolated by PCR using the oligonucleotides *STY85*'UTR for, *STY8Ex4* rev, *STY46Ex7* for, *STY46Ex10* rev and LBa1 (see 2.4). Homozygous *sty8* and *sty46* lines were crossed and double homozygous lines were isolated in the T2 progeny. For the generation of independent *sty17* RNAi lines a 400 bp fragment of *STY17* was amplified using the oligonucleotides *STY17RNAi* for and *STY17RNAi* rev (see 2.4), cloned into the binary vector pB7GWIWG2(II) (Plant Systems Biology, Gent) with the gateway system (Invitrogen) and WT and homozygous *sty8 sty46* mutants were transformed as described in 3.15. Seeds from the progeny of three independent lines were used for molecular and biochemical analysis. For complementation analysis the full length *STY46* and *STY8* cDNA was cloned into the pH2GW7 vector (Plant Systems Biology, Gent) and WT and homozygous *sty8 sty46* mutants were transformed. Segregating lines from the *sty17* RNAi or complemented T2 progeny were either grown on MS medium supplemented with the appropriate antibiotic or checked by PCR for presence of the respective construct if grown on soil.

3.17 Isolation of genomic DNA from *Arabidopsis thaliana*

A small *Arabidopsis* leaf (approx. 0.5-0.75 cm²) was cut and transferred to a 1.5 ml microtube. 200 µl of extraction buffer (200 mM Tris-HCl (pH 7.5), 250 mM NaCl, 0.5% SDS) was added to the tube and the sample was homogenized using a polytron with a pestle. The homogenate was incubated at room temperature (RT) for 3-5 min and then centrifuged at 13000 x g for 10 min. 150 µl of the supernatant were transferred to a new tube. To precipitate the genomic DNA, 150 µl of isopropanol (-20°C) was added to the tube, carefully

mixed and centrifuged at 13000 x g for 15 min at 4°C. The pellet was subsequently air-dried and finally resuspended in 50 µl of distilled water.

3.18 Quantitative RT-PCR analysis

Plantlets grown on MS medium were ground in liquid nitrogen and total RNA was isolated from several seedlings using the Plant RNeasy extraction kit (Quiagen). cDNA was synthesized from 1 µg RNA (DNase-treated) by reverse transcription (MMLV reverse transcriptase, Promega). For quantitative RT-PCR the FastStar DNA Master SYBR-Green Plus kit was used and the reaction was performed in a LightCycler (Roche) using the appropriate pairs of oligonucleotides. 45 cycles were performed as follow: 1 s at 95°C, 7 s at 49°C, 19 s at 72°C and 5 s at 79°C. The relative abundance of all transcripts amplified was normalized to the expression level of 18S rRNA or actin.

3.19 Chlorophyll extraction

Chlorophyll determination of *Arabidopsis* leaves was performed following the method described by (Porra 1989). 200 mg leaf tissue was harvested and incubated in 2 ml DMF for 2 h in the dark. Absorbance was measured at 663, 750 and 645 nm. Chlorophyll concentration was calculated as described (Arnon 1949).

3.20 Spectroscopic analysis

Chlorophyll *a* fluorescence of WT and mutant leaves was measured using a pulse modulated fluorimeter (PAM 101, Waltz, Effeltrich, Germany) as described (Meurer et al. 1996)

3.21 Electron microscopy

Distal pieces (approximately 1 mm² segments) of cotyledons were prefixed in 2.5 % (w/v) glutaraldehyde in 75 mM cacodylate buffer (pH 7,0). Cotyledon segments were rinsed in cacodylate buffer and fixed in 1 % (w/v) osmium tetroxide in the same buffer for 2.5 h at room temperature. The specimens were stained en block with 1 % (w/v) uranyl acetate in 20 % acetone, dehydrated in a graded acetone series and embedded in Spurr's low viscosity epoxy resin (Spurr 1969). Ultrathin sections (50-75nm thick) were cut with a diamond knife

on an Ultramicrotome Leica EM UC6, and post-stained with lead citrate (Reynolds 1963). Micrographs were taken 1800x (overviews) and 11kx, 44kx, 110kx (details) at 80 kV on a Fei Morgagni 268 electron microscope.

3.22 Protein extraction from *Arabidopsis thaliana*

To obtain soluble and total membrane-attached proteins, 50-150 mg of *Arabidopsis* fresh weight was harvested, homogenized in homogenization buffer (50 mM Tris/HCl pH 8, 10 mM EDTA, 2 mM EGTA, 1 mM DTT) using a micropestle and the extract was solubilized in SDS sample buffer. To separate soluble and membrane-attached proteins, the homogenization was followed by centrifugation for 15 min at 4000 rpm. Soluble proteins were contained in the supernatant. Pellet was resuspended in homogenization buffer supplemented with 1 % SDS or directly in SDS sample buffer.

3.23 Isolation and transient transformation of *Arabidopsis thaliana* protoplasts

Mesophyll protoplasts were isolated from leaves of three to four-week-old *Arabidopsis* plants grown on soil. Leaves were cut in small pieces and incubated in the 10 ml enzymes-buffer (1 % Cellulase R10, 0.3 % Macerozyme R10, 40 mM Mannitol, 20 mM KCl, 20 mM MES pH 5.7, 10 mM CaCl₂, 0.1 % BSA) in the dark for 90 min at 40 rpm. Protoplasts were released by shaking 1 min at 80 rpm, filtered with a 100 µm Nylon-membrane and centrifuged 2 min at 100 x g. Protoplasts were resuspended in 500 µl MMg buffer (400 mM Mannitol, 15 mM MgCl₂, 4 mM MES pH 5.7, Osm 540), separated on a gradient made by 9 ml MSC buffer (10 mM MES, 20 mM MgCl₂, 1.2 % sucrose, pH 5.8, Osm 550) and 2 ml MMg buffer via centrifugation 10 min at 75 x g. Intact protoplasts were washed once in W5 buffer (150 mM NaCl, 125 mM CaCl₂, 5 mM KCl, 2mM MES pH 5.7, Osm 550-580) and resuspended in MMg buffer. 100 µl protoplasts (about 4 x 10⁴ protoplasts) were mixed with 10-50 µg DNA (GFP-fusion constructs) and with 110 µl PEG buffer (40 % PEG 4000 (Fluka), 200 mM Mannitol, 100 mM Ca(NO₃)₂) and incubated 15 min in dark. Protoplasts were diluted with 500 µl W5 buffer and collected by centrifugation 2 min at 100 x g. Protoplasts were resuspended in 1 ml

W5 buffer and incubate at 25°C overnight in dark. GFP fluorescence was observed with a TCS-SP5 confocal laser scanning microscope (Leica, Wetzlar, Germany).

3.24 Protein extraction from transformed *Arabidopsis thaliana* protoplasts

Transient-transformed *Arabidopsis* protoplasts were collected via centrifugation 5 min at 800 rpm. Pellet was resuspended in protein extraction buffer (2% mM Tris7HCl pH 7.7, 10 mM MgCl₂, 15 mM EGTA, 150 mM NaCl, 15 mM beta-glycerophosphate, 0.1 % Tween-20, 10 % glycerol, 1 mM DTT, 1 mM NaF, 0.5 mM PMSF, 1x complete protease inhibitor cocktail (Roche)) and frozen in liquid nitrogen. Pellet was melted on ice, vortex and centrifuged 10 min at 13000 rpm. Loading buffer was added to the supernatant, samples were immediately loaded on a SDS polyacrilamide gel and immunoblot analysis was performed with anti-GFP antibody.

3.25 Transient transformation of *Nicotiana benthamiana*

Plantlets of 3-4 weeks old *Nicotiana benthamiana* grown on soil were used for transient transformation. *Agrobacterium tumefaciens* (AGL1) carrying the construct of interest was grown in YEP medium until OD₆₀₀ =0.5. Cells were centrifuged 15 min at 4000 rpm and resuspended in a proper volume of Agromix (10 mM MgCl₂, 10 mM MES/KOH pH 5.6, 150 µM Acetosyringone) in order to have OD₆₀₀=1. Cells were shaken in Agromix for 2 hours in the dark at 23°C and the bacterial solution was infiltrated via a small wound at the lower site of the *Nicotiana benthamiana* leave. *Nicotiana benthamiana* transformed plants protected from direct light for 2-3 days and the transient expression of GFP-fusion proteins was observed with a TCS-SP5 confocal laser scanning microscope (Leica, Wetzlar, Germany).

3.26 Isolation of *Nicotiana benthamiana* protoplasts

3-4 week old transient transformed tobacco plants grown on soil were used. Leaves were cut into 0.1 cm wide stripes and incubated with 1 % Cellulase R10 and 0.3 % Macerozyme R10 in 10 ml F-PIN medium (MS medium PC-vitamins (200 mg/l Myoinositol, 1 mg/l thiamin-HCl, 2 mg/l Ca-panthotenate, 2 mg/l nicotinic acid, 2 mg/l pyridoxin-HCl, 0.02 mg/l biotin), 1 mg/l

6-benzylaminopurin (BAP), 0.1 mg/l α -naphthaleneacetic acid (NAA), 20 mM MES, pH 5.8 (KOH), 80 g/l glucose, Osm 550) for 2 h. The resulting suspension was filtered through 100 μ M Nylon-membrane. 2 ml F-PCN medium (F-PIN, except instead of glucose, sucrose was added as the osmoticum) was overlaid on the filtered suspension and centrifuged for 10 minutes at 70 g. The intact protoplasts were collected from the interface between the F-PIN and F-PCN media, washed with W5 buffer and GFP fluorescence was observed with a TCS-SP5 confocal laser scanning microscope (Leica, Wetzlar, Germany).

4 RESULTS

4.1 Characterization of STY8, STY17 and STY46 auto- and substrate phosphorylation *in vitro*

4.1.1 Phylogeny and conserved domains

The *Arabidopsis* STY8, STY17 and STY46 kinases are plant specific and have homologs in all green plants (i.e. green algae, mosses, ferns, monocots, and dicots), but not in species containing rhodoplasts or complex plastids.

The gene encoding for the STY protein kinase STY8 (At2g17700) is located on chromosome 2, whereas the genes encoding for STY17 (At4g35780) and STY46 (At4g38470) are located on chromosome 4. STY8 and STY17 are very closely related and are located in a larger context of duplicated genes as verified with PGGD (<http://chibba.agtec.uga.edu/duplication>) (Tang et al. 2008).

The three proteins STY8, STY17 and STY46 share 89.3 % amino acids sequence similarity and their primary sequences can be divided into 11 kinase typical subdomains. The activation segment, which is highly conserved among the kinases, localizes in subdomains VII and VIII and is flanked by the conserved DFG and APE motifs. A conserved threonine residue essential for the kinase activity localizes within the activation segment. Three conserved motifs, which are responsible for the kinase specificity, are located in subdomains VI, VIII and XI. Motif 1 includes a lysine residue, conserved among STY8, STY17 and STY46, which is important for the kinase activity. The three kinases also present another conserved domain, called ACT, which is located upstream the kinase subdomain I and might be involved in the kinase regulation (Figure 3).

STY8	MTIKDE--SESCGSRVAVASPSQENP---RHYRMKLDVYSEVLQRLQESNYEEATLPDFEDQLWLHFNRLPARYALDVKVE	76
STY17	MAIKEETEESCGSRVAVASITKESP---RQHRMKLEVYGEVLQRIQESNYEEANFPGFDDLLWLHFNRLPARYALDVNVE	77
STY46	MVMEDN--ESCASRVIFDALPTSQATMDRRERIKMEVFDEVLRRLRQSDIEDAHLPGFEDDLWNHFNRLPARYALDVNVE	78
ACT		
STY8	RAEDVLTHQRLKLAADPATRPFVFEVRSVQVSPRISADS-----DPAVEEDAQSSHQPSGPGVLAPPTFGSSPNFEAIT	150
STY17	RAEDVLTHQRLKLAEDPATRPFVFEVRCVQVSPTLNGNSGDVDPSPDPAVNEDAQSSYNRSR---LAPPTFGSSPNFEALT	154
STY46	RAEDVLMHKRLLHSAYDPCNRPAIEVHLVQVQFAGISAD-----LDSTSNDAHGSSPTRKS--IHPPPAFGSSPNLEALA	151
ACT		
STY8	QGSK--IVEDVDSVNNATLS-TREMHIEITFSTIDKPKLLSQLTSSLGELGLNIQEAHAFSTVDGFSLDFVVDGWSQEET	227
STY17	QAYKD-HAQDDDSAVNAQLPNSRREMHIEITFSTIDRPKLLSQLTSMGLGELGLNIQEAHAFSTADGFSLDFVVDGWSQEET	233
STY46	LAASLSQDEDAADNSVHNNSLYSRRLHEITFSTEDKPKLLFQLTALLAELGLNIQEAHAFSTTDGYSLDVFDVVDGWVPEET	231
ACT		
STY8	DGLRDALSKEIKLKDQPGSKQKSISFFEHDKSSNELIPACIEIPTDGTDEWEIDVTQLKIEKKVASGSYGDVLRHGTYS	307
STY17	EGLKDALKKEIRKFKDQPCSKQKSITFFEHDKSTNELLPACVEIPTDGTDEWEIDMKQLKIEKKVACGSYGELFRGTYS	313
STY46	ERLRISLEKEAAKIELQSQSWPMQQSFSPEKENGQTGARHVPVPIPDGTDVWEINLKHLLKFGHKIASGSYGDLYKGTYS	311
I		
STY8	QEVAIKFLKPDVRNNEMLREFSQEVFIMRKVRHKNVVQFLGACTRSPTLCIVTEFMARGSIYDFLHKQKCAFKLQTLTKV	387
STY17	QEVAIKILKPERVNAEMLRFSQEVYIMRKVRHKNVVQFIGACTRSFNLICIVTEFMTRGSIYDFLHKHKGVPKIQSLLKV	393
STY46	QEVAIKVLKPERLDSLEKEFAQEVFIMRKVRHKNVVQFIGACTKPEHLICIVTEFMGGSVYDYLHKQKGVFKLPTLFKV	391
II motif 1 III motif 2 IV		
STY8	ALDVAKGSYLVHQNNI IHRDLK TANLLMDEHGLVKVDFGVARVQIESGVM AETGTYRWMAPEVIEHKPYNHKADVFSY	467
STY17	ALDVS KGMNYLVHQNNI IHRDLK TANLLMDEHEVVKVDFGVARVQTESGVM AETGTYRWMAPEVIEHKPYDHRADVFSY	473
STY46	AIDICKGSYLVHQNNI IHRDLK AANLLMDENEVVKVDFGVARVKAQTGVM AETGTYRWMAPEVIEHKPYDHRADVFSY	471
V VI VII motif 3 VIII		
STY8	AIVLWELLTGDIPIYAFLTPLQAAGVGVVQKGLRPKIPKKTHPKVKGLLERCWHQDPEQRELFEEIIEMLQQIMKEVNVVV-	546
STY17	AIVLWELLTGELPYSYLTPLQAAGVGVVQKGLRPKIPKETHPKLTELLEK CWQQDPALRPNFAEIIEMLNQLIREVGDDER	553
STY46	GIVLWELLTGKLPYEMTPLQAAGVGVVQKGLRPTIPKNTHPKLAELLERLWEHDSTQREDFSEIIEQLQEI AKEVGEEGE	551
IX X XI		
STY8	-----	-
STY17	HKDKH-----GGYFSGLKKGHR--	570
STY46	EKKKSSTGLGGGIFAALRRSTTHH	575

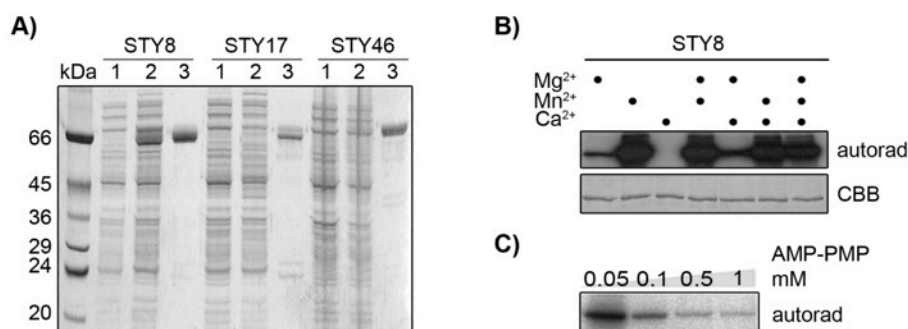
Figure 3. Protein alignment of STY8, STY17 and STY46. The ACT domain and the activation segment are boxed. Conserved motifs (1-3) mediating substrate specificity are colored in blue, the conserved APE and DFG motif flanking the activation segment in yellow. The conserved lysine (position 409 in STY8, 415 in STY17 and 413 in STY46) as well as the threonine, which are essential for kinase activity, are colored in pink.

4.1.2 Characterization of kinase autophosphorylation activity

To characterize the enzymatic properties of the three STY kinases *in vitro*, STY8 (At2g17700), STY17 (At4g35708) and STY46 (At4g38470) full length cDNAs were cloned into a pET21d vector, expressed in *E. coli* and purified via a C-terminal His-Tag on Ni²⁺-sepharose (Figure 4A). In a previous work it was shown that the kinases undergo autophosphorylation in an *in vitro* kinase assay (Martin et al. 2006). To investigate the dependence of the autophosphorylation of STY8 on the presence or absence of cations, 10 mM Mg²⁺, 10 mM Mn²⁺ and 10 mM Ca²⁺ were added during the phosphorylation reaction (Figure 4B). Full autophosphorylation activity was only achieved in the presence of Mn²⁺.

Mg²⁺ only had a slight activating effect, whereas Ca²⁺ alone was not able to promote kinase activity at all, but did not inhibit it either upon simultaneous incubation with Mn²⁺. It has been previously shown that the activity of the three kinases is inhibited when ADP is used as competitor for ATP (Martin et al. 2006). The presence of the non-hydrolyzable ATP analogue AMP-PNP likewise competed with ATP and inhibited the STY8 activity (Figure 4C).

To clarify the necessity of autophosphorylation for kinase activity and substrate phosphorylation, the activity of STY8 wild type and STY8 dephosphorylated was compared. To obtain the STY8 dephosphorylated form, STY8 was treated with λ-phosphatase, re-purified via His-tag in order to remove the phosphatase and the success of dephosphorylation was monitored with ProQ diamond stain (Figure 4D). The activity of phosphorylated STY8 as purified from *E.coli* and dephosphorylated STY8 was compared in an *in vitro* kinase assay using the preprotein of the small subunit of the chloroplast ribulose-1,5-bisphosphate carboxylase/oxygenase (pSSU) as a model substrate. Incorporation of radio-labeled phosphate was much slower for the dephosphorylated STY8 in the case of both autophosphorylation and phosphorylation of the substrate (Figure 4E). STY8 phosphorylates pSSU already after 1.5 min incubation, whereas no pSSU phosphorylation was observed in the case of dephosphorylated STY8 even after 3 min incubation, suggesting that autophosphorylation is important for full activity of STY8.



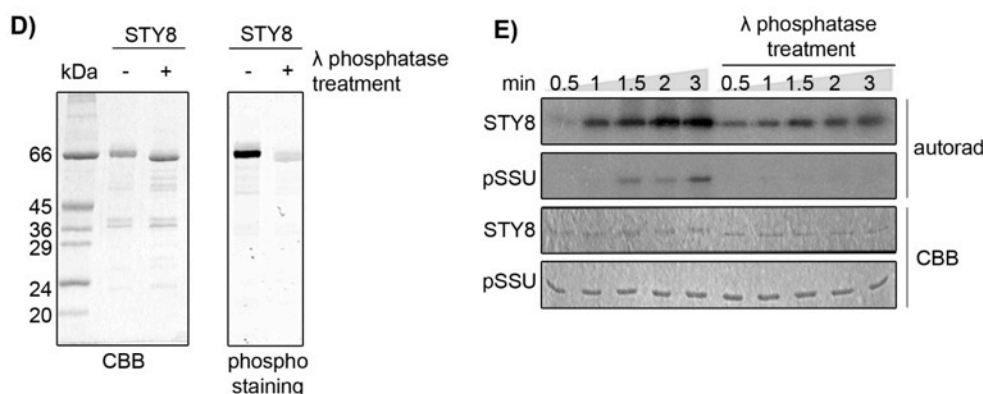


Figure 4. Kinases purification and autophosphorylation activity. **A)** Coomassie stained gel of the purification of the indicated His-tagged recombinant proteins, 1= *E.coli* lysate, 2= *E.coli* lysate after IPTG induction, 3= recombinant protein eluted from Ni^{2+} -sepharose. **B)** An *in vitro* kinase assay was performed with 3 μg of purified STY8 in the presence of Mg^{2+} , Mn^{2+} and/or Ca^{2+} for 10 min and autophosphorylation was detected by autoradiography showing a strong dependence on Mn^{2+} . Coomassie staining shows equal amounts of STY8 (lower panel). **C)** An *in vitro* kinase assay was performed with 3 μg of purified STY8 in the presence of AMP-PNP for 10 min and autophosphorylation was detected by autoradiography. **D)** Complete dephosphorylation of STY8 was analysed with Coomassie stained gel (left panel) and ProQ diamond stained gel (right panel) **E)** STY8 was treated with λ -phosphatase and phosphorylation of STY8 and pSSU was monitored subsequently for the indicated time points. 0.5 μg STY8 and 2 μg pSSU were used.

To better characterize the kinase autophosphorylation, the identification of possible autophosphorylation site(s) became essential. Mass spectrometric analysis (see 7.1 for data from www.phosphat.mpimp-golm.mpg.de (Durek et al. 2009; Heazlewood et al. 2008; Ito et al. 2009)) lead to the identification of a phosphorylated threonine which is conserved in the three kinases. This threonine lies in the activation segment, a conserved region between and including the two three-peptide motifs DFG and APE located in the kinase subdomain VII and VIII respectively (Figure 5A and 3). The threonine was mutagenized by site directed mutagenesis and the activity of the resulting mutants was analysed in *in vitro* kinase assays (Figure 5B). The substitution of the threonine with alanine (STY8-T439A, STY17-T445A, STY46-T443A), a non-phosphorylatable residue, lead to the complete abolishment of the STY8, STY17 and STY46 kinase activity in respect to both auto- and substrate phosphorylation, indicating that phosphorylation of the conserved threonine is required for kinase activity (Figure 5B upper and lower panels). The activity of the three kinases was not restored when the threonine was substituted to aspartic acid (STY8-T439D, STY17-T445D,

STY46-T443D), an amino acid residue commonly used to mimic phosphorylation due to the introduction of negative charge (Figure 5B upper and lower panels). Three additional mutants were generated for STY8 substituting the conserved threonine with glutamic acid (STY8-T439E), the second amino acid residue commonly used to mimic phosphorylation, and with serine (STY8-T439S) and tyrosine (STY8-T439Y), two phosphorylatable residues (Figure 5B upper panel). These mutants did also not present any kinase activity.



Figure 5. Activation segment and autophosphorylation site. A) Sequences of the activation segment of STY8, STY17 and STY46. The conserved three-peptide motifs DFG and APE and the phosphorylated threonine are marked. **B)** *In vitro* kinase assays of STY8, STY17 and STY46 wild type and mutants for the conserved threonine. The threonine residue at position 439 of STY8 was substituted to alanine, aspartic acid, glutamic acid, serine and tyrosine (upper panel). Threonine residues 445 of STY17 and 445 of STY46 were mutated to alanine and aspartic acid (lower panel).

To investigate the molecular mechanism of the threonine autophosphorylation two different approaches were chosen to distinguish between an intramolecular (*in cis*) and an intermolecular (*in trans*) autophosphorylation event. Firstly, a mutated kinase, which lacked any activity but could still be phosphorylated on its threonine in the activation segment, was generated. An exchange of a conserved lysine residue at position 409 (located in subdomain VI) in STY8 to an arginine (STY8-K409R) resulted in complete loss of auto- and substrate phosphorylation (Figure 6A). Increasing amounts of STY8-K409R were used as a substrate

for invariable amounts of wild type STY8 (Figure 6B). In the case of *in trans* phosphorylation of the inactive kinase by the active kinase an increasing phosphorylation signal would be expected. However, since the amount of phosphorylated kinase remained unchanged, phosphorylation is likely to occur via an intramolecular mechanism. In a second approach addressing this question an *in vitro* kinase assay in a smaller (25 μ l) and a larger (250 μ l) reaction volume with equal amounts of wild type STY8 was performed (Figure 6C). Phosphorylation was not decreasing with a larger reaction volume, as would be expected in the case of an intermolecular process due to the dilution, thus also favouring an intramolecular mechanism for the autophosphorylation.

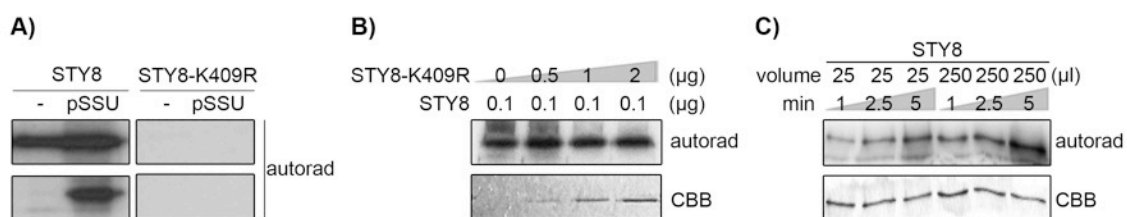


Figure 6. Intramolecular autophosphorylation of STY8. **A)** Kinase assay using STY8 wild type and a mutant in which the lysine at position 409 was substituted with arginine. pSSU was used as substrate. **B)** Increasing amounts of mutated STY8-K409R were added to constant amounts of wild-type STY8 in an *in vitro* kinase assay. Phosphorylation of STY8-K409R did not increase with higher concentrations. The increasing amount of STY8-K409R is shown by Coomassie blue staining (bottom panel) **C)** An *in vitro* kinase assay was performed in a sample volume of 25 or 250 μ l and samples were taken at three time points as indicated. Equal amounts of STY8 are shown by Coomassie blue staining (bottom panel).

4.1.3 Analysis of the conserved ACT domain

A blast search for conserved protein domains revealed that all three kinases contain an additional conserved functional domain upstream of the serine/threonine and tyrosine kinase domains, a so called ACT domain (Figure 3). This domain was named after the first proteins in which it was identified, *aspartate kinase*, *chorismate mutase* and *tyrA* (prephenate dehydrogenase) (Grant 2006) and it has been described as a small molecule binding regulative domain. In STY8, the motif comprises amino acids 185-253. To investigate the

function of the ACT domain in STY8, the amino acids 185-253 were deleted, the mutant protein (STY8- Δ ACT) was expressed in *E. coli*, purified via a C-terminal His-Tag on Ni²⁺-sepharose (Figure 7A) and subjected to an *in vitro* phosphorylation assay with pSSU and pOE23 (Waegemann and Soll 1996) as substrates (Figure 7B). STY8- Δ ACT exhibited higher activity than the STY8 wild type protein. The yield of phosphorylation of pSSU and pOE23 was double when incubated with STY8- Δ ACT than with STY8 wild type, suggesting that the ACT domain could be involved in the regulation of the kinase activity *in planta*. In order to investigate whether the binding of small molecules or other substances to the ACT domain regulates the activity of STY8, kinase assays were performed in the presence of amino acids, malate, oxalacetic acid, sucrose, fructose 1,6-bisphosphate, trehalose, alpha-ketoglutaric acid, spermidine, spermine and putrescine (data not shown). No reproducible alteration in the kinase activity was observed.

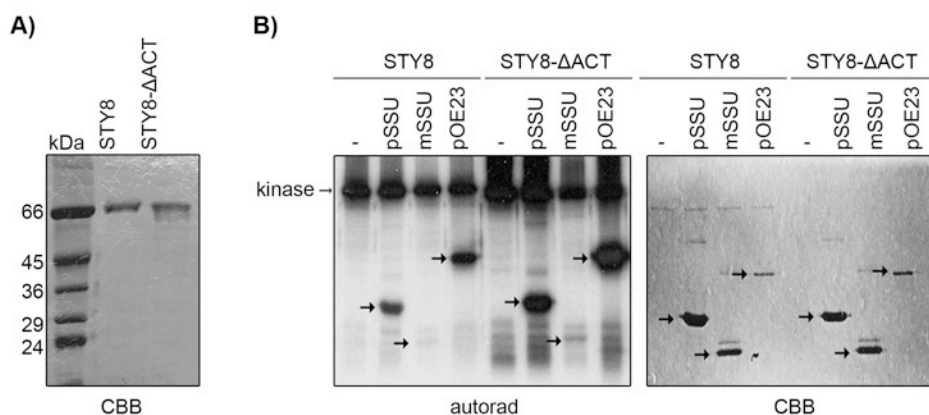


Figure 7. The ACT domain. **A)** Coomassie stained gel of the purification of STY8 and STY8- Δ ACT recombinant proteins. **B)** Kinase assay comparing the activity of STY8 wild type and STY8- Δ ACT, which lack the ACT domain. Phosphorylation of pSSU and pOE23 is shown. mSSU (the mature part of pSSU) is used as a nonphosphorylatable control (left panel). A Coomassie blue gel shows equal loading of proteins (right panel), and the purified proteins are indicated with arrows.

4.1.4 Identification of kinases specific inhibitors

A library of kinase inhibitors comprising 64 different compounds (Cayman, USA) including 44 serine/threonine and 20 tyrosine kinase inhibitors (see 7.2) was screened for substances able to inhibit STY8. Three of the inhibitors tested, JNJ-10198409, Tyrphostin and Janex 1, showed the ability to affect the STY8 auto- and substrate phosphorylation activity, even when applied at low concentration ranging from 0.01 to 10 μM (Figure 8A), whereas DMSO, which was used as solvent for the inhibitors, did not have an impact on the reaction. The inhibitory effect on STY8 autophosphorylation (Figure 8B) and on substrate phosphorylation (Figure 8C) was determined by liquid scintillation counting. Interestingly, JNJ-10198409, Tyrphostin and Janex 1 are typical small molecule tyrosine kinase inhibitors and none of the tested serine/threonine-specific kinase inhibitors showed the ability to effect the STY8 activity. To exclude that JNJ-10198409, Tyrphostin and Janex 1 also have an effect on a typical serine/threonine kinase, the auto- and substrate phosphorylation of a well characterized plant serine/threonine kinase, CPK4, was tested (Hrabak et al. 2003) (Figure 8D). None of the inhibitors affected the phosphorylation of CPK4 indicating a resemblance between the dual specificity STY kinases and classical tyrosine kinases.

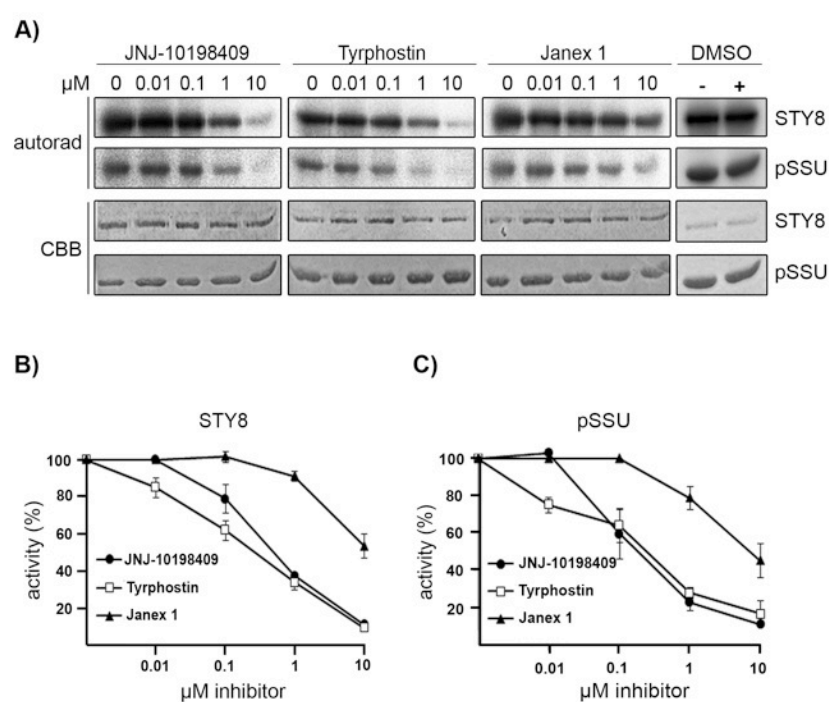
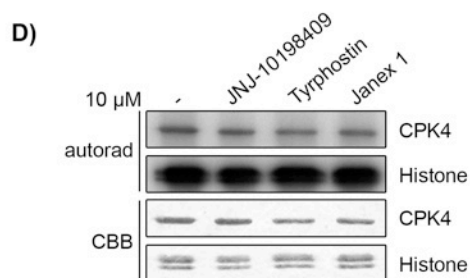


Figure 8. STY8 is inhibited by typical Tyr kinase inhibitors. **A)** The kinase inhibitors JNJ-10198409, Tyrphostin and Janex 1 were added to an *in vitro* kinase assay in increasing amounts. Constant amounts of 1 mg of STY8 and 2 mg of pSSU were used. A control reaction with the highest used concentration of dimethyl sulfoxide (DMSO; corresponding to 0.1% of the reaction volume) is shown. **B)** and **C)** Autophosphorylation of STY8 (B) as well as substrate phosphorylation (pSSU; C) decrease in the presence of kinase inhibitors in a concentration of 0 to 10 mM.



D) The Ser/Thr kinase CPK4 is not inhibited by 10 μ M JNJ-10198409, Tyrphostin or Janex 1.

4.1.5 Characterization of kinases amino acids specificity

The three kinases STY8, STY17 and STY46 belong to the family of dual specificity kinases. Since members of this family have been shown to phosphorylate hydroxyl groups of serines, threonines as well as tyrosines, the amino acid specificity of STY8 was investigated in respect to auto- and substrate phosphorylation. MBP (myelin basic protein), which is phosphorylatable on serine, threonine and tyrosine residues (Reddy and Rajasekharan 2006), was used as substrate. The proteins were subjected to an *in vitro* kinase assay in the presence of 32 P, phosphorylated proteins were excised from an SDS gel and hydrolyzed in 6 M HCl. The hydrolyzed phospho-amino acids were then separated by thin layer chromatography and phosphorylated amino acids were visualized by autoradiography. Phosphorylated amino acids stained with ninhydrin were used as marker. Interestingly, phosphorylation was restricted to serine and threonine residues in the case of both autophosphorylation of STY8 (Figure 9A) and phosphorylation of the model substrate MBP (Figure 9B). To confirm the lack of tyrosine phosphorylation by STY8, the activity of STY8 and Yes, a typical tyrosine kinase of the Src protein kinase family, was compared (Figure 9C). After *in vitro* kinase assay phosphorylated amino acids were detected in immunoblot with specific antisera against phospho-threonine and phospho-tyrosine residues. The substrate protein MBP was efficiently phosphorylated by Yes on tyrosine residues, but not by STY8, even though almost 10 fold STY8 excess over Yes was used. Threonine phosphorylation however, was observed only with STY8, but not with Yes.

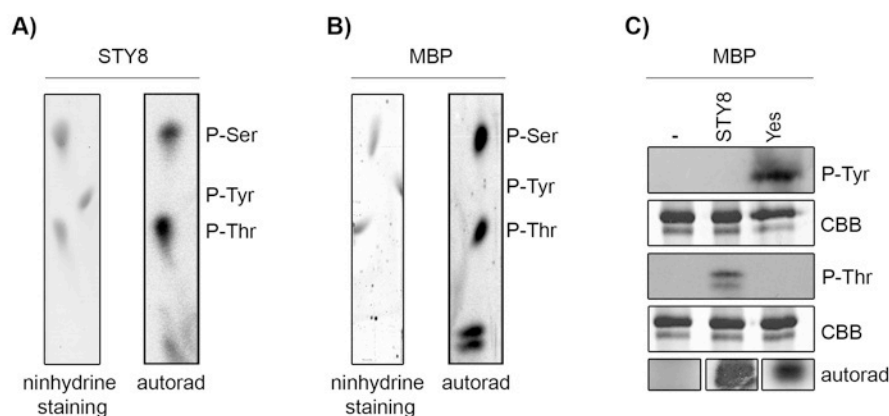


Figure 9. STY8 amino acid specificity. **A)** STY8 and **B)** MBP were phosphorylated in *in vitro* kinase assay and the corresponding bands were cut from a SDS gel and hydrolyzed. Phosphorylated amino acids were subsequently analyzed by TLC and identified by comparison with marker proteins. **C)** MBP was phosphorylated in *in vitro* kinase assay with STY8 and Yes and phosphorylated amino acids were detected with phospho-Thr or phospho-Tyr antibodies. 2 mg of Yes and 15 mg of STY8 were used. Coomassie blue staining of MBP is shown as a loading control and autoradiography show efficient phosphorylation.

4.1.6 Analysis of the substrates phosphorylation

To gain insight whether phosphorylation of preproteins occurs co- or post-translationally, the phosphorylation status of pSSU during *in vitro* translation in a wheat germ lysate, which contains endogenous kinase, was followed. The non-phosphorylatable pSSU S31/34A mutant was used as a control. The ^{35}S labeled translated proteins (Figure 10A, left panel) were purified after the translation reaction via a C-terminal His-tag and separated on 2D gels (Figure 10A, right-upper panel). Three distinct spots were visible in the wild type pSSU sample representing non-phosphorylated pSSU (IEP: 7.71), single (IEP: 6.89) and double (IEP: 6.54) phosphorylated pSSU. In the pSSU S31/34A sample only the non-phosphorylated form (IEP: 7.71) was detected as expected (Figure 10A, right-middle panel). When wild type pSSU was treated with λ -phosphatase prior to 2D gel electrophoresis, also only the non-phosphorylated form of pSSU was detected (Figure 10A right-lower panel). A possible co-translational mechanism of substrate phosphorylation was investigated by stalling the ribosomes to the nascent peptide chain during translation. Wild type pSSU and pSSU S31/34A, both equipped with a C-terminal stalling sequence (Bhushan et al. 2010), were translated *in vitro* (Figure 10B, left panel), purified with a N-terminal His-tag and the

phosphorylation status was visualized in 2D gels (Figure 10B). In this case only the non-phosphorylated form was detected (IEP: 8.21), indicating that the phosphorylation sites are not accessible to the kinase during the translation process, but that phosphorylation of the preproteins rather occurs post-translationally.

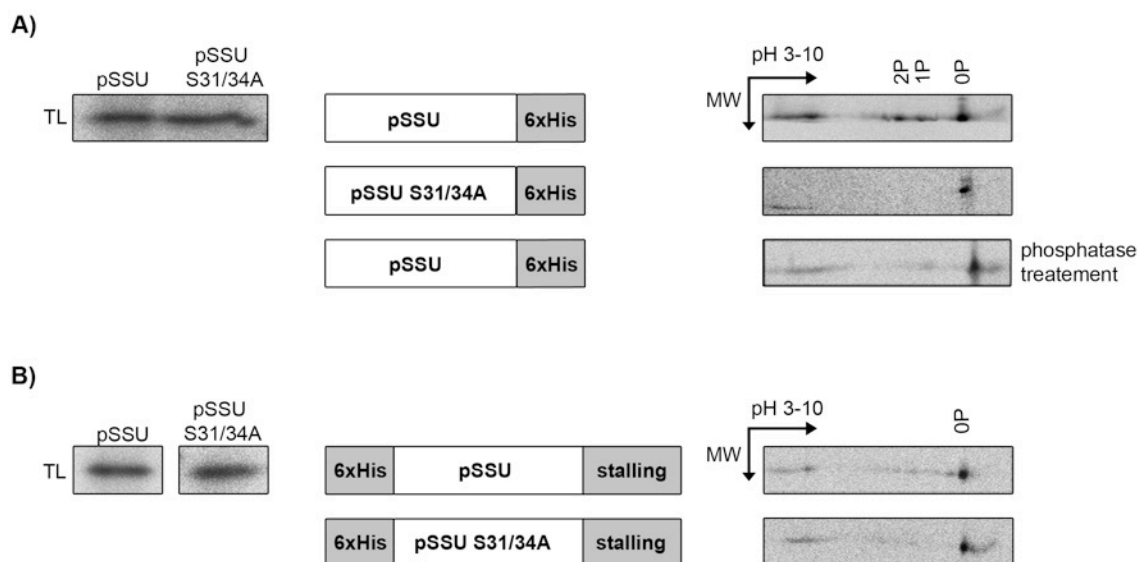


Figure 10. Post-translational phosphorylation. **A)** pSSU was *in vitro* translated in wheat germ lysate and subjected to isoelectric focusing, resulting in three distinct spots corresponding to nonphosphorylated pSSU (0P) and pSSU phosphorylated on one residue (1P) or on both residues (2P; right panel, top). pSSU S31/34A and pSSU dephosphorylated after the translation reaction were used as controls, only showing nonphosphorylated protein (right panels, middle and bottom). TL shows equal translation efficiencies for pSSU and pSSU S31/34A (left panels). **B)** pSSU fused to a C-terminal ribosomal stalling sequence was subjected to *in vitro* translation and again separated by isoelectric focusing. In wild-type pSSU (right panel, top) and pSSU S31/34A (right panel, bottom) only a spot corresponding to the nonphosphorylated pSSU (0P) was detectable. TL shows equal translation efficiencies for pSSU and pSSU S31/34A (left panels)

4.2 *In vivo* characterization of STY8, STY17 and STY46

4.2.1 GFP localization of STY8, STY17 and STY46

The phosphorylation of nuclear encoded chloroplast preproteins is a process that occurs in the cytosol. Therefore, it is reasonable to assume that the kinase(s) responsible for this phosphorylation localize to the cytosol. It has been shown previously that STY8 is a cytosolic protein (Martin et al. 2006). The two homologue kinases STY17 and STY46 likewise do not

comprise any predicted signalling sequences (TargetP (Emanuelsson et al. 2007)). The localisation of STY8, STY17 and STY46 was analysed by expressing C-terminal GFP fusion proteins in isolated *Arabidopsis* protoplasts (Figure 11). Confocal laser scanning microscopy clearly detected the GFP signal in the cytosol.

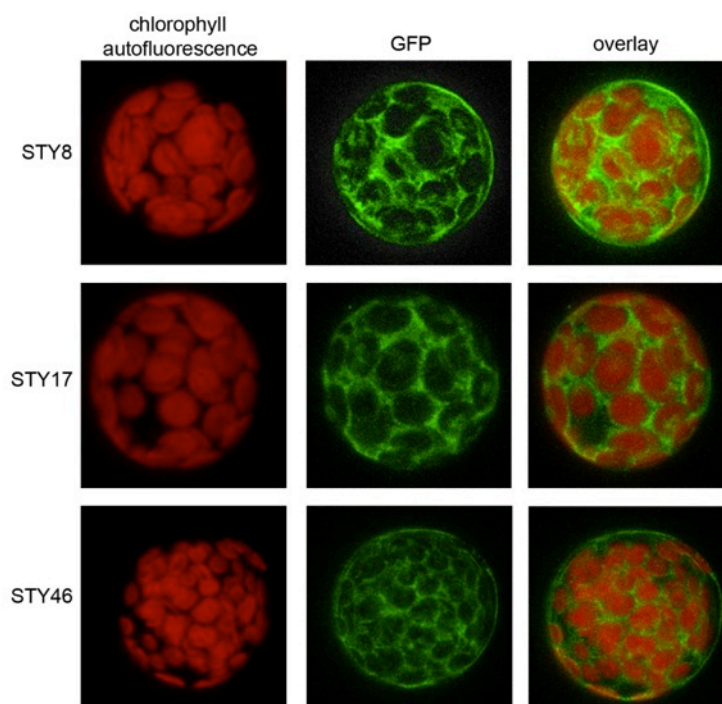


Figure 11. Localization of STY8, STY17 and STY46. The full length cDNA of *STY8*, *STY17* and *STY46* was expressed under control of the 35S promoter as GFP fusion proteins. Left: chlorophyll autofluorescence, middle: GFP fluorescence, right: overlay.

4.2.2 Association analysis of STY8

In order to investigate whether the kinases form high molecular weight complex(s) *in vivo*, the behaviour of the recombinant STY8 and the endogenous STY8 from *Arabidopsis* was compared in size-exclusion chromatography. STY8 was expressed in *E. coli*, purified via a C-terminal His-Tag on Ni²⁺-sepharose and separated on a Superdex-200 column. The elution volume of STY8 was 12.5 mL. Total soluble protein extract from two weeks old *Arabidopsis* leafs was likewise separated on a Superdex-200 column, fractions were collected and

immunodecorated with antisera against STY8 in order to identify the elution volume of the endogenous STY8 (Figure 12). The endogenous STY8 eluted at the same volume as the recombinant STY8, suggesting that STY8 does not form any high molecular weight complex *in vivo*.

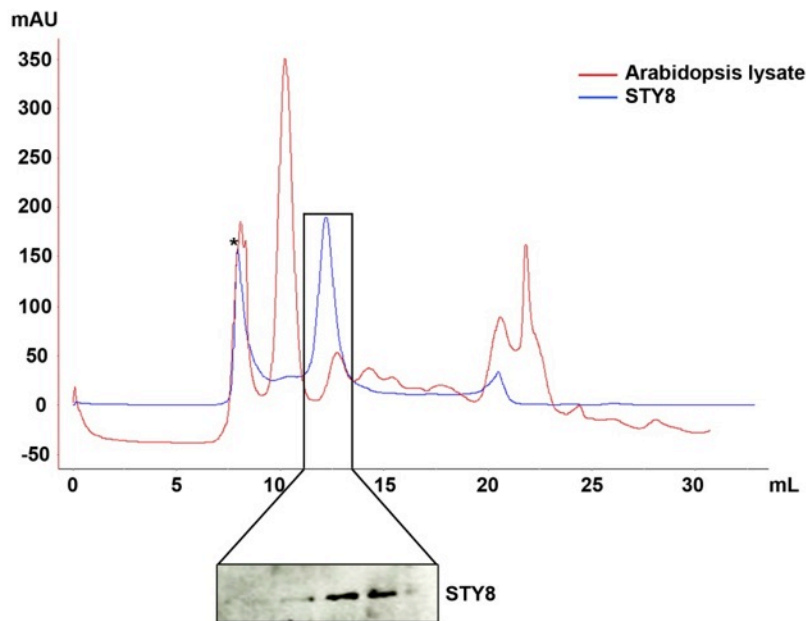


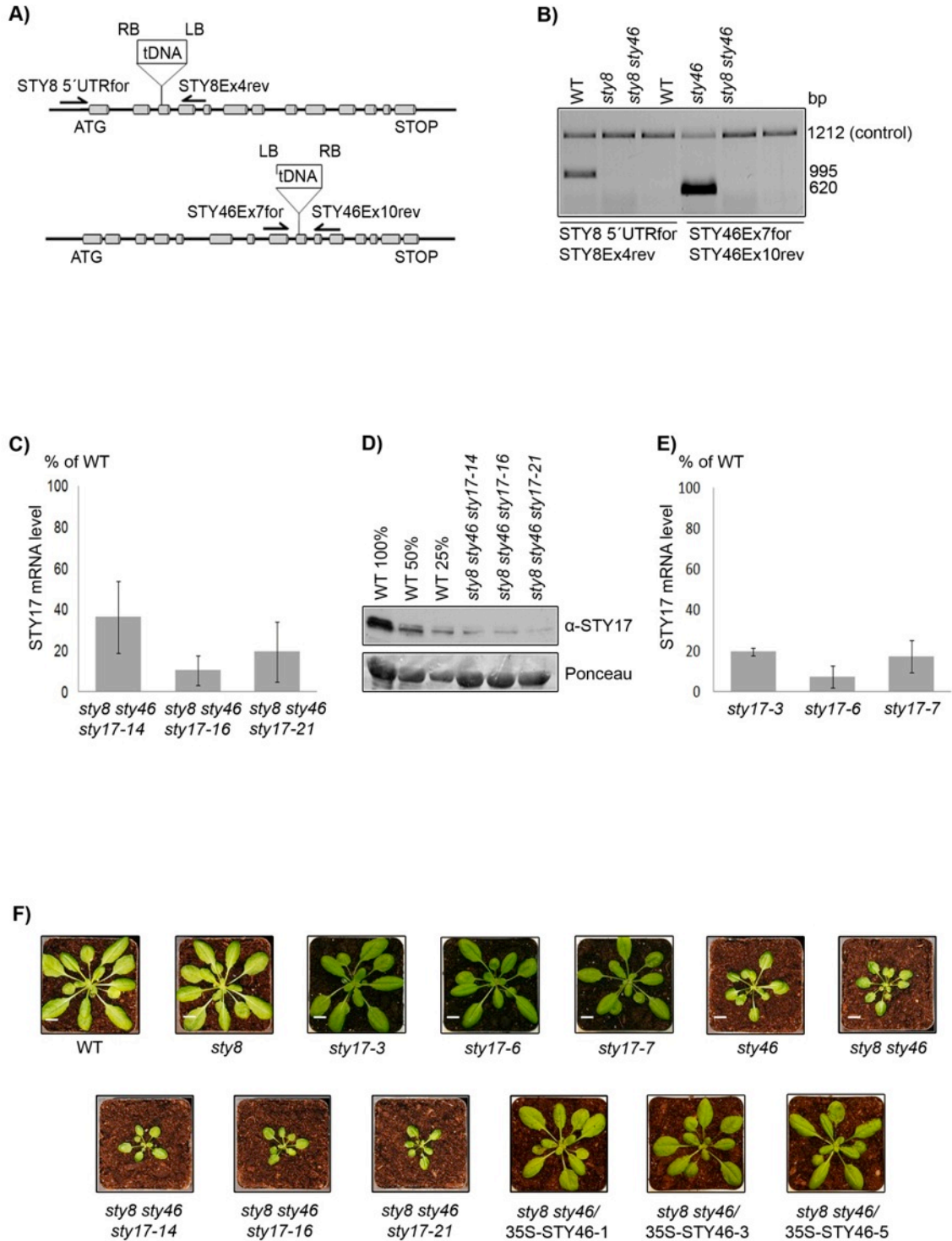
Figure 12. Association analysis of STY8. A) Chromatograms of recombinant STY8 (blue) and *Arabidopsis* total protein extract (red). The high molecular weight peak (asterisk) in the STY8 chromatogram corresponds to protein aggregation, the second peak corresponds to recombinant STY8 (elution volume=12.5 mL). The elution volume of endogenous STY8 was detected by immunodecoration of the fractions with STY8 antiserum.

4.2.3 Generation and characterization of *sty8*, *sty17* and *sty46* *Arabidopsis* mutant lines

To study the effect of transit peptide phosphorylation *in planta*, loss of function mutants for *STY8* and *STY46* were isolated. Homozygous lines with the T-DNA insertion located in exon 3 (*sty8*) and in exon 9 (*sty46*) were obtained (Figure 13A) and crossed to generate double mutants (*sty8 sty46*). The lack of RNA expression was analyzed by RT-PCR (Figure 13B). In either of the single or double mutant lines no residual RNA was detected. Since no T-DNA insertion lines were available for *STY17*, an RNAi approach was applied to generate *sty17* knockdown lines in wild type as well as *sty8 sty46* double mutant background. A 400 bp fragment corresponding to the N-terminal part of *STY17*, which does not contain any of the conserved protein domains, was cloned in sense and antisense orientation into the gateway

vector pB7GWIWG2(II) and wild type as well as in *sty8 sty46* plants were transformed with the construct. Transformants were selected by BASTA resistance and the F2 generation was analyzed on RNA and protein level to verify the extent of STY17 reduction. RNA levels of *STY17* in the double mutant background were significantly reduced to 10-30% in lines 14, 16 and 21 as demonstrated by quantitative RT-PCR (Figure 13C). Analyses on the protein level with specific STY17 antisera confirmed these results showing a reduction to below 25% of wild type protein levels (Figure 13D) in the respective lines, which were consequently used for further analyses. RT-PCR analysis showed a reduction of the RNA levels of *STY17* in the wild type background to 5-20% (Figure 13E). Growth phenotypes of all mutant plants were analyzed under several conditions including long-day (16 h light), short-day (8 h light), constant light (24 h light), low light (10 $\mu\text{mol photons m}^{-2} \text{s}^{-1}$), high light (500 $\mu\text{mol photons m}^{-2} \text{s}^{-1}$) and cold stress (+10°C). *Sty8* single mutants did not show any visible phenotype under all conditions tested, whereas *sty46* single and *sty8 sty46* double mutants were clearly retarded in growth, especially under long day conditions (Figure 13F, upper panel). *Sty17* knockdown mutants in wild type background were undistinguishable from wild type plants (Figure 13F, upper panel). RNAi knockdown in the background of *sty8 sty46* resulted in an even more pronounced retardation of growth (Figure 13F, lower panel). 5 week old mutant plants displayed a delay of bolting by over 1 week in comparison to wild type (Figure 13G), although the principal inflorescence stem reached the same length after 6 weeks. The delayed development was solely due to retardation in growth, since germination was not found to be affected in the mutants. To ensure that the observed phenotype resulted from inactivation of the kinases and was not due to background mutations in any of the lines, complementation of the double mutant *sty8 sty46* was performed. The full length cDNA of *STY8* and *STY46* was cloned under the control of the 35S cauliflower mosaic virus promoter and wild type as well as mutant plants were transformed with the construct. Only the *STY46* cDNA was sufficient to completely restore the wild type phenotype (Figure 13F and G, lower panel) which is consistent with the observation of a growth phenotype in the *sty46* single

mutant. Successful expression of *STY46* in three independent complemented lines is demonstrated by RT-PCR (Figure 13H).



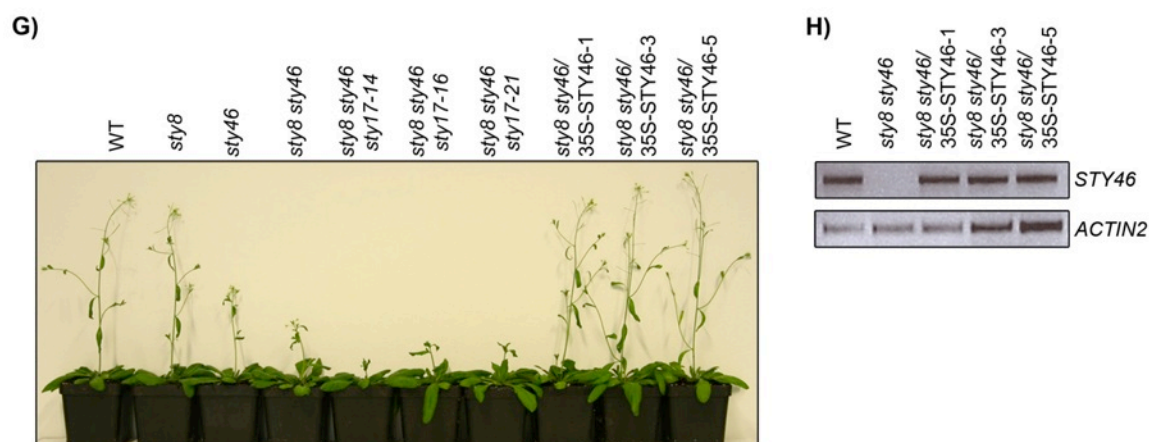


Figure 13. Isolation of *sty8* and *sty46* T-DNA insertion lines, generation of *sty17* RNAi knockdown lines and complementation of the mutants. **A)** Gene model showing the positions and orientations of T-DNA insertions in SALK 072890 (*sty8*) and SALK 116340 (*sty46*). Oligonucleotides used in B are indicated. LB, Left border; RB, right border. **B)** RT-PCR was performed with single and double mutants of *sty8* and *sty46* and the wild type (WT). HCF136 was amplified as a control. **C)** Independent *sty17* RNAi lines (14, 16, and 21) in the background of *sty8 sty46* were analyzed by quantitative RT-PCR. Values were calculated relative to 10^3 molecules of ACTIN2 and expression levels relative to the wild type are given. **D)** Immunoblot analysis of *sty17* RNAi lines (14, 16 and 21) in the background of *sty8 sty46*. For 100%, 20 mg of protein was loaded on a 12% SDS gel, transferred to a PVDF membrane and immunodecorated with specific STY17 antisera. Ponceau staining of the large subunit of Rubisco is shown as a control. **E)** Independent *sty17* RNAi lines (3, 6, and 7) in the wild type background were analyzed by quantitative RT-PCR. Values were calculated relative to 10^3 molecules of ACTIN2 and expression levels relative to the wild type are given. **F)** Phenotype analysis of wild-type, mutant and complemented lines. Plants are shown 4 weeks after germination on soil. Bars = 1 cm. **G)** Flowering phenotype of wild-type and mutant plants 5 weeks after germination. **H)** RT-PCR analysis of the wild type, *sty8 sty46* and *sty8 sty46/35S-STY46* demonstrating the expression of STY46 in the complemented lines.

4.2.4 Analysis of the chloroplast ultrastructure in kinase mutant lines

To verify whether retardation in growth was accompanied by chloroplast ultrastructural changes, wild type and mutant plants were analyzed by transmission electron microscopy. Overviews of the mutant tissues frequently showed cells with slightly smaller vacuoles and plastids which were more round-bodied. Plastids of 7 and 14-days old cotyledons of *sty8 sty46* double mutants were analyzed in more detail. They showed abnormal shape and thylakoid formation was overall affected (Figure 14, 15 and 16). The results of the ultrastructural analysis of the organelles revealed a time-gradient of developmental retardation. In 7-days old cotyledons of wild type plants (Figure 14A and 16A) chloroplasts in

mesophyll cells showed a typically ellipsoidal shape with grana-stacks and stroma thylakoids (Pyke 2007). In 7-days old cotyledons of mutant plants (Figure 14B and 16B) discrepancies to wild type chloroplasts (Figure 14A and 16A) could be observed in every chloroplast of the mesophyll cells. Different and extensive stages of disordered thylakoids were observed. Grana-stacks of thylakoids were only loosely appressed and the lumen was blown up, mainly at both of the chloroplast defined poles, where converging thylakoids were found in wild type ((Pyke 2007) and e.g. Figure 14A, upper panel), but also at the top and the bottom parts of the plastids (Figure 14B, left panel). Plastids from mutant plants contained more and larger membrane bound vesicles, frequently in the vicinity of developing grana-stacks (Figure 14B, right panel). Membrane connections between closely juxtaposed grana-stacks were often missing. In addition the network of stroma thylakoids was only partially developed and the thylakoids appeared more like isolated membrane arrays in many cases. All together, the chloroplasts were less elongated, more disordered and the thylakoids seemed to be improperly arranged in comparison to the wild type (Figure 14 and 16A-B).

In 14-days old cotyledons of mutant plants (Figure 15B and 16 C-E) developing chloroplasts showed frequently grana-stacks with a curved structure and disoriented arrangement. In many cases the grana-stacks lacked a connection to stroma thylakoids and ended in a curved conformation (Figure 15B, upper and middle panel). The thylakoid lumen appeared normal in contrast to seven day old plants. Sometimes star-shaped fragments of vesicular and tubular shape were observed, also in combination with small osmiophilic structures between non-connected grana-stacks (Figure 15B, lower panel, left). These structures are most likely distinct from a typical prolamellar body and have been observed before in electron microscopic studies on plastid differentiation (Menke 1960). Furthermore, in mutant plants stacks of nearly hexagonal arranged vesicular or tubular membranes were regularly found at all anatomical aspects of plastids, meaning the defined poles and at the top and the bottom parts of the plastids (Figure 15B, lower panel right), whereas in wild type these were almost never observed. The ultrastructure of the plastids in cotyledons of complemented

plantlets was fully restored to the wild type phenotype (Figure 16A and E). The transmission electron microscopy experiments have been performed by Dr. Irene Gügel.

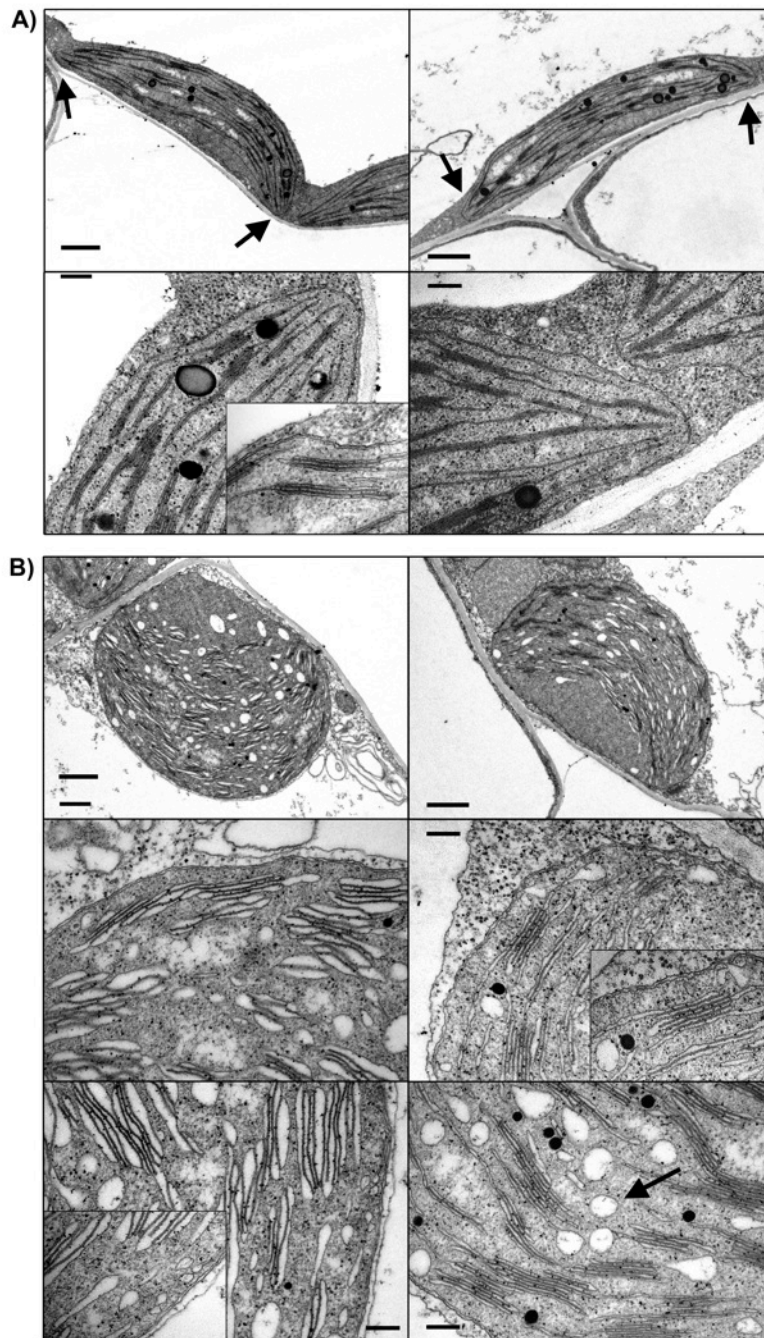


Figure 14. Ultrastructure of chloroplasts from 7-days old cotyledons of *Arabidopsis* plants. A) The wild type. Defined poles are indicated by arrows. **B)** *sty8 sty46*. *sty8 sty46* affects chloroplast morphology and thylakoid ultrastructure in different and extensive stages. Blown-up thylakoids, grana stacks loosely appressed with blown-up lumen (left panels), membrane-bound vesicles mainly in the vicinity of grana stacks indicated by the arrow (right panels) and often missing membrane connections between closely juxtaposed grana stacks are shown. Bars=1 mm (top panels) and 200 nm (middle and bottom panels). The inset magnification is 110,000X.

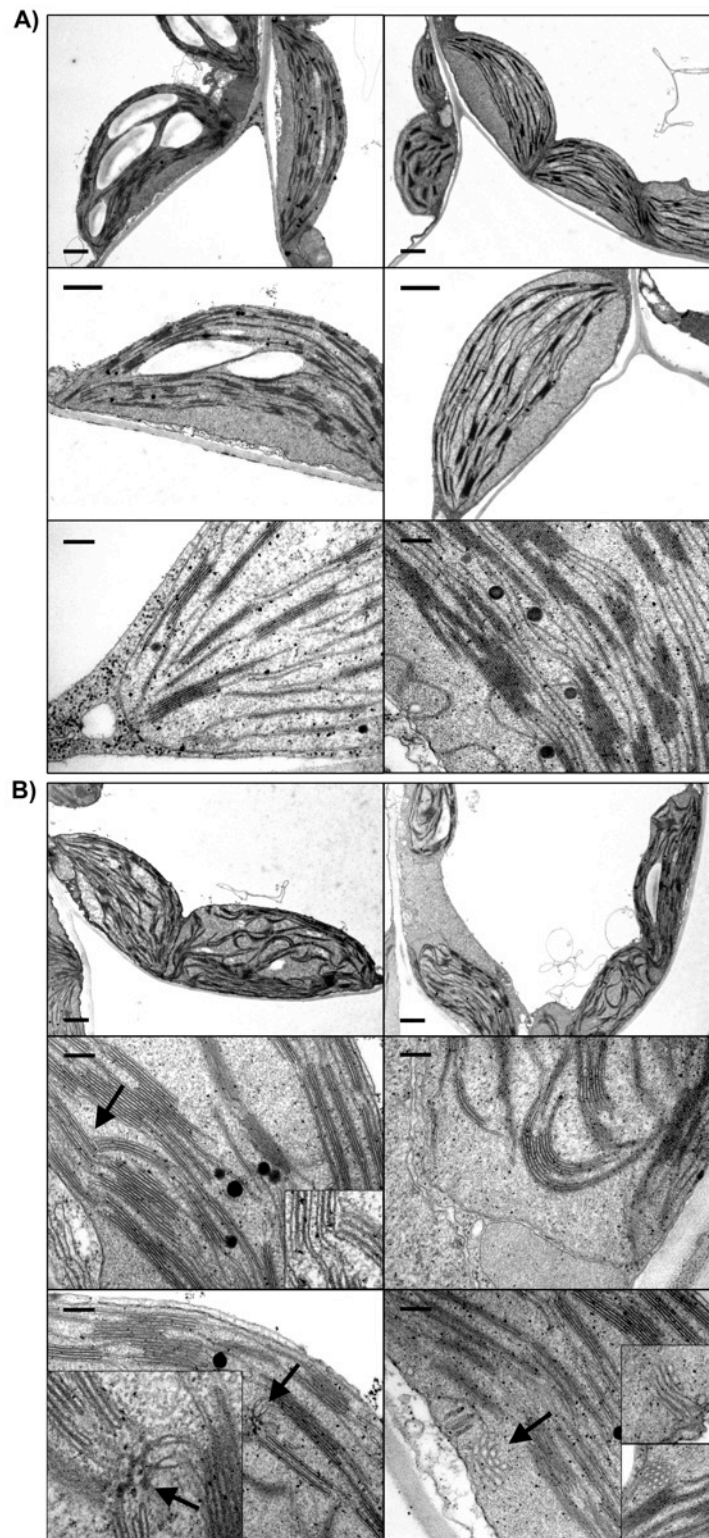


Figure 15. Ultrastructure of chloroplasts from 14-days old cotyledons of *Arabidopsis* plants. A) The wild type. **B)** *sty8 sty46*. *sty8 sty46* chloroplasts with curved structured grana stacks and disoriented arrangement (top panels), grana stacks lacking connection to stroma thylakoids (left middle panel, inset), curved structure of grana stacks (right middle panel), star shaped fragments of vesicular and tubular membranes (left bottom panel) and nearly hexagonal vesicular or tubular membranes (right bottom panel and insets) are shown; described structures are indicated by arrows. Bars=1 μ m (top panels) and 200 nm (middle and bottom panels). Magnification of the insets in the left panels is 110,000X.

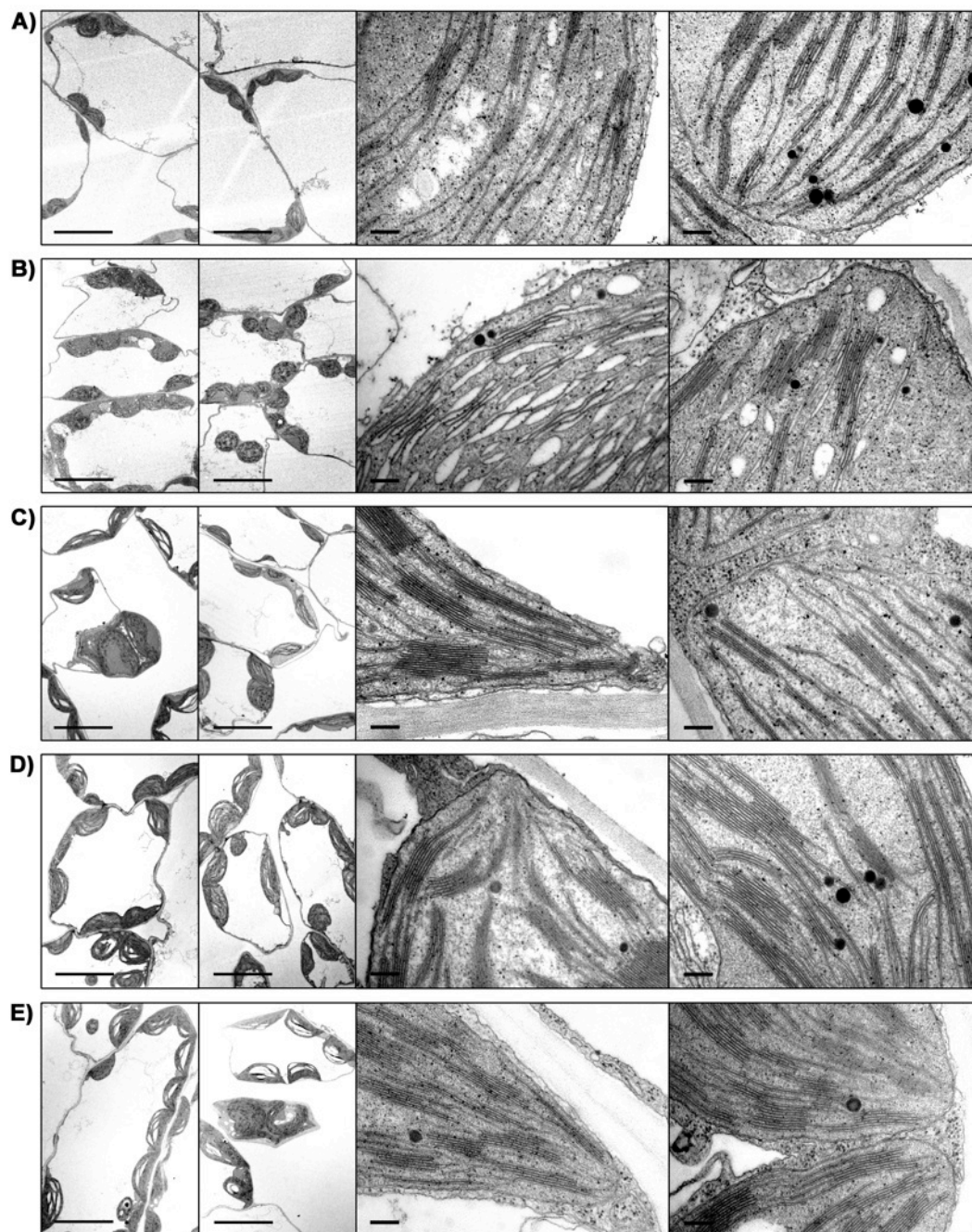


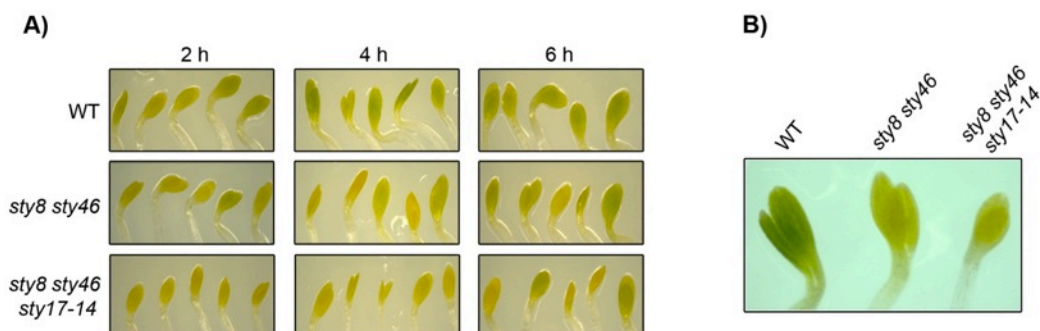
Figure 16. Chloroplast ultrastructure of 7 and 14-days old cotyledons. A) WT (7 d); **B)** *sty8 sty46* (7 d) different and extensive stages of blown-up thylakoids, membrane bound vesicle in vicinity of grana-stacks. **C)** WT (14 d) **D)** *sty8 sty46* (14 d) curved grana-stacks, grana-stacks without membrane connection **E)** *sty8 sty46/35S-STY46* (14 d) complemented line; bar 1 μ m (overviews), 200 nm (details).

4.2.5 Phenotypic analysis of etiolated kinases mutant plants

Chloroplast differentiation from etioplasts to chloroplasts requires the massive influx of preproteins into the organelle to form thylakoids and the photosynthetic machinery. Therefore

seedlings of wild type and mutants were grown in darkness for six days and subsequently transferred to light for several hours to study possible differences during chloroplast differentiation. Interestingly, the greening process was significantly delayed in *sty8 sty46* and *sty8 sty46 sty17* as observed by coloring of the cotyledons (Figure 17A-B) as well as by quantitative measurements of the chlorophyll *a* and *b* content 2, 4 and 6 hours after transition to light (Figure 17C and D). The measurements demonstrate that greening is hampered in the mutants and chlorophyll accumulation only reaches about 50% of wild type level after 2, 4 and 6 h (Figure 17C). Nevertheless, chlorophyll accumulation is not completely impaired as the total chlorophyll concentration increases continuously during the first 6 hours after illumination in mutants and wild type (Figure 17D).

Chlorophyll *a* fluorescence measurements performed during the greening process clearly demonstrated a delay in the photosynthetic performance of PSII in mutant plants. The maximum quantum yield of PSII measured as a ratio of F_v/F_m was severely decreased to 0.22 ± 0.034 in *sty8 sty46 sty17-14* compared to wild type with 0.36 ± 0.011 after 4 h illumination (Figure 17E-F). Measurements after 2 h illumination were not feasible since the signal obtained by the saturating light pulse was hardly above background noise. However, a significant difference in F_v/F_m was observed in the early time period from 4-6 h. Mutant plants only reached the same photosynthetic efficiency as wild type after 22 h illumination (wild type 0.74 ± 0.016 , *sty8 sty46 sty17-14* 0.72 ± 0.01). Chlorophyll *a* fluorescence measurements have been performed by Dr. Jörg Meurer.



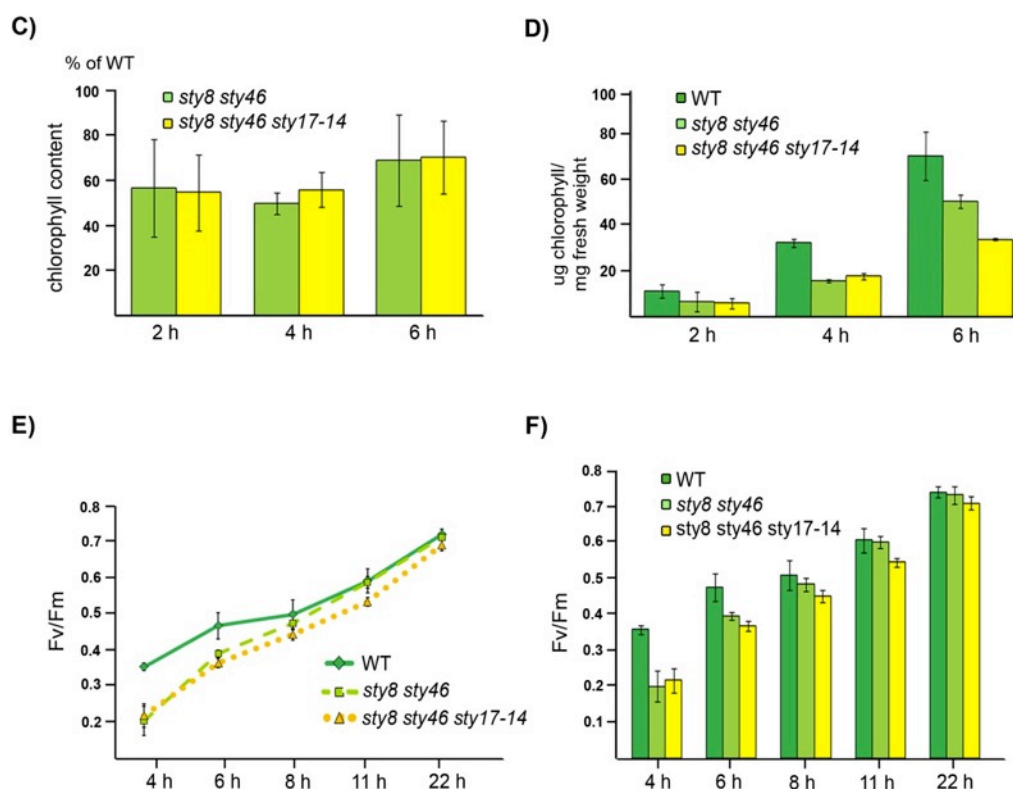


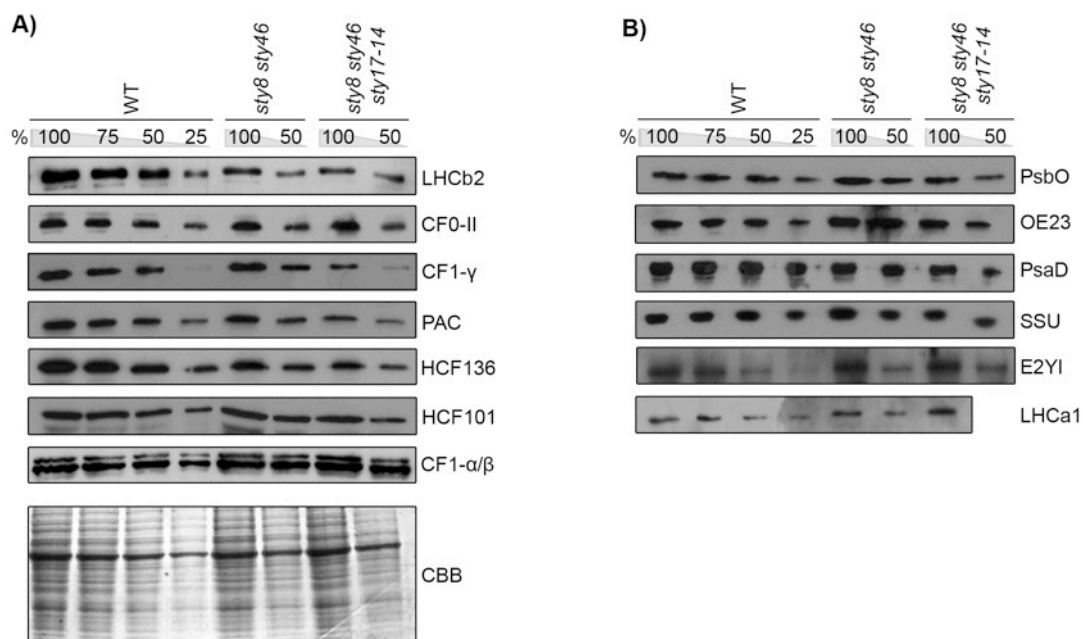
Figure 17. Greening of kinase mutant plants. **A)** Five representative seedlings of the wild type (WT) and mutants are shown 2, 4 and 6 h after illumination. **B)** One representative seedling of the wild type (WT) and mutants is shown 4 h after illumination. **C)** Chlorophyll concentration was measured 2, 4 and 6 h after exposure of etiolated seedlings to light ($50 \mu\text{E m}^{-2} \text{s}^{-1}$). Chlorophyll concentration was reduced to 50% to 60% of wild type level during the entire greening process in double and triple mutants. **D)** Chlorophyll concentration was measured in $\mu\text{g mg}^{-1}$ fresh weight and increases in the wild type and mutants during the first 6 h of illumination ($n = 3$). **E)** and **F)** Fv/Fm was measured at the indicated time points after illumination in wild-type and mutant plants ($n = 3$).

4.2.6 Biochemical characterization of etiolated kinase mutant plants

To elucidate defects of chloroplast development on the protein level, total proteins were isolated 2 h after illumination and immunodecorated with several antisera against chloroplast localized proteins (Figure 18A-B). Several membrane as well as soluble nuclear encoded chloroplast proteins with diverse functions were found to be reduced, mostly showing a stronger effect in the triple mutant. All immunoblots were repeated at least three times and the bands corresponding to the reduced nuclear encoded chloroplast proteins were quantified, showing a reduction to 50-80% (Figure 18C). LHCb2 (light harvesting complex of PSII) displayed the strongest reduction to about 50% of wild type level in the triple mutant

and subunits CF0-II and CFI- γ of the ATP synthase only reached about 60% of wild type levels. Furthermore, PAC (pale cress) (Meurer et al. 1998b), which plays a role in plastid RNA processing, HCF101 (high chlorophyll fluorescence 101) (Schwenkert et al. 2010), a PSI assembly factor, and HCF136 (high chlorophyll fluorescence 136) (Meurer et al. 1998a), a membrane protein involved in early PSII biogenesis, were reduced to 70-80% compared to wild type levels. Strikingly, the plastid encoded CF1 α and β subunits of the ATP synthase were not down regulated, underlining a deficiency in the accumulation of nuclear encoded chloroplast proteins only. However, a number of other nuclear encoded proteins tested were found to be present in comparable amounts to wild type, such as PsaD, PsbO, OE23, LHCa1, SSU and E2YI (Figure 18B).

To verify whether LHCb2, CF0-II, HCF101, PAC preproteins can be phosphorylated by the STY kinases, as has already been shown for two of the down regulated proteins CFI- γ and HCF136 (Martin et al. 2006), chimeric proteins of the transit peptide of LHCb2/CF0-II/HCF101 and mSSU as well as full length HCF101 and PAC were cloned into pET21d vector, expressed in E.coli, purified via a C-terminal His-tag on Ni²⁺-sepharose and subjected to an *in vitro* kinase assay. All proteins but mSSU, which was used as a non-phosphorylatable control, were found to be phosphorylated (Figure 18D).



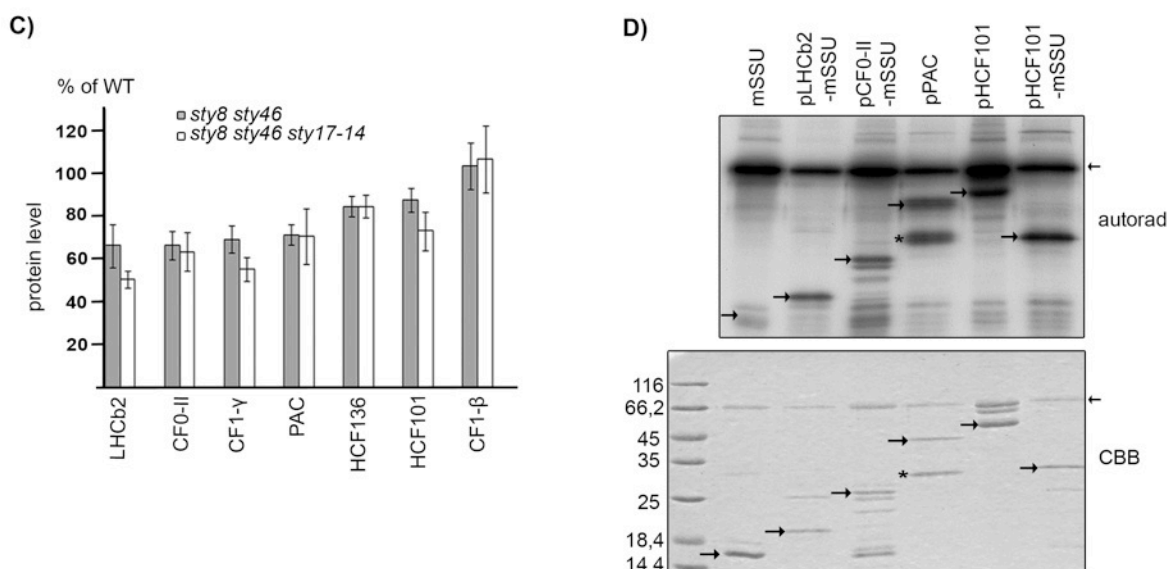


Figure 18. Protein levels of nuclear encoded chloroplast proteins in kinase mutants. A) and B) Immunoblot analysis of wild type (WT) and mutant seedlings isolated 2 h after illumination. Nuclear encoded proteins (LHCb2, CF0-II, CF1-γ, PAC, HCF101, and HCF136 (A) pSbO, OE23, PsaD, SSU, E2YI and LHCA1 (B)) as well as the plastid-encoded CF1-b subunit of the ATP synthase were analyzed. The CF1-b antibody recognizes CF1-b (bottom band) and cross-reacts with CF1-a (top band). A total of 15 mg of protein corresponds to 100% and the bottom panel shows a Coomassie blue-stained gel (CBB) as a loading control. **C)** Quantification of immunoblotting (A) was performed with ImageQuant software (GE Healthcare). All immunoblots were repeated at least three times and the bands corresponding to 50% were quantified. **D)** Quantitative RT-PCR was performed with LHCb2, CF0-II, CF1-γ, PAC, HCF101 and HCF136 to analyze the expression level (n = 3). **E)** Two micrograms of mSSU, pLHCb2-mSSU, pCF0-II-mSSU, pPAC, pHCF101, and pHCF101-mSSU was subjected to an *in vitro* kinase assay with 1 mg of STY8. The positions of the kinase and the purified substrate proteins are marked with arrows in the autoradiograph and in the corresponding Coomassie blue stained gel. A second smaller band is detected in the pPAC sample (marked with an asterisk), which is also phosphorylated and probably contains a degradation product of pPAC.

4.2.7 Gene expression analysis of etiolated kinase mutant plants

The finding that several nuclear encoded chloroplast precursor proteins accumulate slower in etiolated kinase mutant plants indicates a post-translational control of the preprotein import. To rule out any regulatory effects on the transcriptional level of the down regulated chloroplast proteins, expression levels of *LHCb2*, *CF0-II*, *CF1-γ*, *HCF101*, *PAC* and *HCF136*, proteins of which genes were found to accumulate slower, were analyzed by quantitative RT-PCR with RNA isolated from etiolated seedlings 2 h after illumination (Figure 19A). No down regulation of these genes was observed in comparison with wild type, indicating that RNA metabolism is not affected in the mutants. Some of the genes were slightly up regulated,

however not more than 1.3 fold of wild type. To investigate whether other proteins are regulated at a transcriptional level in kinase mutant plants, microarray analyses (Affymetrix ATH1 GeneChip) were performed and the expression levels in wild type and *sty8 sty17 sty46* mutant plants 2 h after illumination were compared. 89 genes were found to be significantly up regulated (see 7.3.1) and 147 were down regulated (see 7.3.2) in the mutant (P -value < 0.1, 1.5-10 fold). Interestingly, among the up regulated genes 18% were found to be chloroplast encoded, especially genes encoding for the NDH complex, suggesting that the mutant plants are trying to compensate the lack of photosynthetic performance possibly by favoring cyclic electron flow (Figure 19B). Among the down regulated genes several kinases were identified (Figure 19C). This finding opens the possibility that STY8, STY17 and STY46 may act in concert with other kinases as components of a signaling cascade.

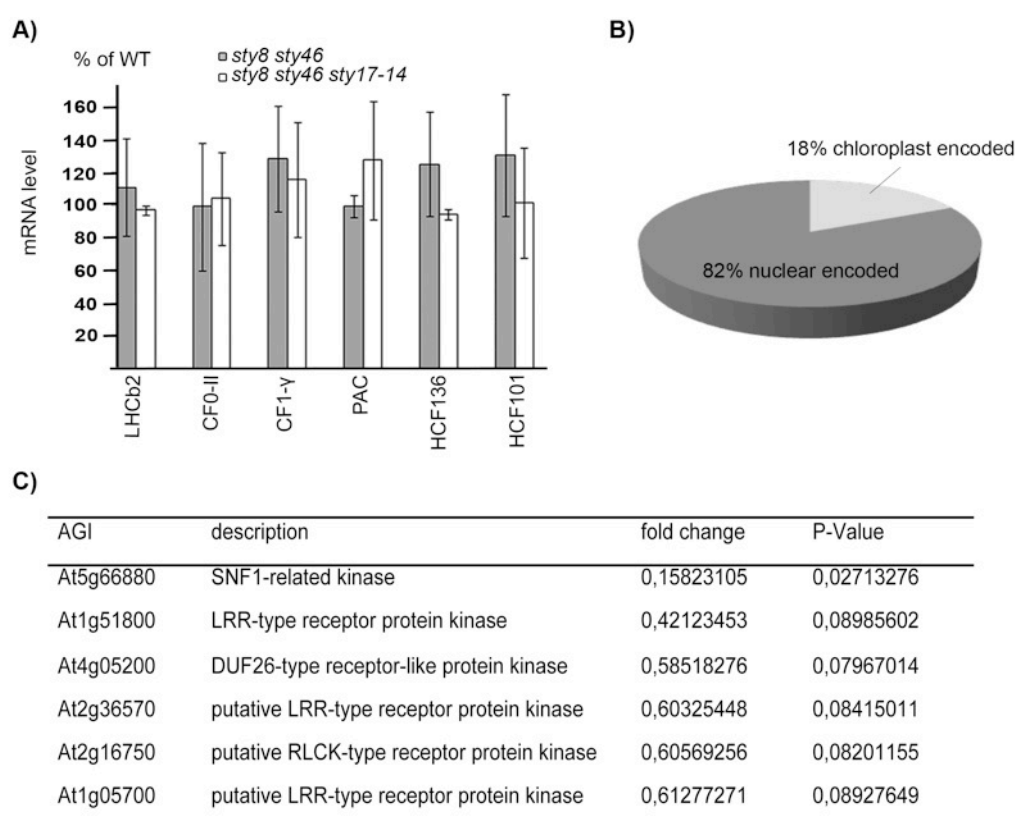


Figure 19. Gene expression analysis of kinase mutant plants. A) Quantitative RT-PCR was performed with LHCb2, CF0- II, CF1- γ , PAC, HCF101 and HCF136 to analyze the expression level ($n = 3$). **B)** Graphical representation of the up regulated genes found in microarray analysis. Among the up regulated genes 18 % were chloroplast encoded and 82 % were nuclear encoded. **C)** List of down regulated kinases identified in *sty8 sty46 sty17* etiolated plants after 2 h of illumination.

4.2.8 Analysis of preprotein import

The molecular characterization of the etiolated kinase mutant plants revealed a defect in the accumulation of nuclear encoded chloroplast proteins in the first hours of illumination, pointing at a possible reduction of the import efficiency related to the lack of precursor phosphorylation. In an attempt to visualize the slowed import process, the import efficiency of several preproteins was analysed in isolated *Arabidopsis* protoplasts. C-terminal GFP fusion proteins were transiently expressed and the localisation of the proteins was microscopically monitored. The import efficiency of pSSU was compared to two mutants: pSSU S31/34A, which is not phosphorylatable, and pSSU S31/34D, which mimics the phosphorylated form of the protein. The localization of pSSU and pSSU S31/34A was similar, the GFP fluorescence overlapped with the chlorophyll autofluorescence indication chloroplast localisation (Figure 20A, upper and middle-upper panels). No residual precursor protein was visible in the cytosol. In contrast, detectable amount of pSSU S31/34D was located in the cytosol showing a pattern similar to the control mutant pSSU T4A (Figure 20A middle-lower and lower), a particular mutant of the *Arabidopsis thaliana* pSSU carrying a mutation of amino acids 33-42 to alanine, of which import deficiency was previously described (Lee et al. 2006). The amount of GFP-fused SSU located in the cytosol (pSSU) and in the chloroplasts (mSSU) was visualised by immunoblotting with GFP antisera (Figure 20B). A reduction of mature SSU was observed in the case of the phosphor-mimicry S31/34D mutant, whereas the amount of mature pSSU S31/34A was identical to pSSU WT. Similarly, in import experiments with isolated chloroplasts from *Pisum sativum* a severe reduction of the import efficiency for pSSU S31/34D as compared to pSSU WT was observed, whereas pSSU S31/34A was efficiently imported (Figure 20C).

As second example pOE23 C-terminal GFP fusion protein and the corresponding mutant pOE23 S22A were also analysed and, like for pSSU, the import efficiency of the mutant was unchanged (Figure 20D).

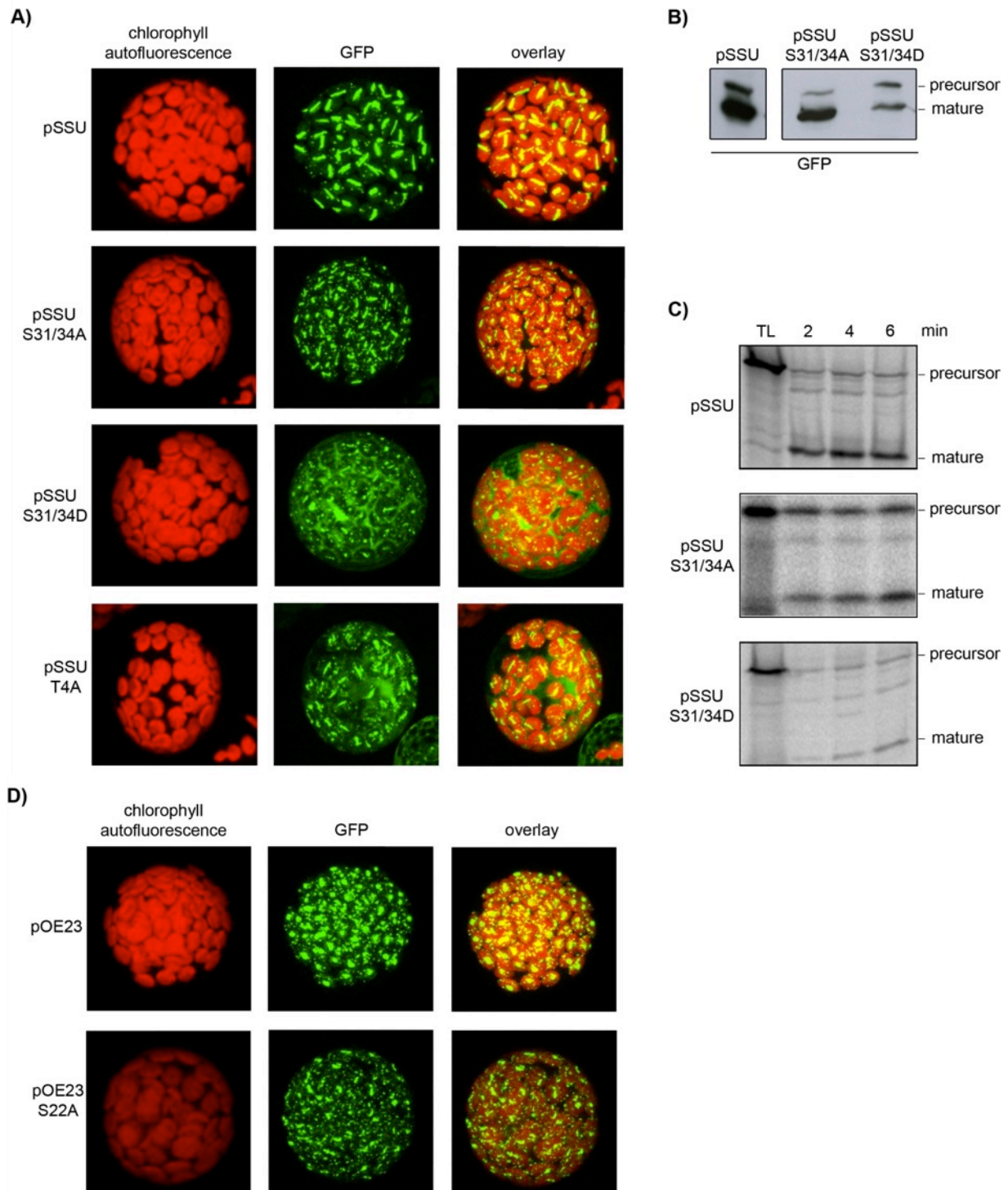


Figure 20. Preproteins import in *Arabidopsis* protoplasts. **A)** *Arabidopsis* protoplasts were isolated and transformed with pSSU, pSSU S31/34A, pSSU S31/34D and pSSU T4A C-terminal GFP fusion proteins. Pictures were obtained by confocal laser scanning microscopy. Chlorophyll fluorescence is shown in red and GFP in green. **B)** Transformed protoplasts were collected 16 h after transformation, lysed, subjected to SDS-PAGE and decorated with GFP antisera. The precursor of SSU and the mature form are shown. **C)** pSSU and pSSU S31/34D were translated in wheat germ lysate and imported into chloroplasts. TL shows 10 % of the translation input. The precursor form and the processed mature form are indicated. **D)** *Arabidopsis* protoplasts were isolated and transformed with pOE23 and pOE23 S22A C-terminal GFP fusion proteins. Pictures were obtained by confocal laser scanning microscopy. Chlorophyll fluorescence is shown in red and GFP in green.

Next, the import efficiency of pSSU was compared in protoplasts isolated from wild type, *sty8 sty17* and *sty8 sty46 sty17 Arabidopsis* plants. The GFP signal was observed only in the chloroplasts, indicating that in the mutants no reduction of the import efficiency occurred (Figure 21A).

Previous analysis of chloroplast ultrastructure (see 4.2.4) and of the greening process (see 4.2.5) indicated that the cotyledons are the main affected leafs in the kinase mutant plants. Therefore, the import efficiency of pSSU was analysed in protoplasts isolated from cotyledons of *Arabidopsis* wild type and *sty8 sty46* plants (Figure 21B). The import efficiency of pSSU resembled the one observed in the case of mesophyll-isolated protoplasts with no deficiency for the mutant.

To exclude that the impossibility to detect import deficiency was due to a too low expression of the GFP fusion proteins in *Arabidopsis* protoplasts, the import of pSSU and the pSSU S31/34A and pSSU T4A mutants was monitored in isolated *Nicotiana benthamiana* protoplasts, a system which permits a high expression of exogenous proteins. *Nicotiana benthamiana* plantlets were transiently transformed with *Agrobacterium tumefaciens* carrying constructs for the expression of C-terminal YFP fusion proteins. Protoplasts were isolated from transformed leafs and analysed with a confocal laser scanner microscope. Even if the YFP fusion proteins were expressed at a very high level, no cytosolic pSSU S31/34A was observed indicating an efficient import (Figure 21C upper and middle panels). In contrast, the import deficient control pSSU T4A clearly accumulated in the cytosol (Figure 21C lower panel).

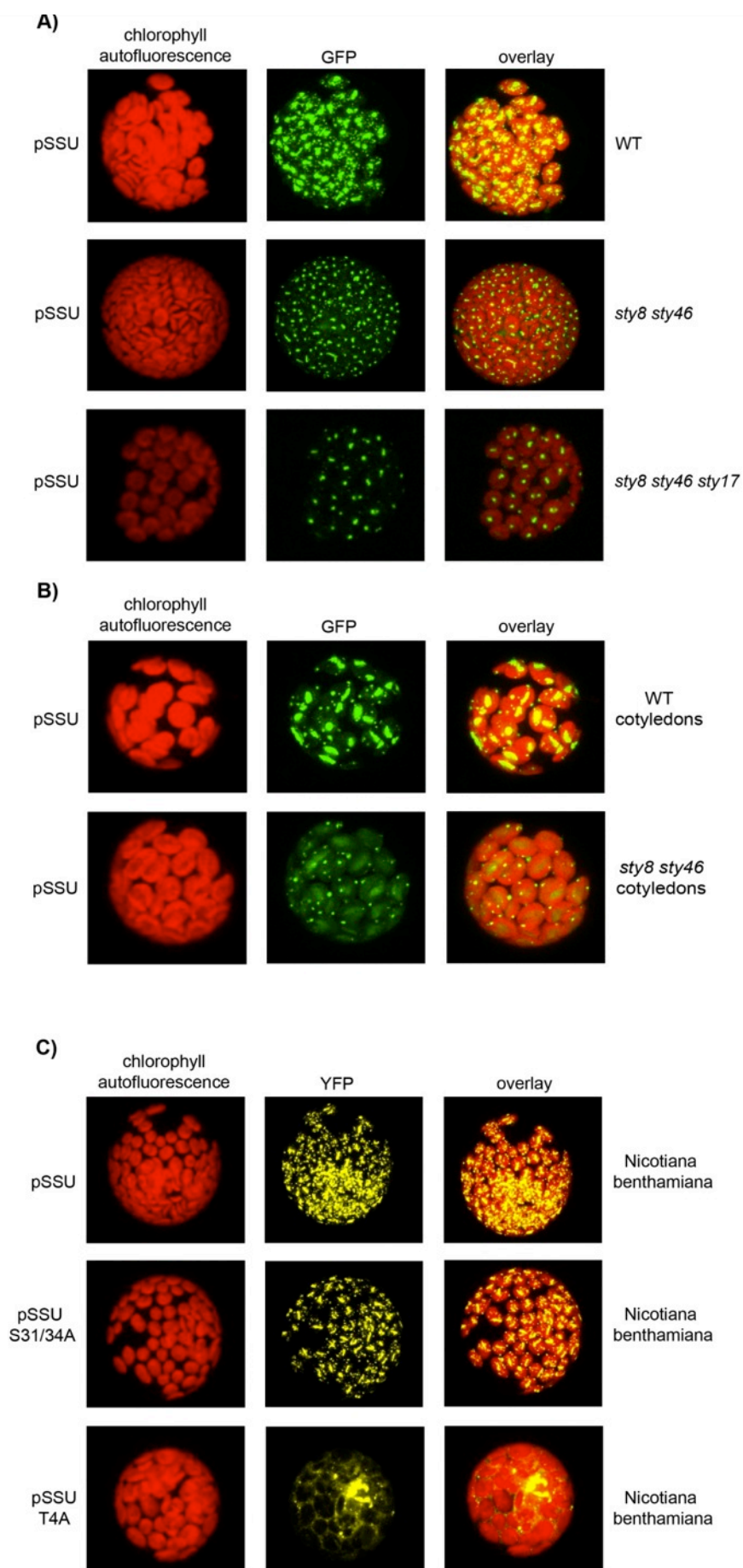
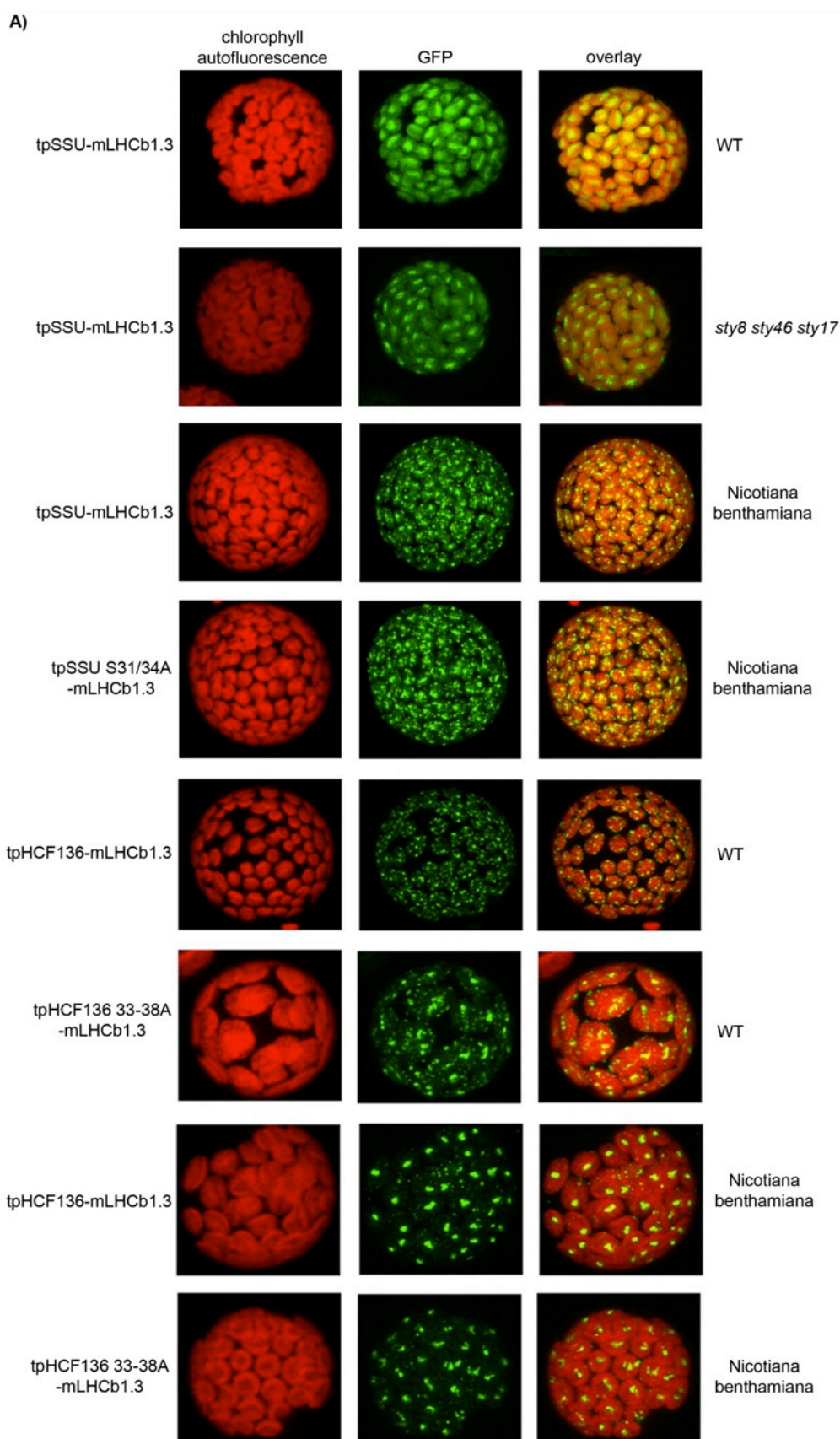


Figure 21. Preproteins import in *Arabidopsis* and *Nicotiana benthamiana* protoplasts. Pictures were obtained by confocal laser scanning microscopy. Chlorophyll fluorescence is shown in red, GFP in green and YFP in yellow. *Arabidopsis* protoplasts were isolated from **A)** wild type, *sty8 sty46* and *sty8 sty46 sty17* plants and **B)** cotyledons of wild type and *sty8 sty46* plants and transformed with pSSU C-terminal GFP fusion proteins. **C)** Protoplasts were isolated from *Nicotiana benthamiana* plantlets transiently transformed with *Agrobacterium tumefaciens* carrying constructs for the expression of pSSU, pSSU S31/34A and pSSU T4A C-terminal YFP fusion proteins.

In another attempt to detect import modification in the absence of preprotein phosphorylation, the transit peptide of pSSU was fused with the mature part of LHCb1.3 generating a chimera. This particular construct retains the phosphorylation site of the transit peptide of pSSU and the presence of the LHCb1.3 sequence confers a higher hydrophobicity that could promote the formation of cytosolic aggregates in the case of slowed down import. The C-terminal GFP fusion of the tpSSU-mLHCb1.3 chimera was expressed in wild type and *sty8 sty46 sty17 Arabidopsis* protoplasts (Figure 22A upper panels). No accumulation of precursor was observed in the cytosol. The same result was obtained by expressing tpSSU-mLHCb1.3 and the mutant tpSSU S31/34A-mLHCb1.3 in *Nicotiana benthamiana* (Figure 22A upper-middle panels).

As second example of high hydrophobic chimeric protein, the transit peptide of HCF136 was fused with the mature part of LHCb1.3. The import efficiency of the wild type GFP fusion construct was compared to the tpHCF136 33-38A-mLHCb1.3 mutant, in which the binding site for 14-3-3 present in the transit peptide of HCF136 was mutated to alanine. No accumulation of precursor was observed in the cytosol, in the case of both expressions in *Arabidopsis* (Figure 22A lower-middle panels) and *Nicotiana benthamiana* protoplasts (Figure 22A lower panels).

No differences in the import efficiency were observed also when the preprotein phosphorylation was abolished by treating the protoplasts with kinase inhibitors. After transient transformation with C-terminal GFP fusion tpSSU-mLHC1.3, *Arabidopsis* protoplasts were incubated with 100 μ M of the kinase inhibitors JNJ-10198409, Tyrphostin and Janex 1, which have been shown to inhibit STY8 (see 4.1.3). Also in this case it was not possible to detect any decrement in the import rate of chloroplast precursor proteins (Figure 22B).



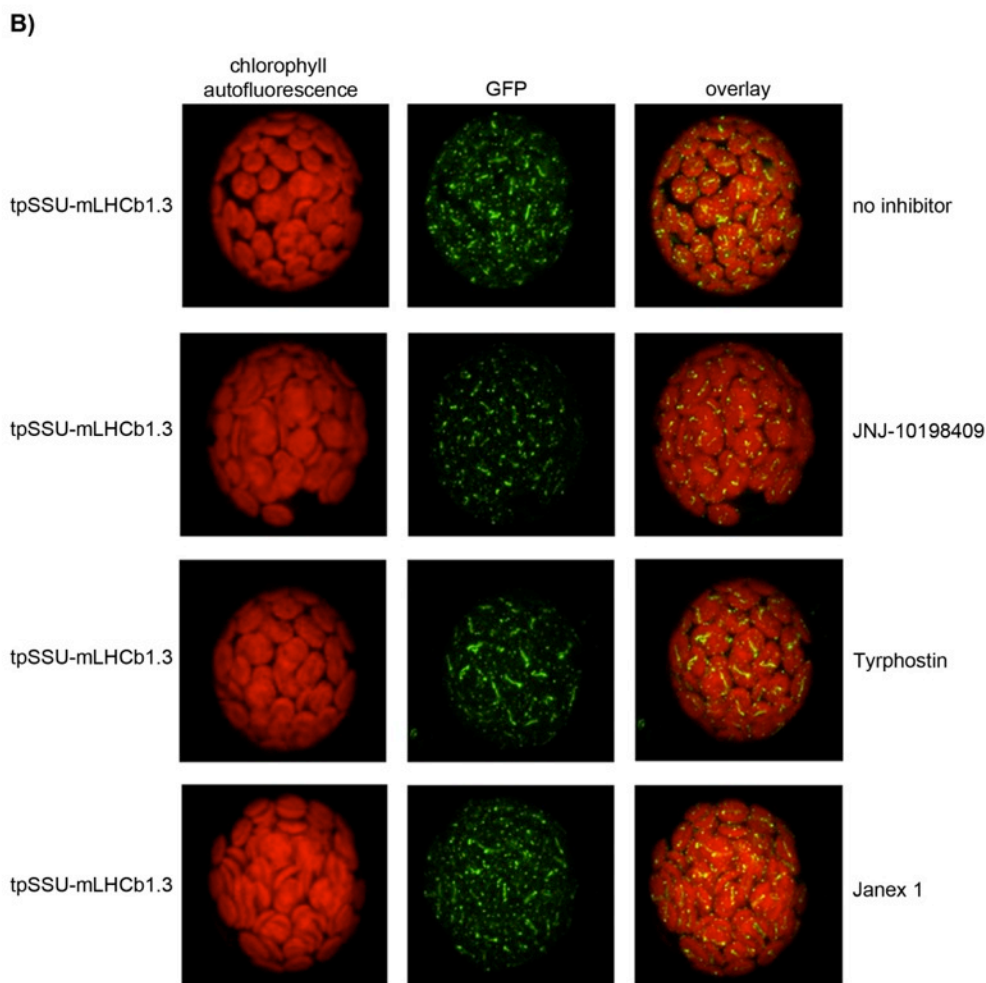


Figure 22. Preproteins import in *Arabidopsis* and *Nicotiana benthamiana* protoplasts. Pictures were obtained by confocal laser scanning microscopy. Chlorophyll fluorescence is shown in red and GFP in green. **A)** *Arabidopsis* protoplasts were isolated from wild type and *sty8 sty46 sty17* plants and transformed with tpSSU-mLHCb1.3 C-terminal GFP fusion proteins. Wild type *Arabidopsis* protoplasts were transformed also with tpHCF136-mLHCb1.3 and tpHCF136 33-38A-mLHCb1.3 C-terminal GFP fusion proteins. Protoplasts were isolated from *Nicotiana benthamiana* plantlets transiently transformed with *Agrobacterium tumefaciens* carrying constructs for the expression of tpSSU-mLHCb1.3, tpSSU S31/34A-mLHCb1.3 tpHCF136-mLHCb1.3 and tpHCF136 33-38A-mLHCb1.3 C-terminal GFP fusion proteins. **B)** *Arabidopsis* protoplasts were isolated from wild type plants and transformed with tpSSU-mLHCb1.3 C-terminal GFP fusion proteins and incubated with 100 μ M of JNJ-10196409, Tyrphostin or Janex-1.

5 DISCUSSION

5.1 *In vitro* characterization of STY8, STY17 and STY46

The cytosolic kinases STY8, STY17 and STY46 have been recently isolated from *Arabidopsis thaliana* as kinases responsible for transit peptide phosphorylation (Martin et al. 2006). These kinases belong to the *Arabidopsis* dual-specificity kinase family and contain typical serine/threonine as well as tyrosine kinase domains (Rudrabhatla et al. 2006). The catalytic domains of the three kinases have 11 conserved sub-domains characteristic of protein kinases and in subdomain VII and VIII is located the activation segment, which is flanked by the two highly conserved three-amino acids motifs DFG and APE. Since little is known about the mechanistic functioning of dual-specificity kinases in plants, a detailed analysis of the STY8, STY17 and STY46 features was performed *in vitro*.

5.1.1 Autophosphorylation of STY8, STY17 and STY46 is important for kinase activity

STY8, STY17 and STY46 perform autophosphorylation in *in vitro* kinase assays. This autophosphorylation appeared to be important for full activity of the kinases, since the dephosphorylated form of STY8 resulted to be much slower in the incorporation of radio-labeled phosphate if compared with wild type STY8. The autophosphorylation site for STY8, STY17 and STY46 was identified in mass spectrometric analysis and it consists in a conserved threonine residue which lies within the activation segment. Mutation of this threonine to a not-phosphorylatable alanine caused the complete loss of kinase activity, indicating that the autophosphorylation of this residue is essential for kinase activity. The phospho-mimicry mutant to which the threonine was substituted with aspartic acid appeared to be likewise not active. The mutations of the conserved threonine to glutamic acid, serine or tyrosine in STY8 also lead to the loss of the kinase activity. The absence of kinase activity in the phospho-mimicry mutant(s) and the impossibility to restore it with the introduction of a phosphorylatable serine or tyrosine residue is not surprising considering that autophosphorylation usually involves a conformational change which leads to the stabilization of the kinase in its active conformation (Nolen et al. 2004). Therefore, it is

reasonable to expect that any modification at the essential autophosphorylation site, even if designed to mimic the phosphorylated state of the kinase, might determine a destabilization of the active conformation leading to the loss of kinase activity.

Kinases can undergo autophosphorylation *in trans* by phosphorylation of an inactive molecule by an active molecule or via an intramolecular mechanism *in cis* as in the case of STY8. Intramolecular phosphorylation is a rather poorly characterized activation mechanism either depending on the help of molecular chaperones, such as HSP90, or involving translational intermediates to overcome conformational hindrances during autophosphorylation (Lochhead 2009). In the present study the autophosphorylation process was analysed *in vitro* in the presence of the recombinant kinase only, thus further analysis will be necessary to verify whether other binding partners are required for STY8 maturation.

5.1.2 The ACT domain might regulate the kinase activity in vivo

Sequence analysis of STY8, STY17 and STY46 revealed the presence of an ACT domain located upstream to the kinase domains. This conserved domain has been described as a small molecule binding regulative domain mainly found in enzymes involved in amino acids and purine metabolism. The deletion of the ACT domain in STY8 lead to an increment of the kinase activity, almost doubled, suggesting a role of this domain in the regulation of the kinase activity possibly upon binding of metabolites or other small molecules. Since the ACT deletion boosted the activity of STY8, it is likely that the binding of ligand(s) to the ACT domain has an inhibitory effect on the kinase activity. Several small molecules and other substances, including amino acids and purines, have been tested for their ability to influence the kinase activity but none of them appeared to alter the activity of STY8. Nevertheless, it cannot be excluded that *in planta* other ligands might come in to play in the regulation of the kinase activity upon binding to the ACT domain, possibly when the metabolites composition of the cell changes upon stress conditions or environmental modifications.

5.1.3 STY8 differs from other plant STY kinases

STY8, STY17 and STY46 belong to the *Arabidopsis* dual-specificity kinase family which members have been shown to phosphorylate hydroxyl groups of serines, threonines as well as tyrosines (Reddy and Rajasekharan 2007; Rudrabhatla et al. 2006). STY8, STY17 and STY46 present three conserved motifs, which are responsible for the substrate specificity, located in subdomain VI, VIII and XI. The first motif (DLKTAN), located in subdomain VI, differs from both typical serine/threonine and tyrosine kinase motifs, which are usually DLKPEN and DLR/AAR/AN, respectively (Hanks et al. 1988). Surprisingly, in the present study it was found that the lysine residue (at position 409 in STY8) lying within this motif is essential for the kinase activity, emphasizing a certain importance of the conservation of this motif. The second motif (GTYRWMAPE) conferring substrate specificity is located in subdomain VIII and lies within the activation segment. This motif is typical for plant dual specificity kinases (Rudrabhatla et al. 2006). The third motif (CW(X)₆RPXF) is located in subdomain XI and is typical for tyrosine kinases. The screening of kinase inhibitors performed in this study revealed that STY8 is inhibited by JNJ-10198409, Tyrphostin, and Janex 1, three specific tyrosine kinase inhibitors. Thus, STY8 appears to share features with tyrosine kinases, most likely structurally, which allows blocking of kinase activity by the tyrosine kinase specific inhibitors. However, STY8 did not show any tyrosine phosphorylation activity, only serine and threonine emerged to be phosphorylated in the case of both auto- and substrate phosphorylation. STY8 seems therefore to differ from classical dual specificity kinases, retaining only the sequence similarity but not the ability to phosphorylate also tyrosine residues. On the one hand it is surprising that STY8 does not phosphorylate tyrosine residues as the STY8 sequence presents a motif 2 typical for dual specificity kinases and a motif 3 typical for tyrosine kinases and as STY8 activity can be inhibited by typical tyrosine kinase inhibitors. On the other hand it has to be considered that tyrosine residues are almost absent in chloroplast transit peptides (Zhang and Glaser 2002), which are STY8 substrates. Therefore, tyrosine phosphorylation is dispensable for the cellular function of STY8, STY17 and STY46 and it might consequently have been lost during evolution.

5.2 *In vivo* characterization of STY8, STY17 and STY46

5.2.1 STY8, STY17 and STY46 are involved in etioplast to chloroplast transition

In the present work, *Arabidopsis* knockout/knockdown mutant lines for STY8, STY17 and STY46 have been extensively analysed in order to elucidate the function of the three kinases *in vivo*. When grown under light conditions, the mutant plants appeared to be retarded in growth but did not show any defect in the photosynthetic activity as well as in the accumulation of nuclear encoded chloroplast proteins (data not shown). However, when the greening process was analysed it was observed that the transition from etioplast to chloroplast was affected in the mutants. After 4 h of light exposition, chlorophyll *a* measurements revealed that in mutant plants Fv/Fm was reduced to 50% of the wild type, whereas wild type and mutants reached the same photosynthetic efficiency after 22 h of illumination, indicating that the phenotype is most prominent early during the greening process. Immunoblot analyses revealed a slowed accumulation of nuclear encoded chloroplast proteins in the mutants to 50-80 % of the wild type level. Notably, the mRNA levels of the reduced proteins were unchanged as well as in the case of chloroplast encoded proteins, pointing at a post-translational defect, the absence of transit peptide phosphorylation, as cause for the slowed protein accumulation. Interestingly, three of the slowed accumulated proteins, HCF136, CF0- γ and LHCII, have been described to be phosphorylated in their transit peptides (Martin et al. 2006; Waegemann and Soll 1996). In the present study it was additionally proven that the other reduced proteins, LHCb2, CF1-II, PAC and HCF101, could likewise be phosphorylated by STY8. In the case of LHCb2, CF1-II and HCF101 it was also possible to show that the phosphorylation occurs within the transit peptide. The slowed accumulation and the transit peptide phosphorylation of HCF136 are particularly interesting because this protein is indispensable for PSII assembly and its reduction correlates with the observed reduction of the photosynthetic activity. Furthermore, HCF136 together with CF0- γ and CF1-II present at least one common 14-3-3 binding motif in their N-terminal sequence at position 33-38, 42-47 and 37-42/48-53, respectively. Contrarily,

among the proteins found not to be reduced, only OE23 has a predicted 14-3-3 binding site. Tobacco pSSU has been shown to be phosphorylated and to bind 14-3-3 (May and Soll 2000). In the present work reduction of the pSSU accumulation in the *Arabidopsis* mutants was not observed. This discrepancy might be explained with the fact that the predicted binding motif from Tobacco pSSU differs slightly from the common 14-3-3 motif and from the motifs found in *Arabidopsis* isoforms. Taken together, these results support the model proposing transit peptide phosphorylation as enhancer for 14-3-3 binding and preprotein import (May and Soll 2000).

5.2.2 STY8, STY17 and STY46 depletion leads to chloroplast ultrastructure modification

STY8, STY17 and STY46 mutant plants show chloroplast ultrastructural changes in cotyledons. Analysis of 7-days old cotyledons on the ultrastructural level revealed distinct changes between wild type and mutants concerning the formation and shape of thylakoids. The defined poles appeared unstructured, thylakoids were less appressed and the thylakoid lumen was swollen. Possibly, this is due to the lack of several photosynthetic membrane and luminal proteins or proteins involved in lipid trafficking and thylakoid formation as has been observed in photosynthesis mutants, such as mutants deficient in the ATP synthase assembly (Benz et al. 2009; Bosco et al. 2004). The massive accumulation of vesicles may be due to the retarded development, since vesicle trafficking is involved in the formation of thylakoids (Joyard et al. 1998; Westphal et al. 2003). In 14-days old mutant plants the phenotype was less severe, however thylakoids still often appeared disordered and unstructured. Apart from the observed defects in cotyledons, a general retardation in growth was observed in the mutants, indicating that any disturbance at the cotyledon stage has a more severe impact in the plant differentiation and development. In line with this idea, no ultrastructural changes have been observed in differentiated chloroplasts. This indicates that the STY kinases play an important role in particular early in the plant development. During germination and immediately upon illumination in the cotyledons etioplasts are converted into

chloroplast to facilitate the transition from heterotrophic to autotrophic growth and enable seedlings to photosynthesize. To be performed efficiently, this process requires not only chloroplast encoded proteins but also the massive influx of nuclear encoded protein into the chloroplasts. Therefore, the defect in chloroplast biogenesis observed in STY8, STY17 and STY46 mutant plants hints at a regulatory or kinetic function of transit peptide phosphorylation during chloroplast development by facilitating preprotein import. Beside de-etiolation, the STY kinases might also be important in other developmental stages which require the massive influx of nuclear encoded chloroplast proteins, such as cell differentiation and growth. Therefore the physiological relevance of STY kinases is most pronounced during differentiation phases and less important or even dispensable during phases of maintenance as in fully differentiated adult leave tissue.

5.3 Chloroplast precursor phosphorylation

5.3.1 Transit peptide phosphorylation is not essential for import into chloroplasts

In the present study, an extensive analysis on preprotein import in isolated protoplasts was performed in order to investigate whether a less efficient import caused by the lack of phosphorylation could be visualized by accumulation of preproteins in the cytosol. The comparison of GFP fusion proteins, pSSU and pOE23, with their non-phosphorylatable mutants revealed similar accumulation of fusion proteins. Similarly, no differences in preprotein accumulation were observed when the experiments were performed using expression of GFP proteins in Tobacco, mediated by transient transformation with *Agrobacterium tumefaciens*. When GFP fusion proteins were expressed in protoplasts isolated from *sty8 sty46* and *sty8 sty17 sty46* mutant plants, both from cotyledons and true leaves, the import appeared to yield similar quantities of imported protein as in the wild type protoplasts. Also the addition of kinase inhibitors or the use of high hydrophobic chimeras did not interfere with the protein accumulation of GFP fusion proteins in isolated protoplasts. Taken together these results suggest that transit peptide phosphorylation is not essential for preprotein import, however caution is necessary to interpret the above data because they

only represent an end-point measurement, since no kinetic analysis are possible in this experimental setup. Nevertheless, the present study has demonstrated that *in planta* the absence of the STY kinases responsible for this phosphorylation leads to slowed accumulation of nuclear encoded chloroplast proteins. Furthermore, it has been previously shown that transit peptide phosphorylation is necessary for the formation of the guidance complex which enhances the import rate of chloroplast preproteins (May and Soll 2000). Therefore, the failure in the detection of slowed import of GFP fusion proteins might be due to different reasons. First, protoplasts from green leaves were used, in which transit peptide phosphorylation appears not to be physiological relevant as it has been discussed previously in this work. Second, the GFP fusion proteins are highly overexpressed in protoplasts, condition that does not resemble the physiological expression of chloroplast precursor proteins in the cell. Thirdly, it cannot be excluded that in isolated protoplasts the import is slightly slowed but that the precursors do not accumulate in the cytosol due to a fast protein turnover that leads to preprotein degradation.

5.3.2 Transit peptide dephosphorylation is essential for import into chloroplasts

A first indication that chloroplast preproteins need to be dephosphorylated to be efficiently imported into the chloroplast was obtained performing import experiment in the presence of the phosphatase inhibitor NaF. The addition of the unspecific phosphatase inhibitor NaF prohibits import of phosphorylated preproteins. Furthermore, import is hindered by introduction of a thiophosphate group which is significantly slower dephosphorylated, suggesting that the activity of a phosphatase might be required for successful import (Waegemann and Soll 1996). Following this notion, it was investigated whether the dephosphorylation of the transit peptide is a prerequisite for efficient import. Therefore, a phospho-mimicry mutant of the model substrate pSSU was generated and transiently expressed as GFP fusion in *Arabidopsis* isolated protoplasts. The phospho-mimicry mutant appeared to accumulate in the cytosol, pointing at a slowed import. Taken together these results indicate that dephosphorylation of precursor proteins is an important step for efficient

import, implying that not only phosphorylation but also dephosphorylation by a yet unidentified phosphatase regulates import of nuclear encoded proteins into the chloroplast. Therefore it might be speculated that these modifications of chloroplast transit peptides are an important developmental mechanisms to regulate chloroplast biogenesis on a post-translational level allowing the plant to react dynamically in response to environmental changes.

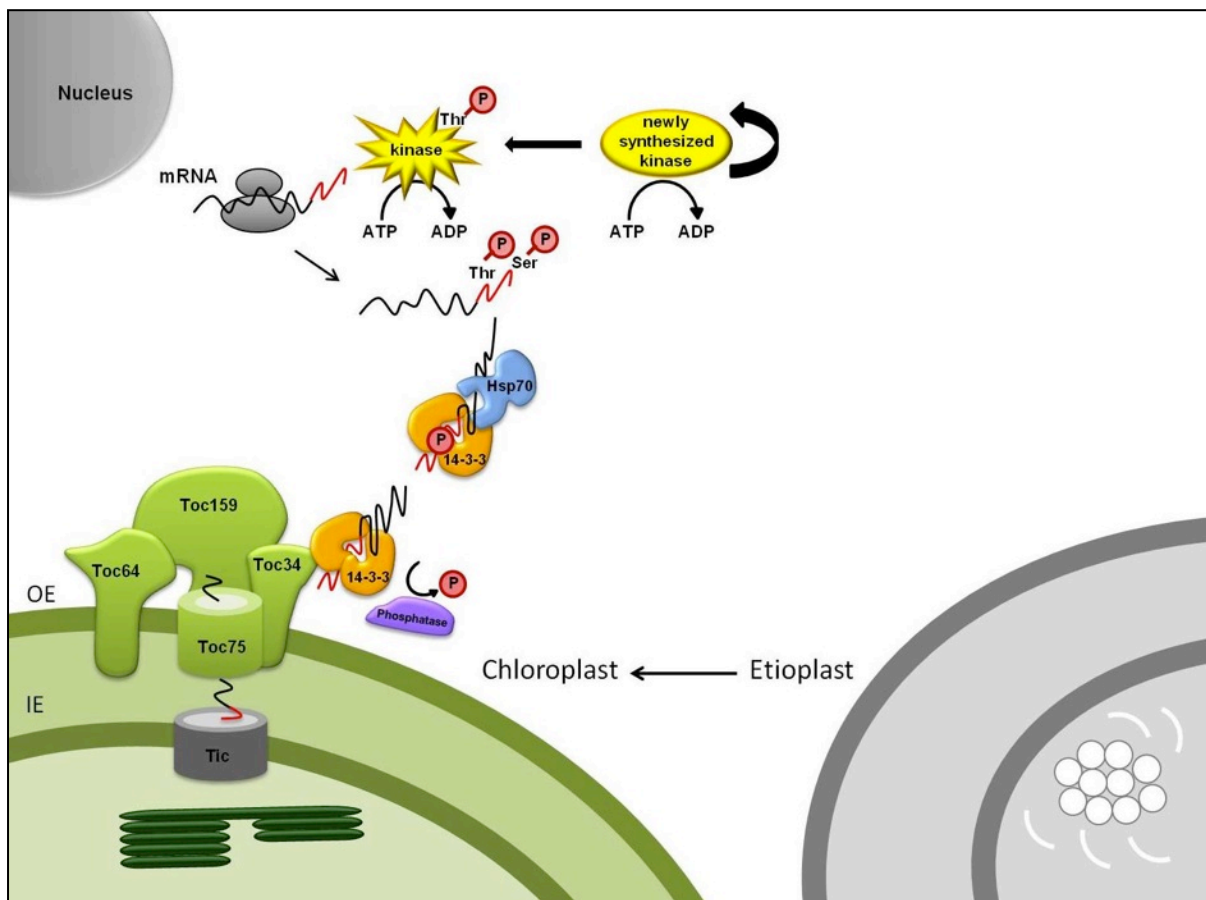


Figure 23. Model of cytosolic phosphorylation of chloroplast transit peptides. The cytosolic kinases are phosphorylated by an intramolecular event resulting in active kinase molecules, which can subsequently post-translationally phosphorylate chloroplast transit peptides on serine and threonine residues. Phosphorylation and 14-3-3 binding enhances association with the Toc receptor, from where the proteins are imported after dephosphorylation by an as yet unidentified protein phosphatase. Transit peptide phosphorylation is responsible for efficient chloroplast biogenesis and is involved in the transition from etioplast to chloroplast.

5.4 Future perspectives

The present study contributes to the comprehension of the mechanisms regulating protein import into the chloroplasts at a cytosolic level. The role of transit peptide phosphorylation and in particular the kinases responsible for this phosphorylation have been dissected in detail. Nevertheless, some work remains to be done in order to completely shed light on the cytosolic regulation of protein import.

Since so far the formation of the cytosolic guidance complex has been shown only in wheat germ lysate (May and Soll 2000), an important goal would be to prove the formation of this complex also *in vivo*. This approach is challenging because the process is extremely transient and short lived. One possibility to approach this question could be the use of a construct harboring a truncated transit peptide of pSSU (amino acids 1-47), which is not fully imported into the chloroplast and remains longer in the cytosol (Figure 24). The GFP fusion of this protein expressed in isolated protoplasts can be immunoprecipitated using GFP antisera coupled to Protein A sepharose and detected by immunoblotting with GFP antisera. Stable *Arabidopsis* transgenic lines expressing this construct, both in wild type and in the STY kinase mutants background, could be generated to subject larger amounts of plant material to the analyses. With this method it would be possible to assess the 14-3-3 and HSP70 binding capacity of transit peptides *in vivo* in wild type and mutant plants by co-immunoprecipitation with the GFP-tagged truncated transit peptide and detection with 14-3-3/HSP70 antisera. Moreover it would also be possible to identify putative additional interaction partners by co-immunoprecipitation and subsequent silverstaining and mass spectrometric analyses.

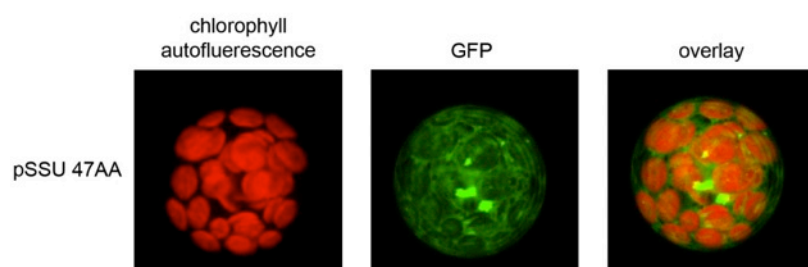


Figure 24. A truncated variant of pSSU accumulate in the cytosol. The first 47 amino acids of pSSU from Tobacco were fused N-terminally to GFP and expressed transiently in *Arabidopsis* protoplasts. GFP and chloroplast fluorescence were monitored with a confocal laser scanning microscope.

Another interesting and challenging goal would be the identification of the phosphatase responsible for the transit peptide dephosphorylation. The *Arabidopsis* genome harbors 150 phosphatases (Kerk et al. 2002; Kerk et al. 2008). However, the list of possible candidates can be reduced since phosphatases with an already known function or a clear prediction of a signaling peptide for mitochondria or chloroplasts (TargetP) can be excluded because the expected phosphatase could localize in the cytosol or at the outer envelope membrane. Tyrosine specific phosphatases can be also excluded, since transit peptides are only phosphorylated on serine and threonine residues. A possible approach to further shorten the list would be to perform import experiment in the presence of different specific phosphatase inhibitors. The biochemical and physiological features of the remaining phosphatases could then be used to identify the respective phosphatase.

6 REFERENCES

- Andres, C., Agne, B., and Kessler, F. (2010), 'The TOC complex: preprotein gateway to the chloroplast', *Biochim Biophys Acta*, 1803 (6), 715-23.
- Arnon, D. J. (1949), 'Copper enzymes in isolated chloroplasts. Polyphenoloxidase in *Beta vulgaris*', *Plant Physiol*, 24, 1-15.
- Balsera, M., Soll, J., and Buchanan, B. B. (2010), 'Redox extends its regulatory reach to chloroplast protein import', *Trends Plant Sci*, 15 (9), 515-21.
- Benz, M., et al. (2009), 'Alb4 of Arabidopsis promotes assembly and stabilization of a non chlorophyll-binding photosynthetic complex, the CF1CF0-ATP synthase', *Mol Plant*, 2 (6), 1410-24.
- Bhushan, S., et al. (2010), 'Structural basis for translational stalling by human cytomegalovirus and fungal arginine attenuator peptide', *Mol Cell*, 40 (1), 138-46.
- Bosco, C. D., et al. (2004), 'Inactivation of the chloroplast ATP synthase gamma subunit results in high non-photochemical fluorescence quenching and altered nuclear gene expression in Arabidopsis thaliana', *J Biol Chem*, 279 (2), 1060-9.
- Bridges, D. and Moorhead, G. B. (2005), '14-3-3 proteins: a number of functions for a numbered protein', *Sci STKE*, 2005 (296), re10.
- Bruce, B. D. (2000), 'Chloroplast transit peptides: structure, function and evolution', *Trends Cell Biol*, 10 (10), 440-7.
- Clough, S. J. and Bent, A. F. (1998), 'Floral dip: a simplified method for Agrobacterium-mediated transformation of Arabidopsis thaliana', *Plant J*, 16 (6), 735-43.
- de la Fuente van Bentem, S. and Hirt, H. (2009), 'Protein tyrosine phosphorylation in plants: More abundant than expected?', *Trends Plant Sci*, 14 (2), 71-6.
- Dougherty, M. K. and Morrison, D. K. (2004), 'Unlocking the code of 14-3-3', *J Cell Sci*, 117 (Pt 10), 1875-84.
- Durek, P., et al. (2009), 'Detection and characterization of 3D-signature phosphorylation site motifs and their contribution towards improved phosphorylation site prediction in proteins', *BMC Bioinformatics*, 10, 117.

- Emanuelsson, O., et al. (2007), 'Locating proteins in the cell using TargetP, SignalP and related tools', *Nat Protoc*, 2 (4), 953-71.
- Fellerer, C., et al. (2011), 'Cytosolic HSP90 Cochaperones HOP and FKBP Interact with Freshly Synthesized Chloroplast Preproteins of Arabidopsis', *Mol Plant*.
- Grant, G. A. (2006), 'The ACT domain: a small molecule binding domain and its role as a common regulatory element', *J Biol Chem*, 281 (45), 33825-9.
- Hanks, S. K., Quinn, A. M., and Hunter, T. (1988), 'The protein kinase family: conserved features and deduced phylogeny of the catalytic domains', *Science*, 241 (4861), 42-52.
- Heazlewood, J. L., et al. (2008), 'PhosPhAt: a database of phosphorylation sites in *Arabidopsis thaliana* and a plant-specific phosphorylation site predictor', *Nucleic Acids Res*, 36 (Database issue), D1015-21.
- Hrabak, E. M., et al. (2003), 'The Arabidopsis CDPK-SnRK superfamily of protein kinases', *Plant Physiol*, 132 (2), 666-80.
- Hunter, T. (1987), 'A thousand and one protein kinases', *Cell*, 50 (6), 823-9.
- Ito, J., et al. (2009), 'A survey of the Arabidopsis thaliana mitochondrial phosphoproteome', *Proteomics*, 9 (17), 4229-40.
- Ivey, R. A., 3rd, Subramanian, C., and Bruce, B. D. (2000), 'Identification of a Hsp70 recognition domain within the rubisco small subunit transit peptide', *Plant Physiol*, 122 (4), 1289-99.
- Joyard, J., et al. (1998), 'The biochemical machinery of plastid envelope membranes', *Plant Physiol*, 118 (3), 715-23.
- Kerk, D., Templeton, G., and Moorhead, G. B. (2008), 'Evolutionary radiation pattern of novel protein phosphatases revealed by analysis of protein data from the completely sequenced genomes of humans, green algae, and higher plants', *Plant Physiol*, 146 (2), 351-67.
- Kerk, D., et al. (2002), 'The complement of protein phosphatase catalytic subunits encoded in the genome of Arabidopsis', *Plant Physiol*, 129 (2), 908-25.

- Kovacs-Bogdan, E., Soll, J., and Bolter, B. (2010), 'Protein import into chloroplasts: the Tic complex and its regulation', *Biochim Biophys Acta*, 1803 (6), 740-7.
- Krupa, A., Anamika, and Srinivasan, N. (2006), 'Genome-wide comparative analyses of domain organisation of repertoires of protein kinases of *Arabidopsis thaliana* and *Oryza sativa*', *Gene*, 380 (1), 1-13.
- Lazo, G. R., Stein, P. A., and Ludwig, R. A. (1991), 'A DNA transformation-competent *Arabidopsis* genomic library in *Agrobacterium*', *Biotechnology (N Y)*, 9 (10), 963-7.
- Lee, D. W., et al. (2006), 'Functional characterization of sequence motifs in the transit peptide of *Arabidopsis* small subunit of rubisco', *Plant Physiol*, 140 (2), 466-83.
- Lochhead, P. A. (2009), 'Protein kinase activation loop autophosphorylation in cis: overcoming a Catch-22 situation', *Sci Signal*, 2 (54), pe4.
- Luan, S. (2002), 'Tyrosine phosphorylation in plant cell signaling', *Proc Natl Acad Sci U S A*, 99 (18), 11567-9.
- Martin, T., et al. (2006), 'A protein kinase family in *Arabidopsis* phosphorylates chloroplast precursor proteins', *J Biol Chem*, 281 (52), 40216-23.
- May, T. and Soll, J. (2000), '14-3-3 proteins form a guidance complex with chloroplast precursor proteins in plants', *Plant Cell*, 12 (1), 53-64.
- Mayer, M. P. and Bukau, B. (2005), 'Hsp70 chaperones: cellular functions and molecular mechanism', *Cell Mol Life Sci*, 62 (6), 670-84.
- Menke, W. (1960), 'Einige Beobachtungen zur Entwicklungsgeschichte der Plastiden von *Elodea canadensis*.', *Z Naturf* 15, 800-04.
- Meurer, J., Berger, A., and Westhoff, P. (1996), 'A nuclear mutant of *Arabidopsis* with impaired stability on distinct transcripts of the plastid psbB, psbD/C, ndhH, and ndhC operons', *Plant Cell*, 8 (7), 1193-207.
- Meurer, J., et al. (1998a), 'A nuclear-encoded protein of prokaryotic origin is essential for the stability of photosystem II in *Arabidopsis thaliana*', *EMBO J.*, 17 (18), 5286-97.
- Meurer, J., et al. (1998b), 'The PAC protein affects the maturation of specific chloroplast mRNAs in *Arabidopsis thaliana*', *Mol. Gen. Genet.*, 258 (4), 342-51.

- Nakrieko, K. A., Mould, R. M., and Smith, A. G. (2004), 'Fidelity of targeting to chloroplasts is not affected by removal of the phosphorylation site from the transit peptide', *Eur J Biochem*, 271 (3), 509-16.
- Nolen, B., Taylor, S., and Ghosh, G. (2004), 'Regulation of protein kinases; controlling activity through activation segment conformation', *Mol Cell*, 15 (5), 661-75.
- Paetzel, M., et al. (2002), 'Signal peptidases', *Chem Rev*, 102 (12), 4549-80.
- Porra, R.J. , Thompson, W.A, Kriedemann, P.E. (1989), 'Determination of accurate extinction coefficients and simultaneous equations for assaying chlorophylls a and b extracted with four different solvents: verification of the concentration of chlorophyll standards by atomic absorption spectroscopy', *Biochimica et Biophysica Acta* 975 384-94.
- Pyke, K. (2007), 'Plastid biogenesis and differentiation', in R. Bock (ed.), *Cell and Molecular Biology of Plastids*. (Berlin-Heidelberg: Springer), 1-28.
- Qbadou, S., et al. (2006), 'The molecular chaperone Hsp90 delivers precursor proteins to the chloroplast import receptor Toc64', *EMBO J*, 25 (9), 1836-47.
- Reddy, M. M. and Rajasekharan, R. (2006), 'Role of threonine residues in the regulation of manganese-dependent arabidopsis serine/threonine/tyrosine protein kinase activity', *Arch Biochem Biophys*, 455 (2), 99-109.
- Reddy, M. M. and Rajasekharan, R. (2007), 'Serine/threonine/tyrosine protein kinase from Arabidopsis thaliana is dependent on serine residues for its activity', *Arch Biochem Biophys*, 460 (1), 122-8.
- Reynolds, E.S. (1963), 'The use of lead citrate at high pH as an electron opaque stain in electron microscopy', *Journal of Cell Biology* 17, 208.
- Rudrabhatla, P., Reddy, M. M., and Rajasekharan, R. (2006), 'Genome-wide analysis and experimentation of plant serine/ threonine/tyrosine-specific protein kinases', *Plant Mol Biol*, 60 (2), 293-319.
- Schleiff, E., Jelic, M., and Soll, J. (2003), 'A GTP-driven motor moves proteins across the outer envelope of chloroplasts', *Proc Natl Acad Sci U S A*, 100 (8), 4604-9.

- Schleiff, E., et al. (2002), 'Structural and guanosine triphosphate/diphosphate requirements for transit peptide recognition by the cytosolic domain of the chloroplast outer envelope receptor, Toc34', *Biochemistry*, 41 (6), 1934-46.
- Schwenkert, S., Soll, J., and Bolter, B. (2011), 'Protein import into chloroplasts--how chaperones feature into the game', *Biochim Biophys Acta*, 1808 (3), 901-11.
- Schwenkert, S., et al. (2010), 'Chloroplast HCF101 is a scaffold protein for [4Fe-4S] cluster assembly', *Biochem J*, 425 (1), 207-14.
- Schwenkert, S., et al. (2006), 'Psbl affects the stability, function, and phosphorylation patterns of photosystem II assemblies in tobacco', *J Biol Chem*, 281 (45), 34227-38.
- Spurr, A. E. (1969), 'A low-viscosity epoxy resin embedding medium for electron microscopy', *J Ultrastruct Res* 26, 31-41.
- Summy, J. M., et al. (2003), 'The SH4-Unique-SH3-SH2 domains dictate specificity in signaling that differentiate c-Yes from c-Src', *J Cell Sci*, 116 (Pt 12), 2585-98.
- Tang, H., et al. (2008), 'Synteny and collinearity in plant genomes', *Science*, 320 (5875), 486-8.
- Waagemann, K. and Soll, J. (1995), 'Characterization and isolation of the chloroplast protein import machinery', *Methods Cell Biol*, 50, 255-67.
- Waagemann, K. and Soll, J. (1996), 'Phosphorylation of the transit sequence of chloroplast precursor proteins', *J Biol Chem*, 271 (11), 6545-54.
- Westphal, S., Soll, J., and Vothknecht, U. C. (2003), 'Evolution of chloroplast vesicle transport', *Plant Cell Physiol*, 44 (2), 217-22.
- Zhang, X. P. and Glaser, E. (2002), 'Interaction of plant mitochondrial and chloroplast signal peptides with the Hsp70 molecular chaperone', *Trends Plant Sci*, 7 (1), 14-21.

7 APPENDIX

7.1 Phosphorylated residues in STY8, STY17 and STY46

Protein	Modified peptide	Enrichment	Tissue	Score
AT2G17700	G(pT)Y(*C)(pS)QEVAIK			17
AT2G17700	VQIE(s)GV(oxM)(t)AE(t)G(t)(y)R	TiO2 or Fe-IMAC	seedling	78,92
AT2G17700	VQIE(s)GV(oxM)(t)AE(t)G(t)(y)R	TiO2 or Fe-IMAC	rosette	110,3
AT2G17700	VQIE(s)GV(oxM)(t)AE(t)G(t)(y)R	TiO2 or Fe-IMAC	rosette	104,49
AT2G17700	VQIE(s)GV(oxM)(t)AE(t)G(t)(y)R	TiO2 or Fe-IMAC	rosette	97,33
AT2G17700	VQIE(s)GV(oxM)(t)AE(t)G(t)(y)R	TiO2 or Fe-IMAC	rosette	3131
AT2G17700	VQIE(s)GV(oxM)(t)AE(t)G(t)(y)R	TiO2 or Fe-IMAC	rosette	3767
AT2G17700	VQIE(s)GV(oxM)(t)AE(t)G(t)(y)R	TiO2 or Fe-IMAC	rosette	1844
AT2G17700	VQIE(s)GV(oxM)(t)AE(t)G(t)(y)R	TiO2 or Fe-IMAC	rosette	85,67
AT2G17700	VQIE(s)GV(oxM)(t)AE(t)G(t)(y)R	TiO2 or Fe-IMAC	seedling	2883
AT2G17700	VQIE(s)GV(oxM)(t)AE(t)G(t)(y)R	TiO2 or Fe-IMAC	rosette	3435
AT2G17700	VQIE(s)GVM(t)AE(t)G(t)(y)R	TiO2 or Fe-IMAC	rosette	3993
AT2G17700	VQIE(s)GVM(t)AE(t)G(t)(y)R	TiO2 or Fe-IMAC	rosette	3021
AT2G17700	VQIE(s)GVM(t)AE(t)G(t)(y)R	TiO2 or Fe-IMAC	rosette	2665
AT2G17700	VQIE(s)GVM(t)AE(t)G(t)(y)R	TiO2 or Fe-IMAC	rosette	132,53
AT2G17700	VQIE(s)GVM(t)AE(t)G(t)(y)R	TiO2 or Fe-IMAC	rosette	84,75
AT2G17700	VQIE(s)GVM(t)AE(t)G(t)(y)R	TiO2 or Fe-IMAC	rosette	81,73
AT2G17700	VQIESGV(oxM)(pT)AETGTYR	TiO2	cell culture	98
AT2G17700	VQIESGVM(pT)AETGTYR	Fe-IMAC	cell culture	47239
AT2G17700	VQIESGVM(pT)AETGTYR	TiO2 or Fe-IMAC	rosette	40,01
AT2G17700	VQIESGVM(pT)AETGTYR	TiO2	cell culture	93
AT2G17700	VQIESGVM(pT)AETGTYR			93
AT2G17700	VQIESGVM(pT)AETGTYR	TiO2 or Fe-IMAC	rosette	3345
AT2G17700	VQIESGVM(pT)AETGTYR	Ga2+	seedling	33,9
AT2G17700	VQIESGVM(pT)AETGTYR	TiO2 or Fe-IMAC	rosette	92,16
AT4G35780	AVVA(s)I(t)KE(s)PR	TiO2 or Fe-IMAC	rosette	1307
AT4G35780	AVVA(s)I(t)KE(s)PR	TiO2 or Fe-IMAC	rosette	36,15
AT4G35780	VQ(t)E(s)GV(oxM)(t)AE(t)G(t)(y)R	TiO2 or Fe-IMAC	seedling	60,78
AT4G35780	VQ(t)E(s)GV(oxM)(t)AE(t)G(t)(y)R	TiO2 or Fe-IMAC	seedling	2101
AT4G35780	VQTESGVM(pT)AETGTYR			44
AT4G38470	AQTGVM(pT)AETGTYR	TiO2	cell culture	54
AT4G38470	AQTGVM(pT)AETGTYR	TiO2 or Fe-IMAC	seedling	75,33
AT4G38470	AQTGVM(pT)AETGTYR			54
AT4G38470	AQTGVM(pT)AETGTYR	Fe-IMAC	cell culture	15067
AT4G38470	AQTGVM(pT)AETGTYR	Ga2+	seedling	68
AT4G38470	AQTGVM(pT)AETGTYR	Ga2+	seedling	
AT4G38470	AQTGVM(pT)AETGTYR	TiO2 or Fe-IMAC	seedling	16497
AT4G38470	IELQ(s)Q(s)WP(oxM)QQ(s)F(s)P EKENGQ(t)GAR	TiO2 or Fe-IMAC	seedling	79,33
AT4G38470	IELQSQSWPMQQ(s)F(s)PEK			33
AT4G38470	IELQSQSWPMQQ(s)F(s)PEK	TiO2	cell culture	33

AT4G38470	ISADLDSTSNAGH(pS)SPTR	TiO ₂ or Fe-IMAC	seedling	1871
AT4G38470	ISADLDSTSNAGHS(pS)PTR	TiO ₂ or Fe-IMAC	seedling	1925
AT4G38470	ISADLDSTSNAGHS(pS)PTR	TiO ₂ or Fe-IMAC	seedling	2601
AT4G38470	LDSTSNAGHS(pS)PTR	TiO ₂ or Fe-IMAC	seedling	1597
AT4G38470	LDSTSNAGHS(pS)PTR	TiO ₂ or Fe-IMAC	seedling	19360

7.2 Kinase inhibitory library tested with STY8

Inhibitor	Target	Inhibition of STY8
CAY10578	CK2	NO
Lauric Acid Leelamide	PDK	NO
N,N-Dimethylsphingosine	sphingosine kinase	NO
SB 203580	p38 MAPK	NO
AS-252424	PI3K	NO
AG-17	EGF (PTK)	NO
PD 98059	MAPK	NO
Piceatannol	IκBα kinase	NO
Imatinib (mesylate)	PTK	NO
JNJ-10198409	PTK	YES
SB216763	GSK3	NO
Sphingosine Kinase Inhibitor 2	Sphingosine kinase	NO
HA-1077 (hydrochloride)	Rho-kinase	NO
H-8 (hydrochloride)	PKA and PKG	NO
NSC 210902	CK2	NO
Arachidonic Acid Leelamide	PDK	NO
CAY10561	ERK2	NO
PD 169316	MAPK	NO
Triciribine	Akt-1, -2, and -3	NO
D-erythro-Sphingosine C-18	sphingosine kinases	NO
O-1918	non-CB ₁ /CB ₂ receptor	NO
RG-13022	EGF (PTK)	NO
AG-123	EGF (PTK)	NO
Wortmannin	PT3K	NO
LFM-A13	BTK and Polo-like kinase	NO
Myricetin	JAK1/STAT3/MEK1	NO
Leelamine (hydrochloride)	PDK	NO
AS-604850	PI3Kγ	NO
AG-1296	PDGF (PTK)	NO
CAY10572	Cdc7	NO
NH125	Histidine kinases	NO
AG-825 (tyrphostin)	EGFR (PTK)	NO
(R)-Roscovitine	CDKs	NO
AG-1478	PTK	YES
L-threo-Sphingosine C-18	Proteinkinase C	NO
AG-494 (tyrphostin)	PTK	NO

AG-370 (tyrphostin)	PTK	NO
AG-82 (tyrphostin)	PTK	NO
CAY10575	IKK- ϵ	NO
CAY10571	p38 MAPK	NO
CCT018159	HSP90	NO
Leelamine	PDK	NO
Olomoucine	CDKs	NO
AG-183 (tyrphostin)	PTK	NO
AS-605240	PI3K γ , α , β , and δ	NO
AG-99 (tyrphostin)	PTK	NO
PD 0325901	MEK	NO
ZM 336372	Raf-1	NO
PI-103	PI3K	NO
PI3-Kinase α Inhibitor 2	PI3K α	NO
RG-1462 (tyrphostin)	PTK	NO
CAY10577	CK2	NO
Erbstatin Analog	PTK	NO
Janex-1	JAK3	YES
CAY10576	IKK- ϵ	NO
U-0126	MEK1/MEK2	NO
ML-9	serine/threonine	NO
LY294002	PI3K	NO
AG-490 (tyrphostin)	PTK	NO
HDBA	EGF	NO
Y-27632 (hydrochloride)	Rho-kinase	NO
AG-18 (tyrphostin)	PTK	NO

7.3 Results of microarray analysis for etiolated *sty8 sty17 sty46*

7.3.1 Up-regulated genes in *sty8 sty17 sty46*

Gene Name	Fold	Pi Value	Gene Information
At2g16005	10,40	0,084	not assigned no ontology
At3g25830	6,21	0,089	secondary metabolism isoprenoids terpenoids
At3g60140	3,58	0,058	misc.gluco-, galacto- and mannosidases
At3g48360	3,46	0,046	protein.degradation ubiquitin E3 BTB/POZ Cullin3 BTB/POZ
At1g10070	3,07	0,058	amino acid metabolism synthesis branched chain group common branched-chain amino acid aminotransferase Co-factor and vitamine metabolism pantothenate branched-chain amino acid aminotransferase
At5g20790	3,03	0,088	35.2 not assigned unknown
At1g74670	3,03	0,044	hormone metabolism gibberelin induced-regulated-responsive-activated
At2g47880	3,02	0,044	Redox glutaredoxins

At5g20150	2,85	0,058	Stress abiotic
At2g22980	2,77	0,058	Protein degradation serine protease
NdhH	2,70	0,072	PS lightreaction cyclic electron flow-chlororespiration
At2g29090	2,69	0,072	misc.cytochrome P450
At5g47240	2,65	0,058	nucleotide metabolism salvage NUDIX hydrolases
At5g38020	2,55	0,097	hormone metabolism salicylic acid synthesis-degradation
At2g18050	2,54	0,058	DNA synthesis/chromatin structure histone
At5g06760	2,44	0,080	Development late embryogenesis abundant
At4g37220	2,39	0,080	not assigned no ontology
At1g55240	2,32	0,098	not assigned unknown
Rps16	2,22	0,072	Protein synthesis ribosomal protein prokaryotic chloroplast 30S subunit S16
At1g03090	2,19	0,058	amino acid metabolism degradation branched-chain group leucine
At1g77760	2,15	0,072	N-metabolism nitrate metabolism.NR
At1g14240	2,15	0,072	nucleotide metabolism degradation
At1g80440	2,14	0,098	Protein degradation ubiquitin E3 SCF FBOX
At1g15380	2,11	0,094	Biodegradation of Xenobiotics lactoylglutathione lyase
ycf3	2,10	0,089	Protein assembly and cofactor ligation
At4g02280	2,09	0,089	major CHO metabolism degradation sucrose Susy
At1g15045	2,08	0,058	not assigned no ontology
At5g52300	2,04	0,090	Stress abiotic cold
At4g37610	1,97	0,098	Protein degradation ubiquitin E3 BTB/POZ Cullin3 BTB/POZ
At5g49450	1,95	0,072	RNA regulation of transcription bZIP transcription factor family AND not assigned unknown
NdhG	1,94	0,066	PS light reaction
AccD	1,92	0,076	lipid metabolism FA synthesis and FA elongation Acetyl CoA Carboxylation
At2g22990	1,92	0,072	Protein degradation serine protease
psbG (ndh)	1,90	0,080	PS ligh treaction
At2g41190	1,87	0,074	Transport amino acids
At1g66110	1,87	0,072	not assigned unknown
Rpl33	1,87	0,072	Protein synthesis ribosomal protein prokaryotic chloroplast 50S subunit L33
At3g49160	1,86	0,097	Glycolysis cytosolic branch pyruvate kinase (PK)
NdhA	1,85	0,076	PS lightreaction cyclic electron flow-chlororespiration
At1g16260	1,85	0,072	Signalling receptor kinases wall associated kinase
At2g30540	1,83	0,073	Redox glutaredoxins
At4g35770	1,83	0,080	Development unspecified
At2g18700	1,83	0,081	minor CHO metabolism trehalose.potential TPS/TPP
At1g21400	1,82	0,072	amino acid metabolism degradation branched-chain group shared AND Co-factor and vitamine metabolism pantothenate 2-dehydropantoate 2-reductase
At2g07000	1,82	0,097	not assigned unknown
At2g02710	1,81	0,072	Signalling light

At5g26200	1,78	0,072	Transport metabolite transporters at the mitochondrial membrane
psbF	1,78	0,091	PS.lightreaction photosystem II. PSII polypeptide subunits
At3g02040	1,78	0,084	lipid metabolism lipid degradation lysophospholipases glycerophosphodiester phosphodiesterase
At1g19510	1,76	0,080	RNA regulation of transcription MYB domain transcription factor family
psbE	1,75	0,080	PS lightreaction photosystem II.PSII polypeptide subunits
psal	1,72	0,080	PS lightreaction photosystem I.PSI polypeptide subunits
At1g58180	1,72	0,091	TCA / org. Transformation carbonic anhydrases
At2g21210	1,72	0,080	hormone metabolism auxin induced-regulated-responsive-activated
At1g19050	1,71	0,091	RNA regulation of transcription.ARR
At5g47900	1,71	0,091	not assigned unknown
At3g10450	1,70	0,080	Protein degradation
At2g46680	1,70	0,080	RNA regulation of transcription HB,Homeobox transcription factor family
ycf9 psbZ	1,69	0,083	PS lightreaction photosystem II.PSII polypeptide subunits
At2g43760	1,69	0,083	Co-factor and vitamins metabolism molybdenum cofactor
rps12.2	1,69	0,099	Protein synthesis ribosomal protein prokaryotic chloroplast 30S subunit S12
At1g01330	1,68	0,084	not assigned no ontology pentatricopeptide (PPR) repeat-containing protein
At3g07310	1,67	0,080	not assigned.unknown
At2g25900	1,66	0,097	RNA regulation of transcription C3H zinc finger family
At4g28703	1,66	0,084	not assigned unknown
NdhJ	1,66	0,089	PS lightreaction
At3g06070	1,66	0,089	not assigned unknown
At5g66650	1,65	0,091	not assigned unknown
At5g57655	1,64	0,097	minor CHO metabolism others Xylose isomerase
At3g57520	1,64	0,090	minor CHO metabolism raffinose family raffinose synthases putative
At3g45300	1,63	0,082	amino acid metabolism degradation branched-chain group leucine
At1g20070	1,63	0,084	not assigned unknown
At2g07741	1,62	0,097	mitochondrial electron transport / ATP synthesis F1-ATPase AND transport metal AND not assigned no ontology
At3g10020	1,61	0,084	not assigned unknown
At1g70290	1,61	0,089	minor CHO metabolism trehalose potential TPS/TPP
At5g44410	1,61	0,084	Misc nitrilases, *nitrile lyases, berberine bridge enzymes, reticuline oxidases, troponine reductases
At3g59940	1,60	0,089	Protein degradation ubiquitin E3 SCF FBOX
ycf10_cemA	1,60	0,097	not assigned unknown

ycf6 petN	1,58	0,097	PS lightreaction cytochrome b6/f
At2g45950	1,58	0,089	Protein degradation ubiquitin E3 SCF SKP
At4g15660	1,58	0,088	Redox glutaredoxins
At1g80160	1,57	0,090	Biodegradation of Xenobiotics lactoylglutathione lyase
At2g26980	1,56	0,097	Protein postranslational modification
At4g19500	1,56	0,099	stress.biotic.PR-proteins
At1g64050	1,54	0,097	not assigned unknown
At1g54260	1,54	0,099	RNA regulation of transcription.MYB domain transcription factor family
Rps4	1,53	0,100	Protein synthesis ribosomal protein prokaryotic chloroplast 30S subunit S4
At5g28230	1,51	0,100	Transport metabolite transporters at the envelope membrane
At5g57050	1,51	0,098	hormone metabolism abscisic acid signal transduction AND 29.4 protein postranslational modification

7.3.2 Down-regulated genes in *sty8 sty17 sty46*

Gene Name	Fold	Pi Value	Gene Information
At4g38470	0,05	0,003	protein postranslational modification
At4g33720	0,06	0,044	stress biotic
At4g27170	0,10	0,003	development storage proteins
At5g66880	0,16	0,027	protein postranslational modification
At4g27160	0,16	0,052	development storage proteins
At4g12480	0,18	0,047	misc protease inhibitor/seed storage/lipid transfer protein (LTP) family protein
At4g27140	0,18	0,084	development storage proteins
At5g40590	0,20	0,044	not assigned no ontology DC1 domain containing protein
At5g04970	0,22	0,076	cell wall pectin esterases misc
At5g19890	0,22	0,072	misc peroxidases
At1g52070	0,23	0,082	hormone metabolism jasmonate induced-regulated-responsive-activated
At3g05600	0,17	0,058	misc misc2
At5g62210	0,27	0,060	development unspecified
At1g49570	0,27	0,044	misc peroxidases
At5g39110	0,28	0,044	stress abiotic unspecified
At5g04120	0,30	0,061	glycolysis cytosolic branch phosphoglycerate mutase
At3g23800	0,32	0,058	metal handling
At1g53490	0,34	0,046	RNA regulation of transcription unclassified
At5g46050	0,35	0,058	transport peptides and oligopeptides
At3g18000	0,35	0,080	lipid metabolism Phospholipid synthesis AND not assigned unknown
At4g10270	0,36	0,061	stress abiotic touch/wounding
At4g14980	0,36	0,063	not assigned no ontology DC1 domain containing

			protein
At5g38930	0,37	0,071	stress abiotic unspecified
At4g16260	0,38	0,044	misc beta 1,3 glucan hydrolases glucan endo-1,3-beta-glucosidase
At4g26220	0,38	0,058	secondary metabolism phenylpropanoids lignin biosynthesis CCoAOMT
At4g08770	0,39	0,076	misc peroxidases
At4g36430	0,39	0,076	misc peroxidases
At3g45160	0,40	0,080	not assigned unknown
At5g43520	0,40	0,084	not assigned no ontology DC1 domain containing protein
At4g30280	0,40	0,058	cell wall modification
At4g16563	0,40	0,084	protein degradation aspartate protease
At2g16630	0,41	0,099	not assigned no ontology proline rich family
At4g37800	0,41	0,084	cell wall modification
At5g14920	0,41	0,046	hormone metabolism gibberelin induced-regulated-responsive-activated
At3g13610	0,41	0,094	DNA unspecified
At3g54040	0,42	0,044	signalling in sugar and nutrient physiology
At1g51800	0,42	0,090	signalling receptor kinases misc
At3g14210	0,42	0,046	secondary metabolism sulfur-containing glucosinolates degradation myrosinase AND misc GDSL-motif lipase
At4g36110	0,42	0,097	hormone metabolism auxin induced-regulated-responsive-activated
At1g53070	0,43	0,080	protein postranslational modification
At1g15550	0,43	0,084	hormone metabolism gibberelin synthesis-degradation GA3 oxidase
At1g13420	0,44	0,084	lipid metabolism "exotics" (steroids, squalene etc)
At3g14850	0,44	0,072	not assigned unknown
At5g06720	0,45	0,075	misc peroxidases
At1g76210	0,45	0,074	not assigned unknown
At5g13870	0,45	0,058	cell wall modification
At2g41480	0,45	0,058	misc peroxidases
At4g15620	0,45	0,058	not assigned no ontology
At2g17700	0,45	0,052	protein postranslational modification
At1g02200	0,46	0,080	secondary metabolism wax
At2g02010	0,46	0,058	amino acid metabolism synthesis central amino acid metabolism GABA Glutamate decarboxylase
At5g58570	0,47	0,074	not assigned unknown
At4g30290	0,47	0,061	cell wall modification
At5g66690	0,47	0,080	secondary metabolism phenylpropanoids lignin biosynthesis
At5g01790	0,48	0,089	not assigned unknown
At2g42610	0,48	0,091	not assigned unknown
At3g61820	0,48	0,058	RNA regulation of transcription unclassified
At4g33790	0,48	0,080	lipid metabolism lipid degradation beta-oxidation acyl

			CoA reductase
At3g05770	0,48	0,058	not assigned unknown
At1g28290	0,49	0,058	stress abiotic unspecified
At5g03350	0,49	0,088	misc myrosinases-lectin-jacalin
At2g41090	0,49	0,080	signalling calcium
At4g13210	0,49	0,072	cell wall degradation pectate lyases and polygalacturonases
At2g26440	0,49	0,097	cell wall pectin*esterases PME
At1g18250	0,49	0,080	stress biotic
At2g47010	0,49	0,080	not assigned unknown
At5g08260	0,50	0,061	protein degradation serine protease
At5g20740	0,50	0,089	misc invertase/pectin methylesterase inhibitor family protein
At3g51350	0,51	0,072	not assigned unknown
At3g62150	0,51	0,076	transport ABC transporters and multidrug resistance systems
At2g46140	0,51	0,099	development late embryogenesis abundant
At4g08040	0,52	0,080	hormone metabolism ethylene synthesis-degradation 1-aminocyclopropane-1-carboxylate synthase
At1g10550	0,52	0,058	cell wall modification
At5g49630	0,52	0,087	transport amino acids
At5g66280	0,52	0,100	cell wall precursor synthesis GMD
At1g80760	0,52	0,086	transport Major Intrinsic Proteins NIP
At1g59940	0,52	0,088	RNA regulation of transcription ARR
At5g35735	0,53	0,091	hormone metabolism auxin induced-regulated-responsive-activated
At1g70270	0,53	0,077	not assigned unknown
At1g19900	0,53	0,076	Biodegradation of Xenobiotics
At3g59220	0,53	0,088	signalling G-proteins
At3g61490	0,54	0,086	cell wall degradation pectate lyases and polygalacturonases
At1g26560	0,54	0,072	misc gluco-, galacto- and mannosidases
At4g22490	0,54	0,084	misc protease inhibitor/seed storage/lipid transfer protein (LTP) family protein
At4g02290	0,54	0,072	misc gluco-, galacto- and mannosidases endoglucanase
At5g12110	0,54	0,080	protein synthesis elongation
At1g29670	0,54	0,091	misc GDSL-motif lipase
At1g24020	0,54	0,086	stress abiotic unspecified
At2g18010	0,54	0,093	hormone metabolism auxin induced-regulated-responsive-activated
At3g11340	0,55	0,098	misc UDP glucosyl and glucuronyl transferases
At2g41100	0,55	0,084	signalling calcium
At1g59500	0,55	0,084	hormone metabolism auxin induced-regulated-responsive-activated
At5g59090	0,55	0,089	protein degradation subtilases

At5g08000	0,55	0,080	not assigned no ontology
At5g45070	0,55	0,082	stress biotic receptors
At3g44720	0,55	0,082	amino acid metabolism synthesis aromatic aa phenylalanine arogenate dehydratase / prephenate dehydratase
At2g42540	0,55	0,084	stress abiotic cold
At4g02700	0,55	0,099	transport sulphate
At4g38850	0,56	0,088	hormone metabolism auxin induced-regulated-responsive-activated
At4g30170	0,56	0,084	misc peroxidases
At4g02330	0,57	0,080	cell wall pectin*esterases misc
At2g47550	0,57	0,076	cell wall pectin*esterases PME
At5g01180	0,57	0,089	transport peptides and oligopeptides
At2g18140	0,57	0,086	misc peroxidases
At2g36090	0,57	0,088	protein degradation ubiquitin E3 SCF FBOX
At1g02360	0,58	0,089	stress biotic
At1g73830	0,58	0,084	RNA regulation of transcription bHLH,Basic Helix-Loop-Helix family
At3g20260	0,58	0,080	protein synthesis ribosomal protein eukaryotic 60S subunit L34
At4g05200	0,59	0,080	signalling receptor kinases DUF 26
At1g78370	0,59	0,090	misc glutathione S transferases
At4g25100	0,59	0,082	redox dismutases and catalases
At4g22770	0,59	0,080	RNA regulation of transcription putative transcription regulator
At5g03090	0,59	0,084	not assigned unknown
At3g23540	0,60	0,091	not assigned unknown
At2g40330	0,60	0,090	stress abiotic unspecified
At4g21830	0,60	0,089	stress abiotic AND not assigned no ontology
At2g28900	0,60	0,084	protein targeting mitochondria
At2g38010	0,60	0,085	lipid metabolism "exotics" (steroids, squalene etc) sphingolipids ceramidase
At4g14130	0,60	0,080	cell wall modification
At2g36570	0,60	0,084	signalling receptor kinases leucine rich repeat III
At2g16750	0,61	0,082	protein postranslational modification kinase receptor like cytoplasmatic kinase VI
At3g25780	0,61	0,099	hormone metabolism jasmonate synthesis-degradation allene oxidase cyclase
At1g15210	0,61	0,084	transport ABC transporters and multidrug resistance systems
At1g75390	0,61	0,097	RNA regulation of transcription bZIP transcription factor family AND not assigned unknown
At1g33560	0,61	0,097	stress biotic PR-proteins
At2g22500	0,61	0,084	metabolite transporters at the mitochondrial membrane
At3g52500	0,61	0,097	protein degradation
At5g22500	0,61	0,082	lipid metabolism lipid degradation beta-oxidation acyl

			CoA reductase
At5g07030	0,61	0,091	RNA regulation of transcription putative transcription regulator
At1g05700	0,61	0,089	signalling receptor kinases misc
At5g33370	0,61	0,097	misc GDSL-motif lipase
At5g08640	0,62	0,098	secondary metabolism flavonoids flavonols
At5g50335	0,62	0,084	not assigned unknown
At2g41010	0,62	0,095	stress abiotic drought/salt AND signalling calcium
At5g21100	0,62	0,097	redox ascorbate and glutathione ascorbate
At2g02100	0,63	0,085	stress biotic
At3g03020	0,63	0,097	not assigned unknown
At3g50440	0,63	0,091	not assigned no ontology
At1g17830	0,63	0,091	not assigned unknown
At1g21880	0,65	0,100	not assigned no ontology
At5g23480	0,65	0,091	not assigned unknown
At5g15780	0,65	0,095	stress abiotic unspecified
At1g26100	0,65	0,091	redox ascorbate and glutathione
At2g44300	0,65	0,099	lipid metabolism lipid transfer proteins etc
At3g62770	0,66	0,097	transport misc
At4g38660	0,66	0,100	stress biotic
At1g76410	0,66	0,098	protein degradation ubiquitin E3 RING

ACKNOWLEDGEMENTS

First, I would like to thank Prof. Dr. Soll for giving me the possibility to perform my PhD work in his lab.

I would also like to thank my direct supervisor Serena for her constant support and help during the last three years.

Big thanks to Kathi, Tine and Regina for sharing with me the lab fun and troubles (and lots of chocolate).

Many thanks to all my colleagues for the good time spent together, in particular special thanks to Sabine for her unconditional friendship, Ingo for fighting my bad mood moment with “Gummibärchen” and the Italian connection from downstairs for the motivation coffees.

Thanks also to Hans-Jörg, Maxi and Ingrid from the IMPRS coordination office for their unpayable help in every situation.

Many thanks to the people who contributed with experiments and materials to this project: Irene for the electron microscopy, Dr. J.Meurer for the PSII PAM measurements, Katrin, Julia and Karl for the Affimetrix analysis and Prof. Dr. U. Vothknecht and Claudia Sippel for providing the *sty8 sty46 Arabidopsis* lines.

CURRICULUM VITAE**Personal details**

First name: Giorgia
 Family name: Lamberti
 Date of birth: 10th of July 1984
 Place of birth: Bolzano/Bozen, Italy
 Nationality: Italian

Education and research experience

1998-2003 High school (Liceo scientifico), Bolzano, Italy
 Score: 95/100

09/2003-09/2006 Bachelor in Molecular Biology (score of 110/110), University of Padova, Italy.

04/2006-07/2006 Bachelor Thesis “Strategy of epitope mapping of the thylakoidal protein cpPHI1 through expression of its fragments in *E.coli*”. Work carried out in Prof. Elisabetta Bergantino’s lab, Department of Biology, University of Padova, Italy

09/2006-07/2008 Master in Molecular Biology completed with First Class Honours (score of 110/110, with distinction), University of Padova, Italy

09/2007-07/2008 Master Thesis “Molecular dissection of the interaction between Cdc48 and its cofactors Ufd2 and Ufd3 in *Saccharomyces cerevisiae*”. Work carried out in Prof. Alexander Buchberger’s lab (official supervisor Prof. Stefan Jentsch), Department of Molecular Cell Biology, Max Planck Institute of Biochemistry, Martinsried, Germany

10/2008-present PhD graduate student (IMPRS-LS student membership) in the lab of Prof. Dr. J. Soll at the “*Ludwig-Maximilians-Universität München*” (LMU München), Munich, Germany
 Thesis topic: “Characterization of the *Arabidopsis thaliana* STY8, STY17 and STY46 protein kinase family”

LIST OF PUBLICATIONS**Publications:**

Böhm S.*, Lamberti G.*, Fernández-Sáiz V., Stapf C., Buchberger A. (2011) Cellular functions of Ufd2 and Ufd3 in proteasomal protein degradation depend on Cdc48 binding. *Mol Cell Biol* 31, 1528-1539

* These authors contributed equally to this work

Lamberti G., Gügel I.L., Meurer J., Soll J., Schwenkert S. (2011) The cytosolic kinases STY8, STY17, and STY46 are involved in chloroplast differentiation in *Arabidopsis*. *Plant Physiol* 157(1):70-85

Lamberti G., Drurey C., Soll J., Schwenkert S. (2011) The phosphorylation state of chloroplast transit peptides regulates preprotein import. *Plant Signaling & Behavior* Volume 6 Issue 12, in press

Presentations at international meetings:

Lamberti G., Soll J., Schwenkert S. "How can phosphorylation regulate protein targeting from cytosol to chloroplast?", Poster. FEBS/EMBO Advanced Lecture Course in Cellular and Molecular Biology of Membranes; 08.06.-19.06.2009: Cargese, Corsica, France.

Lamberti G., Gügel I.L., Soll J., Schwenkert S. "Transit peptide phosphorylation: a regulatory step in etioplast to chloroplast transition?", Poster. FEBS Workshop: Plant Organellar Signaling-from Algae to Higher Plants; 31.08.-03.09.2011; Primòsten, Croatia.

EHRENWÖRTLICHE VERSICHERUNG

Ich versichere hiermit ehrenwörtlich, dass die vorgelegte Dissertation von mir selbständig und nur unter Verwendung der angegebenen Hilfsmittel und Quellen angefertigt wurde.

München, den

Giorgia Lamberti

Erklärung

Hiermit erkläre ich, dass ich zuvor nicht versucht habe, anderweitig eine Dissertation einzureichen oder mich einer Doktorprüfung zu unterziehen. Die vorliegende Dissertation wurde keiner weiteren Prüfungskommission weder in Teilen noch als Ganzes vorgelegt.

München, den

Giorgia Lamberti